

Functional analysis of two components of the chloroplastic TIC complex

Dissertation der Fakultät für Biologie
der
Ludwig-Maximilians-Universität München

vorgelegt von

Natalie Schuck

München
2013



Erstgutachter: Prof. Dr. J. Soll
Zweitgutachter: PD Dr. C. Bolle

Tag der Abgabe: 23. Mai 2013
Tag der mündlichen Prüfung: 18. Juni 2013

Summary

In plants the majority of chloroplast proteins is encoded in the nucleus and has to be transported posttranslationally into the organelle. For this purpose, the TOC and TIC (Translocon at the Outer/Inner envelope of Chloroplasts) mediate the import of precursor proteins into the chloroplast by guiding them across the two membranes. Both multiprotein complexes comprise a number of well-defined subunits. In this work, two TIC components were investigated concerning their molecular function.

First, the intermembrane space (IMS) protein Tic22, which was shown to be involved in the guidance of preproteins from the TOC complex through the IMS to the TIC complex, was analyzed. For this purpose, double knock-out mutants, lacking two (Tic22III and Tic22IV) of the three isoforms in *Arabidopsis thaliana* (*A. thaliana*) were used to characterize the protein with regard to further functional and structural features. A third protein (Tic22V), potentially representing a third isoform of Tic22, was also studied in terms of its function in wildtype and *tic22III/IV* double mutant plants by gene silencing and the analysis of single knock-down mutants. Due to the fact that Tic22 is highly conserved within numerous plastid-containing organisms, the importance of this conservation with regard to further functional properties beside the role of Tic22 in protein import was investigated in this work.

The second part of this work deals with the characterization of Tic62, a protein which is localized at the thylakoids, the inner envelope and in the stroma of chloroplasts. Tic62 was shown to possess FNR binding activity, an enzyme, which mediates the last step of linear electron flow (LEF) by transferring electrons from ferredoxin to NADP^+ , thus generating the reduction equivalent NADPH, which is required in numerous metabolic pathways in the plastid. At the thylakoids, Tic62 was shown to tether FNR to the membrane in the same way as Trol (thylakoid rhodanese-like protein), which is localized in the thylakoid membrane. Both proteins Tic62 and Trol contain serine-proline-rich repeats (Ser/Pro rich repeats), which were shown to possess high binding affinity for FNR. Although the interaction between Tic62/Trol and FNR is indisputable, the importance of this interaction as well as tethering of the enzyme to the thylakoid membrane is still under debate. For this purpose, Tic62 and Trol double knock-out mutants (*tic62trol*) were analyzed in respect to potential photosynthetic and metabolic alterations in respective *Arabidopsis thaliana* mutant plants.

Zusammenfassung

In Pflanzen ist die Mehrheit der chloroplastidären Proteine im Kern kodiert und muss posttranslational in das Organell transportiert werden. Zu diesem Zweck vermitteln der TOC und TIC (Translocon at the Outer/Inner envelope of Chloroplasts) Komplex den Import von Vorstufenproteinen in Chloroplasten, indem sie diese über die beiden Membranen dirigieren. Beide Multiproteinkomplexe umfassen eine Anzahl klar definierter Proteine. In dieser Arbeit wurden zwei TIC Komponenten bezüglich ihrer molekularen Funktion untersucht.

Zunächst wurde das Intermembranraum-(IMS)-Protein Tic22 analysiert, bei dem es sich erwiesen hatte, dass es an der Überführung der Vorstufenproteine vom TOC Komplex über den IMS zum TIC Komplex beteiligt ist. Zu diesem Zweck wurden Doppel-*knockout*-Mutanten, denen zwei (Tic22III und Tic22IV) der drei Isoformen in *Arabidopsis thaliana* (*A. thaliana*) fehlen, dazu verwendet, das Protein hinsichtlich weiterer funktionaler und struktureller Merkmale zu charakterisieren. Ein drittes Protein (Tic22V), das möglicherweise eine weitere Isoform von Tic22 darstellt, wurde ebenso bezüglich ihrer Funktion in Wildtyp- und *tic22IIIxIV* Doppelmutanten Pflanzen durch Genstilllegung und das Analysieren von Einzel-*knockdown*-Mutanten untersucht. Aufgrund der Tatsache, dass Tic22 in zahlreichen plastidhaltigen Organismen hochkonserviert ist, wurde in dieser Arbeit die Bedeutung dieser Konservierung im Hinblick auf weitere strukturelle Eigenschaften neben der Beteiligung von Tic22 im Proteinimport, untersucht.

Der zweite Teil dieser Arbeit befasst sich mit der Charakterisierung von Tic62, einem Protein, das an den Thylakoiden, der inneren Hüllmembran und im Stroma von Chloroplasten lokalisiert ist. Es wurde gezeigt, dass Tic62 FNR-Bindungsaktivität besitzt, ein Enzym, das den letzten Schritt des linearen Elektronenflusses (LEF) durch eine Übertragung der Elektronen von Ferredoxin auf NADP^+ vermittelt, wodurch das Reduktionäquivalent NADPH generiert wird, welches in zahlreichen Stoffwechselwegen im Plastid benötigt wird. Es wurde gezeigt, dass Tic62 FNR auf die gleiche Weise wie Trol (thylakoid rhodanese-like protein), das an der Thylakoidmembran lokalisiert ist, an den Thylakoiden verankert. Beide Proteine, Tic62 und Trol, enthalten Serin-Prolin reiche Wiederholungen (Ser/Pro rich repeats), die sich als eine hohe Bindeaffinität für FNR besitzend erwiesen. Obwohl die Interaktion zwischen Tic62/Trol und FNR unumstritten ist, wird die Bedeutung dieser Interaktion sowie die Bindung des

Enzyms an die Thylakoidmembran immer noch diskutiert. Zu diesem Zweck wurden Tic62 und Trol Doppel-*Knockout*-Mutanten (*tic62trol*) im Hinblick auf etwaige photosynthetische und metabolische Veränderungen in jeweiligen *Arabidopsis thaliana* Mutantepflanzen untersucht.

Table of contents

Summary	I
Zusammenfassung.....	II
Table of contents.....	IV
Abbreviations	VII
1. Introduction.....	1
1.1 Protein import into chloroplasts	1
1.2 Tic22 and its evolutionary conservation	4
1.4 The function of Tic62 and Trol and their interplay with FNR.....	6
1.5 Metabolic processes connected to photosynthesis	7
1.6 Aims of this work.....	9
2. Materials.....	10
2.1 Chemicals.....	10
2.2 Enzymes.....	10
2.3 Oligonucleotides.....	10
2.4 Vectors and constructs	12
2.5 Molecular weight markers and DNA standards	13
2.6 Antibodies.....	13
2.7 Strains.....	13
2.8 Plant material	13
3. Methods	14
3.1 Plant methods	14
3.1.1 Growth of <i>A. thaliana</i>	14
3.1.2 Cross fertilization of <i>A. thaliana</i>	14
3.1.3 Stable transformation of <i>A. thaliana</i>	15
3.1.4 Chlorophyll fluorescence measurements of PSII.....	15
3.2 Microbiology methods	15
3.2.1 Media and growth	15
3.2.2 Bacteria transformation	16
3.3 Molecular biology methods.....	16
3.3.1 Polymerase Chain Reaction (PCR)	16
3.3.2 Cloning strategies	17
3.3.3 Isolation of DNA plasmids from <i>Escherichia coli</i>	17

3.3.4 Preparation of genomic DNA of <i>A. thaliana</i>	17
3.3.5 Determination of DNA and RNA concentrations.....	17
3.3.6 Characterization of plant T-DNA insertion lines.....	18
3.3.7 DNA sequencing	18
3.3.8 RNA extraction and Real-Time RT-PCR (qRT-PCR).....	18
3.3.9 Microarray analysis	19
3.4 Biochemical methods	19
3.4.1 Determination of protein concentration.....	19
3.4.2 Protein extraction of <i>A. thaliana</i>	19
3.4.3 SDS-PAGE (polyacrylamide gelelectrophoresis)	20
3.4.4 Immunodetection.....	20
3.4.5 Blue Native PAGE.....	21
3.4.6 <i>In vitro</i> transcription and translation	21
3.4.7 <i>A. thaliana</i> chloroplast isolation.....	22
3.4.8 <i>A. thaliana</i> chloroplast isolation and fractionation.....	22
3.4.9 <i>Pisum sativum</i> chloroplast isolation and protein import	22
3.4.10 Protein expression, purification and crystallization	23
3.5 Metabolite analysis	23
3.6 Microscopy	24
3.7 Computational analysis	24
4. Results	25
4.1 Characterization of Tic22 in <i>A. thaliana</i>	25
4.1.1 The Tic22 protein family in <i>A. thaliana</i>	25
4.1.2 Generation of Tic22 mutants in <i>A. thaliana</i>	29
4.1.3 Phenotypic characterization of the <i>tic22IIIxIV</i> double mutant	31
4.1.4 Photosynthetic performance of WT and <i>tic22dm</i> plants	36
4.1.5 Molecular analysis of separated leaf parts.....	37
4.1.6 Immunoblot of Lhc proteins in <i>A. thaliana</i> WT and <i>tic22dm</i> chloroplasts	41
4.1.7 Analysis of the gene regulation in WT and <i>tic22dm</i> by DNA-Microarray analysis.....	42
4.1.8 Gene silencing of TIC22V by RNAi	46
4.1.9 Isolation of TIC22V knock-out mutants.....	49
4.1.10 Localization of Tic22V.....	51
4.1.11 Structural analysis of <i>Synechocystis sp.</i> Tic22 by X-Ray crystallography.....	52
4.2 Characterization of Tic62/Trol and their relation to FNR.....	57
4.2.1 Generating <i>tic62trol</i> double mutants.....	57

4.2.2 Localization of FNR in <i>tic62trol</i>	60
4.2.3 Thylakoidal complex composition in <i>tic62trol</i>	61
4.2.4 Phenotypic and photosynthetic analysis of <i>tic62trol</i>	63
4.2.5 Metabolic pathways influenced in <i>tic62trol</i> plants.....	63
5. Discussion	67
5.1 Characterization of Tic22 in <i>A.thaliana</i>	67
5.1.1 General properties of the Tic22 isoforms in <i>A.thaliana</i>	67
5.1.2 Tic22V might play a role during pollen development	69
5.1.3 The knock-out of Tic22III and Tic22IV leads to a chlorotic phenotype and altered thylakoid composition.....	69
5.1.4 Tic22dm reveals an altered gene expression	70
5.1.5 <i>Tic22dm</i> reveals a reduced OE33 content in the margins.....	71
5.1.6 <i>Tic22dm</i> plants contain an altered plastid gene expression	71
5.1.7 Potential flexible loops might avoid the crystallization of synTic22	73
5.2 Tic62 and Trol and their potential role in photosynthetic processes	76
6. References	80
7. Supplementary data	91
7.1 DNA Microarray analysis	91
Curriculum vitae	100
Danksagung	101
Eidesstattliche Versicherung	102
Erklärung	102

Abbreviations

2D	two dimensional
aa	amino acids
AP	alkaline phosphatase
ATPase	CF ₀ CF ₁ ATP synthase
<i>A.thaliana</i>	<i>Arabidopsis thaliana</i>
ATP	adenosine triphosphate
β-ME	β-mercaptoethanol
bp	base pair
BCA	bicinchoninic acid
BCIP	5-bromo-4-chloro-3-indolyl phosphate
BLAST	basic local alignment search tool
BN-PAGE	blue-native polyacrylamide gel electrophoresis
CaM	calmodulin
CEF	cyclic electron flow
Chl	chlorophyll
cDNA	complementary DNA
Col-0	Columbia 0 ecotype
Cys	cysteine
Cytb ₆ f	cytochrome b ₆ f complex
Cyt c	cytochrome c
DNA	deoxyribonucleic acid
dNTP	deoxynucleotide triphosphates
DTT	dithiothreitol
<i>E. coli</i>	<i>Escherichia coli</i>
ECL	enhanced chemiluminescence
EDTA	ethylenediaminetetraacetic acid
FBPase	fructose-1,6-biphosphatase
Fd	ferredoxin
FNR	ferredoxin-NADP(H) oxidoreductase
FTR	ferredoxin-thioredoxin oxidoreductase
F ₀	minimal chlorophyll fluorescence (in the dark)
F _m	maximal chlorophyll fluorescence (in the light)
F _v	variable chlorophyll fluorescence
F _s	steady-state chlorophyll fluorescence
F _v /F _m	maximal quantum yield of PSII
GAPDH	glyceraldehyde-3-phosphate dehydrogenase
GFP	green fluorescent protein
GL	growth light
GTP	guanosine-5'-triphosphate
<i>G.theta</i>	<i>Guillardia theta</i>
he	heterozygous
Hepes	(4-(2-hydroxyethyl)-1-piperazineethanesulfonic acid)

His	histidine
ho	homozygous
IE	inner envelope
IMS	intermembrane space
IP	isoelectric point
Kan	kanamycin
kDa	kilo Dalton
LB	Left Border (TDNA)
LEF	linear electron flow
LHC	light harvesting complex
MDH	malate dehydrogenase
Met	methionine
mRNA	messenger RNA
MS	Murashige and Skoog
MW	molecular weight
NAD	nicotinamide adenine dinucleotide
NADP ⁺	nicotinamide adenine dinucleotide phosphate, oxidized form
NADPH	nicotinamide adenine dinucleotide phosphate, reduced form
NDH	NAD(P)H dehydrogenase
NPQ	non-photochemical quenching
NTR	NADPH-thioredoxin reductase
OD	optical density
OE	outer envelope
OEC	oxygen evolving complex (of PSII)
OEP	outer envelope protein
PAGE	polyacrylamide gel electrophoresis
PCR	polymerase chain reaction
Pi	inorganic phosphate
PMSF	phenylmethylsulfonyl fluoride
PQ	plastoquinon
<i>P.sativum</i>	<i>Pisum sativum</i>
<i>P.falciparum</i>	<i>Plasmodium falciparum</i>
PSI, PSII	photosystem I, photosystem II
PVDF	polyvinylidene fluoride
RNA	ribonucleic acid
RNAi	RNA interference
ROS	reactive oxygen species
rpm	revolutions per minute
RT-PCR	reverse-transcription polymerase chain reaction
RT	room temperature
RuBisCo	ribulose-1,5-bisphosphate carboxylase/oxygenase
SD	standard deviation
SE	standard error
SDS	sodium dodecyl sulphate
SPP	stromal processing peptidase

SSU	small subunit of ribulose-1,5-biphosphatase carboxylase/oxygenase
T-DNA	Transfer-DNA
TEM	transmission electron microscopy
TIC	translocon at the inner envelope of chloroplasts
<i>tic22dm</i>	Tic22IIIxIV double mutant
<i>tic22IVsm</i>	Tic22IV single mutant
<i>tic62trol</i>	Tic62xTrol double mutant
TM	transmembrane domain
TOC	translocon at the outer envelope of chloroplasts
<i>T.gondii</i>	<i>Toxoplasma gondii</i>
TP	transit peptide
TPR	tetratricopeptide repeat
Tris	tris(hydroxymethyl) aminomethane
Trx	thioredoxin
UTR	untranslated region
v/v	volume per volume
VDAC	voltage dependent anion channel
w/v	weight per volume
WT	wildtype
x g	times the force of gravity

1 Introduction

1.1 Protein import into chloroplasts

Plastids are a heterogeneous family of organelles which are found in plant and algal cells. Most prominent are the chloroplasts, comprising important biochemical and metabolic processes such as photosynthesis and the synthesis of fatty acids and amino acids. For these processes, the translocation of proteins into plastids constitutes a crucial event. Chloroplasts originated from an endosymbiotic event in which an early eukaryotic cell engulfed an ancient cyanobacterium. Since the endosymbiont kept both of its membranes, the resulting organelle is surrounded by a double membrane (Martin *et al.*, 1998; Gould *et al.*, 2008). Due to the massive transfer of more than 90% of their genetic information to the host nucleus during evolution, the organelle had to evolve a mechanism to transport nucleus-encoded and cytosolic-synthesized chloroplast proteins back into the plastid (Martin *et al.*, 1998 and 2002; Leister *et al.*, 2003). This process is mediated by two translocation machineries in the outer (OE) and the inner (IE) envelope of the chloroplast (Figure 1), called TOC (translocon at the outer envelope of chloroplasts) and TIC (translocon at the innner envelope of chloroplasts), commonly known as mediating the “general import pathway” of precursor proteins (Benz *et al.*, 2009; Jarvis, 2008; Schwenkert, 2011, Figure 1). The TOC core complex consists of the β -barrel membrane channel Toc75 (Hinnah *et al.*, 2002) and the two associated receptor proteins Toc159 and Toc34, representing integral GTPases at the OE (Hirsch *et al.*, 1994; Kessler *et al.*, 1994; Perry and Keegstra, 1994; Seedorf *et al.*, 1995; Jelic *et al.*, 2002, Aronsson *et al.*, 2011). These receptor proteins are responsible for the recognition of nuclear-encoded proteins, which are synthesized in the cytosol and whose final destination is the chloroplast. A third receptor, Toc64, is dynamically associated to the core translocon and was shown to recognize preproteins associated with Hsp90 containing complexes (Sohrt and Soll, 2000; Qbadou *et al.*, 2006 and 2007). Furthermore, it is discussed that chaperones like Hsp70 and Hsp90 and regulatory proteins like 14-3-3 form complexes with freshly synthesized preproteins to guide them to the chloroplast surface and to keep them in an import-competent state (May and Soll, 2000; Fellerer *et al.*, 2011, Flores-Pérez and Jarvis, 2013). Proteins destined for chloroplasts are generally synthesized as precursor proteins, containing an N-terminal targeting sequence. This is first recognized by Toc34 and subsequently by Toc159 which facilitates movement through the Toc75 channel

(Waagemann and Soll, 1995; Bruce, 2000). Toc12 was originally found to form an intermembrane space complex together with Tic22, Toc64 and an Hsp70 chaperone (Becker *et al.*, 2004; Ruprecht *et al.*, 2010), but was recently discovered to represent the closest homolog to the chaperone DnaJ-J8 in *Arabidopsis thaliana* (*A.thaliana*), indicating more likely a stromal localization (Chiu *et al.*, 2010).

Upon reaching the intermembrane space of the organelle, the IE associated protein Tic22 is thought to facilitate the transport of the precursor protein to the TIC complex (Kouranov *et al.*, 1997), where it is translocated through the IE channel Tic110, representing the best characterized component of the TIC translocon, into the stroma of the chloroplast (Inaba *et al.*, 2003 and 2005; Balsera *et al.*, 2009). Another integral membrane component of the TIC translocon is Tic20, which was recently described as a second channel in the IE (Kovács-Bogdán *et al.*, 2011). Tic40, a co-chaperone, is anchored to the IE with its N-terminal domain and exposes its C-terminal part into the stroma, where it interacts with Tic110 and the stromal chaperone Hsp93. The C-terminus of Tic40 was originally found to possess two distinct domains: the TPR (tetratricopeptide) domain of Tic40 is thereby thought to enable the interaction with Tic110, whereas the Sti1 (Hip/Hop-like) domain of Tic40 was shown to enhance the ATPase activity of Hsp93 (Chou *et al.*, 2003). Hsp93 is thought to build the “motor-complex” together with Tic40, providing the energy for protein translocation supplied by ATP hydrolysis. In contrast, recent studies predict two Sti1 (stress inducible protein) domains instead of the TPR domain, which is located in tandem at the C-terminus of the protein (Balsera *et al.*, 2009b). However, the structure and detailed interaction of Tic40 remains to be resolved.

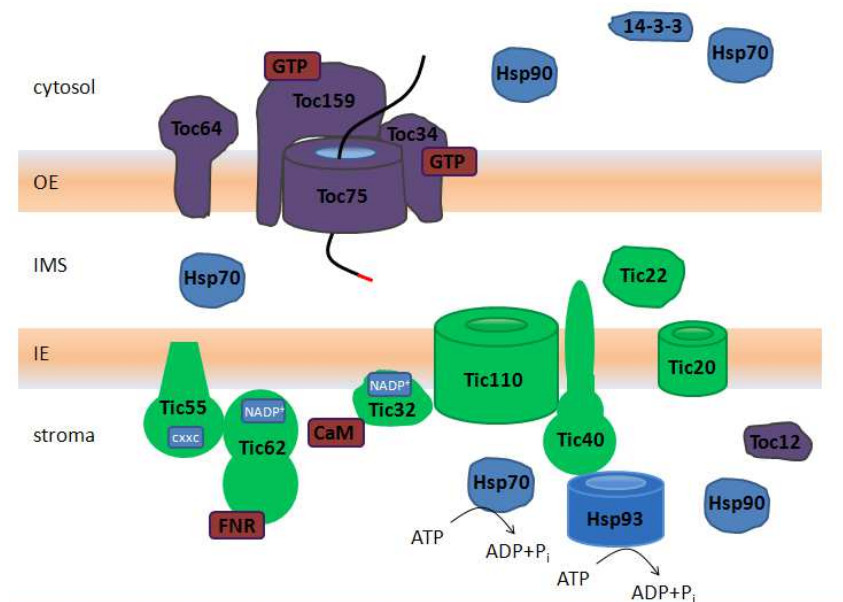


Figure 1 Schematic overview of the translocon at the outer (Toc) and inner (Tic) envelope of chloroplasts

The precursor protein (black line) is translocated from the cytosol to the stroma by the two multiprotein complexes Toc and Tic (see text for details). In the stroma, the N-terminal transit peptide (red line extension at the precursor protein) is cleaved by the stromal processing peptidase and the mature protein can reach its final destination in the chloroplast.

After entering the stroma, the N-terminal transit peptide is cleaved by a stromal processing peptidase (Richter and Lamppa, 1999) and the mature protein is subsequently directed to its final destination in the chloroplast. Thereby, stromal Hsp70 and Hsp93 are thought to provide the energy for this translocation process by ATP hydrolysis as mentioned above (Constan *et al.*, 2004; Su and Li, 2010). Current data propose in addition that stromal Hsp90, which is integrated in a chaperone complex, facilitates preprotein translocation into the stroma (Inoue *et al.*, 2013). At the stromal side of the TIC complex, three proteins build the so called redox-regulon: Tic62, Tic55 and Tic32 are known to react to the chloroplast metabolic redox state by representing targets for regulatory signals, and hence regulate the import rate of at least a subgroup of preproteins accordingly. The two dehydrogenases Tic62 and Tic32 react to the changing redox state of the chloroplast (Chigri *et al.*, 2006; Stengel *et al.*, 2008; Benz *et al.*, 2009), calcium/calmodulin (CaM) signaling takes place by binding CaM to Tic32 (Chigri *et al.*, 2006) and stromal thioredoxin might interact with Tic110 and possibly with Tic55, enabling the tight regulation of cell signals and the protein demand of the chloroplast.

1.2 Tic22 and its evolutionary conservation

Tic22 is a nuclear-encoded protein of the Tic complex and was originally identified together with Tic20 in *P.sativum* by crosslinking the protein to translocating preproteins at an early intermediate stage, when the preprotein has entered the intermembrane space, but had not accessed the stromal compartment (Kouranov *et al.*, 1997). Furthermore, it was shown that Tic22 is peripherally bound to the outer face of the IE, whereas Tic20 is an integral IE protein and that the two proteins associate with other TOC and TIC components (Kouranov *et al.*, 1998). This indicates that Tic22 might function at the same stage of import as Tic20, which was identified by crosslinking to an incoming preprotein (Kouranov *et al.*, 1998; Chen *et al.*, 2002) and later on biochemically determined to possess channel activity in the IE (Kovács-Bogdán *et al.*, 2011). These results along with the interaction with other components of the translocation machinery (Hörmann *et al.*, 2004) led to the suggestion that Tic22 represents a linker for incoming preproteins, forming the connection between outer and inner envelope (Soll and Schleiff, 2004). Tic22 itself is imported into the IMS of chloroplasts via the general import pathway, but the exact mechanism of the translocation to the IMS as well as the detailed function of the protein is still under debate (Kouranov *et al.*, 1999; Vojta *et al.*, 2007). In *A. thaliana*, two Tic22 isoforms – Tic22III (At3g23710), Tic22IV (At4g33350) - have been identified to be components of the Tic translocon. A third protein - Tic22V (At5g62650) – might belong to this family, but is not characterized yet. However, the specified functions of the Tic22 isoforms in *A. thaliana* are almost unknown and, additionally, the correlation between the isoforms in vascular plants and Tic22 in other organisms is an auspicious topic in current science. Thus, the first part of this thesis deals with the characterization of Tic22 in *A. thaliana* by analyzing Tic22III and Tic22IV double knock-out mutants (*tic22dm*), representing the foundation for further research in this topic.

Several studies revealed Tic22 to be an evolutionary conserved protein throughout several organisms, including cyanobacteria (*Anabaena*, *Synechocystis sp.* PCC6803), plants (*A.thaliana*, *Pisum sativum*), green algae (*Clamydomonas reinhardtii*), red algae (*Cyanidioschizon melorae*), cryptomonades (*Guillardia theta*) and parasites such as *Plasmodium falciparum* and *Toxoplasma gondii* (Figure 2). This conservation indicates an important function of the protein for these organisms, which has not been investigated in detail so far. However, it is widely accepted that all plastids evolved by a single endosymbiotic event (Martin and Herrmann, 1998; Lopez-Juez, 2007).

Synechocystis sp. PCC6803 Tic22 (synTic22) was initially found to be localized in the periplasm (Fulda *et al.*, 1999), however in a more recent study it was mainly detected in the thylakoid membrane of cyanobacteria (Fulda *et al.*, 2002). In these studies, synTic22 was supposed to play a role in electron transport at the thylakoid membrane and thus be involved in photosynthetic processes. Moreover, recent data suggest an involvement of synTic22 in membrane biogenesis (PhD thesis Ingo Wolf, LMU Munich), which was also shown for Tic22 of the multicellular cyanobacterium *Anabaena*, where Tic22 was found to interact with the outer membrane biogenesis factor Omp85 *in vitro* and *in vivo* (Tripp *et al.*, 2012). Furthermore, a single putative TIC22 gene was found to be present in *Chlamydomonas reinhardtii*, although it could not be observed in other green algae including *Ostreococcus lucimarinus* and *Ostreococcus tauri* (Robbens *et al.*, 2007; Kalanon and McFadden, 2008), indicating a specific loss in the prasinophyte lineage after the divergence of chlorophytes (Kalanon and McFadden, 2008). With this bioinformatic approach, TIC22 was also found in the genome of the red algae *Cyanidioschizon melorae* and in the moss *Physcomitrella patens*.

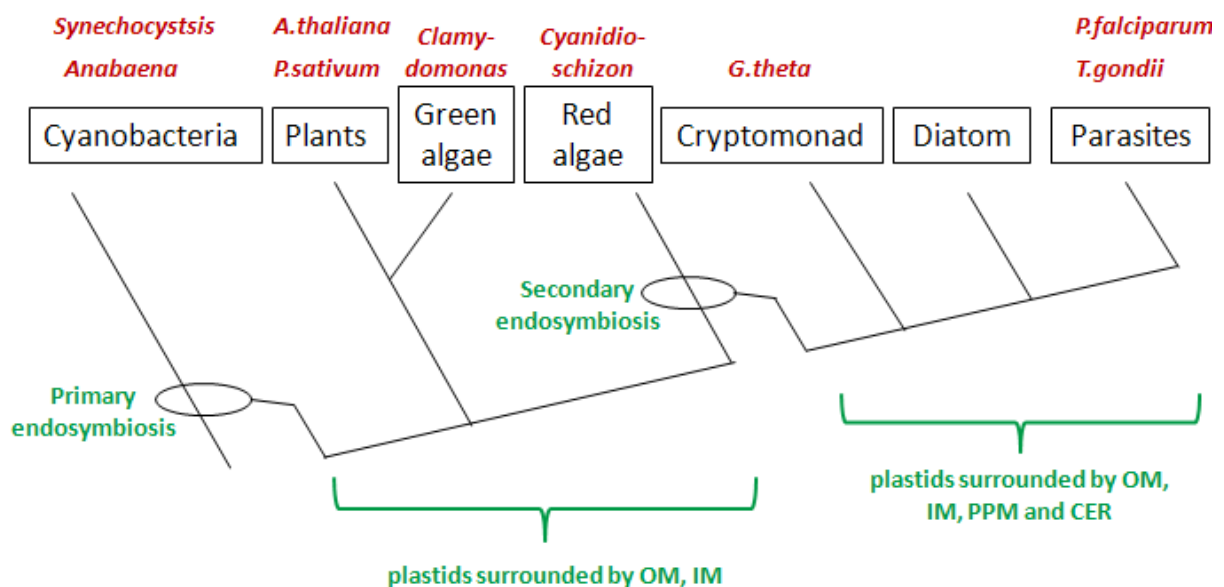


Figure 2 Overview of the organisms comprising Tic22 orthologs (modified from McFadden and van Dooren, 2004)

Tic22 is highly conserved within evolution and found in cyanobacteria, plants, green and red algae, cryptomonads, diatom and parasites. Red letters depict the organisms, which are mentioned in this work. Green letters depict the endosymbiosis events and the resulting membrane systems. Apicoplasts, which evolved during secondary endosymbiosis, are surrounded by four membranes.

1.3 The function of Tic62 and Trol and their interplay with FNR

In plants and cyanobacteria, oxygenic photosynthesis converts absorbed sunlight into chemical energy in terms of ATP and sugars and additionally the reduction equivalent NADPH is generated. The light-induced linear electron transfer (LEF) leading to the generation of ATP and NADPH is carried out by the multiprotein complexes photosystem I and II (PSI and PSII), the cytochrome b_6/f complex (cyt b_6/f) and small electron carriers such as plastoquinone (PQ) and plastocyanin (PC).

At PSI the last step of electron transfer occurs by transferring the electron to ferredoxin and finally to NADP⁺. This reaction is accomplished by the ferredoxin-NADP(H)-oxidoreductase (FNR), a 35 kDa flavoenzyme, which was shown to be one of the key enzymes in photosynthetic processes. Both, ATP and NADPH, are used in the Calvin-Benson cycle in the stroma and in further metabolic processes (see below).

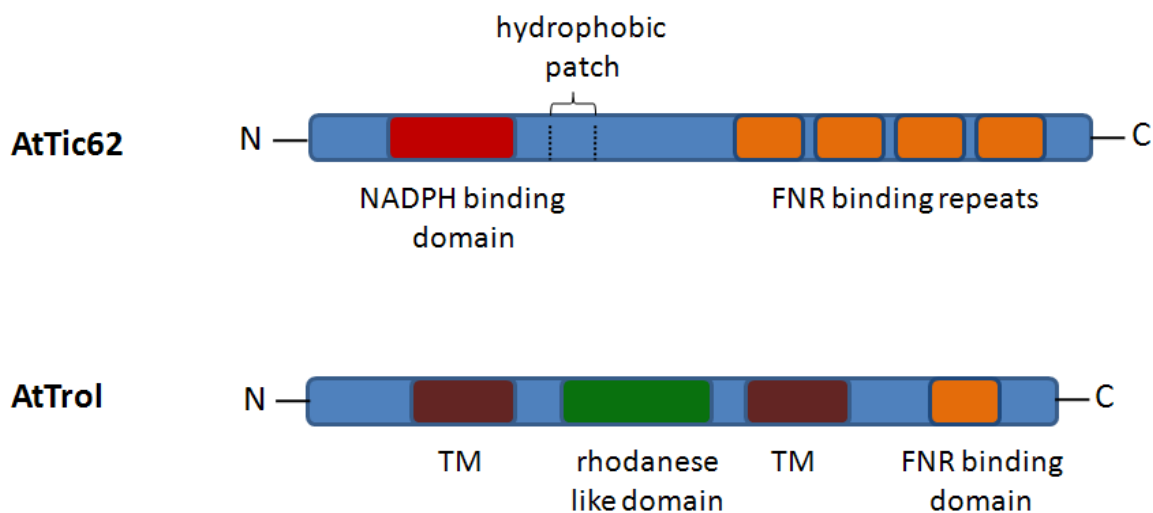


Figure 3 Schematic description of the functional domains of AtTic62 (according to Benz *et al.*, 2009) and Trol (according to Juric *et al.*, 2009)

The N-terminal part of AtTic62 comprises the dehydrogenase domain (red) and a hydrophobic patch, which is thought to mediate membrane attachment. The C-terminal part of AtTic62 possesses a series of Ser/Pro rich repeats (orange), mediating the interaction with FNR. The mature protein Trol contains two transmembrane domains (brown), which span the thylakoid membrane. In between these domains, Trol possesses a potentially inactive rhodanese-like domain due to an exchange from cysteine to aspartate. The C-terminus comprises one Ser/Pro rich motif, mediating binding to FNR.

So far, two proteins have been described to function in FNR binding to the membrane (Figure 3): first the Tic translocon component Tic62 is thought to be responsible for the storage of the FNR at the thylakoids, probably displaying a regulation system during the day/night cycle. Tic62 is encoded by a single copy gene in *A.thaliana* (At3g18890) and has originally been characterized as a so-called redox sensor protein due to its dehydrogenase activity. Furthermore, it was found to shuttle between IE, stroma and thylakoid membrane

dependent on metabolic $\text{NADP}^+/\text{NADPH}$ ratio and the specific interaction with FNR is also dependent on the redox state (Küchler *et al.*, 2002; Stengel *et al.*, 2008). Reducing conditions lead to a favored soluble localization in the stroma and binding to FNR, whereas oxidized conditions cause an attachment to the IE and the thylakoid membrane. The interaction of Tic62 with FNR is mediated by the C-terminal region, which is only found in vascular plants (Balsera *et al.*, 2007). Additionally, the N-terminal part of Tic62, which has approximately the same size as the C-terminus, contains the NADPH binding domain as well as a hydrophobic patch, which is thought to enable the reversible membrane binding and thus the shuttling of the protein. In contrast to the C-terminus, the N-terminal part of Tic62 is highly conserved in all oxyphototrophic organisms as paralogs are even found in green sulfur bacteria (Balsera *et al.*, 2007).

Second, similar aspects were found for the thylakoid rhodanese-like protein Trol which has been found to be anchored within the thylakoid membrane and to represent a docking station for FNR at the membrane. The C-terminus of Trol comprises a highly conserved sequence motif (KPPSSP), which was shown to possess a high affinity to FNR. This domain was shown to be necessary for high-affinity interaction between Tic62 and FNR, suggesting that both Tic62 and Trol possess similar properties in binding FNR (Balsera *et al.*, 2007; Benz *et al.*, 2009; Juric *et al.*, 2009).

1.4 Metabolic processes connected to photosynthesis

NADPH and ATP that are generated in photosynthetic light reactions are used in several metabolic processes in the chloroplast and in the cytosol. The majority of reduction equivalents NADPH and ATP are required in the Calvin Benson cycle reactions, in order to fix CO_2 and to reduce sugars for further metabolic pathways. Thereby, the reduction of 3-phosphoglycerate (PGA) to glyceraldehyde 3-phosphate (G3P) serves as the initial point for the production of hexose phosphates, representing the precursors for the production of sucrose and starch (reviewed in Zeeman *et al.*, 2007 and 2010). The key step during starch synthesis involves the enzyme ADP-glucose pyrophosphorylase (AGPase), catalyzing the conversion of glucose-1-phosphate to ADP-glucose by using ATP as an energy source. ADP-glucose subsequently provides the glucosyl group to the non-reducing end of a starch molecule, which serves as the major storage form of chemical energy in plants. Moreover, the AGPase was found to be one of the targets, reduced and thereby activated by thioredoxin (Trx). Trxs are small molecules containing a conserved amino acid sequence

(WCG/PPC), which is known to possess a thiol-disulfide oxidoreductase activity. Due to their low redox potential, Trxs comprise strong reductive activities (reviewed in Gelhaye *et al.*, 2005). In chloroplast, Trxs are known to regulate numerous metabolic pathways including Calvin-Benson cycle, fatty acid biosynthesis, nitrogen and sulfur metabolism and starch biosynthesis (for reviews see Buchanan and Balmer, 2005; Lindahl and Kieselbach, 2009). They obtain their reductive activity by electron uptake of ferredoxin, catalyzed by the ferredoxin-thioredoxin-reductase (FTR) in the stroma of chloroplasts and the NADPH-thioredoxin-reductase (NTR) in the cytosol. In the chloroplast, FTR transfers electrons from ferredoxin to thioredoxin, which then activates enzymes like AGPase by reducing their disulfide bridges. Another Trx target, NADP malate dehydrogenase (NADP-MDH) is used to generate malate, which is transported into the cytosol via an oxalacetate-malate-transporter (OMT), representing the connection between redox signals in the plastid and the surrounding cell, known as the malate valve of chloroplasts (Scheibe, 2004; Hebbelmann *et al.*, 2012). NADP-MDH catalyzes the conversion of oxalacetate to malate consuming NADPH, thus re-generating the electron acceptor NADP^+ , especially under conditions when CO_2 assimilation is restricted. However, knock-out mutants lacking NADP-MDH exhibit WT-appearance even under high-light conditions, indicating the involvement of compensatory strategies to protect the plants from oxidative stress (Hebbelmann *et al.*, 2012). The reduction equivalents are furthermore required for several other metabolic pathways, including reactions where enzymes are activated by Trx. Thus, the regulation by the FNR and FTR systems displays a well arranged interplay between photosynthetic light reactions and metabolic pathways, which is a promising topic in understanding the fascinating adaptability of the plant to environmental changes.

1.5 Aims of this work

Most of the components of the TIC translocon have been described extensively in numerous studies, but the exact function of Tic22, which is thought to represent the connection between the TOC and the TIC translocon during the import of nuclear-encoded preproteins, is largely unknown. Hence, the first part of the study deals with the functional and structural characterization of Tic22 in *A.thaliana*. Moreover, the evolutionary conservation of Tic22 suggests an important function of the protein within numerous organisms. This function was investigated by analyzing Tic22 double knock-mutants with regard to their phenotype, nuclear and plastidic gene expression and preprotein import behavior in *A.thaliana*. Furthermore, as structural features of proteins can provide further indications for functional properties, this study contains crystallization trials of Tic22.

In the second part of this work, two strategies have been chosen to characterize the interaction of Tic62 and Trol with FNR, in order to clarify the importance of tethering this photosynthetic key enzyme to the thylakoid membrane. On the one hand, biochemical approaches were carried out to investigate the functional relation of Tic62 and Trol with FNR. On the other hand, metabolic contents were analyzed to shed light on the link of photosynthetic processes with the activity and localization of FNR as well as with the metabolism in the chloroplast.

Since FNR was found to be photosynthetically active in the stroma and not necessarily in the membrane-bound state, the function of this FNR-binding to the thylakoids remains to be investigated. Moreover, it is conceivable that FNR might be involved in further redox processes and that the knock-out of both binding partners at the thylakoids might lead to changes in metabolic pathways, thus potentially influencing the electron transport during light reactions in photosynthesis.

2 Material

2.1 Chemicals

All chemicals used in this work were purchased from Applichem (Darmstadt, Germany), Fluka (Buchs, Switzerland), Biomol (Hamburg, Germany), Difco (Detroit, USA), Sigma-Aldrich (Steinheim, Germany), GibcoBRL (Paisley, UK), Merck (Darmstadt, Germany), Roth (Karlsruhe, Germany), Roche (Penzberg, Germany) und Serva (Heidelberg, Germany).

Radiolabeled amino acids ($[^{35}\text{S Met}]$) were obtained from DuPont-NEN (Dreieich, Germany).

2.2 Enzymes

Restriction enzymes were obtained from MBI Fermentas (St. Leon-Rot, Germany), New England Biolabs GmbH (Frankfurt am Main, Germany). T4-ligase was purchased from MBI Fermentas (St. Leon-Rot, Germany) and Invitrogen (Karlsruhe, Germany). Taq Polymerase was obtained from Diagonal (Münster, Germany), Eppendorf, MBI Fermentas, Clontech (Saint-Germainen-Laye, France), Finnzymes (Espoo, Finland) and Bioron (Ludwigshafen am Rhein, Germany). Reverse transcriptase was obtained from Promega (Madison, USA), RNase free DNase I from Roche (Mannheim, Germany) and RNase from GEHealthcare (Uppsala, Sweden). Cellulase R10 and Macerozyme R10 for digestion of the plant cell wall were from Yakult (Tokyo, Japan) and Serva (Heidelberg, Germany).

2.3 Oligonucleotides

Oligonucleotides were ordered from Metabion (Martinsried, Germany) in standard desalted quality. They were used for cloning, genotyping mutant lines and for Real-Time RT PCR (Table 1).

Table 1: Oligonucleotides used in this work

Name	Sequence (5'-3' orientation)	Application
At Tic62 Ex5 fwd NS	ATATGCTGTATTGGTGCTAGCGAGAAAG	Genotyping mutant lines
At Tic62 Ex8 rev NS	AGTCGGTCTCTCCATTCTCCAGGTC	Genotyping mutant lines
LB1	GCCTTTTCAGAAATGGATAAATAGCCTTGCTTCC	Genotyping SAIL mutant lines
LBb1	GCGTGGACCGCTTGCTGCAACT	Genotyping SALK mutant lines
mTic22 IV fwd BglII NEU	GATCAGATCTTAGTCGCTAAAGCTCTCG	Cloning in pRSetA for overexpression
mTic22 IV rev NcoI	GATCCCATGGTTACTCTTTGATCAAATCC	Cloning in pRSetA for overexpression
mTic22 pea fwd SacII	GATCCCGCGGTGGTAACACGTCGC	Cloning in pHUE
mTic22 pea rev HindIII	GATCAAGCTTTTAAAGCAATAACTTCTTGC	Cloning in pHUE
peaTic22 EcoRI fwd	GATCGAATTCATGGAGTCTCAGG	Cloning in pET21b
peaTic22 HindIII rev	GATCAAGCTTAGCAATAACTTC	Cloning in pET21b
pOpOff seq fw	CTCAACTTTTATCTTCTCTGCTTACAC	Genotyping RNAi constructs
pOpOff seq rev	GGGTTTCGAAATCGATAAGCTTGCGC	Genotyping RNAi constructs
popOff-INT seq fw	TGAGCTTTGATCTTTCTTTAAACTG	Genotyping RNAi constructs
popOff-INT seq rev	TGTTAGAAATCCAATCTGCTTGTA	Genotyping RNAi constructs

RB1 pROK	GGGTAACCTAAGAGAAAAGAGCG	Genotyping SALK mutant lines
syn Tic22 rev HindIII	GATCAAGCTTTTACTTAGGTTGTTGGG	Cloning in pRSetA
synTic22 fwd BamHI	GATCGGATCCATGAAATCCTTACTCC	Cloning in pRSetA
synTic22 fwd SacII	GATCCCCGGTGGTATGAAATCCTTAC	Cloning in pHUE
synTic22 rev HindIII	GATCAAGCTTTTACTTAGGTTGTTGGGC	Cloning in pHUE
synTic22 Üex EcoRI rev +GC	CGCCCAACAACCTAAGGCGAATTCGATC	Cloning in pET21b
synTic22 Üex Nde fwd	GATCCATATGTTGCCACCGAAGAGG	Cloning in pET21b
T7 Terminator long	GCTAGTTATTGCTCAGCGG	Genotyping T7 vectors
T-DNA GABI (#361)	GGACGTGAATGTAGACACGTCG	Genotyping GABI mutant lines
Tic22 III fwd ATG	ATGAATTCAAACATTTTCCACCATC	Genotyping mutant lines
Tic22 III fwd Pos. 216	AGAATCTCTCGATTCAATTCTGGTAAGG	Genotyping mutant lines
Tic22 III rev Pos 501	CTTTTGAACCTTCTTTCTCATACGAGG	Genotyping mutant lines
Tic22 IV for ATG	ATGGAGTCATCAGTGAACCCAATCC	Genotyping mutant lines
Tic22 IV fwd Pos 811	GAAAACAGAGCAAACCGATAGACT	Genotyping mutant lines
Tic22 IV rev Ex3	GGAAATCCCTTCAACTTTTAGCAAGT	Genotyping mutant lines
Tic22 IV rev Pos 802	CAAACCGATAGACTTGCTCCGG	Genotyping mutant lines
Tic22III 387C03 rev_NEU	CCAACACAAACTCCTCATTCTG	Genotyping mutant lines
Tic22III for	CTATGAATTCAAACATTTTCCAC	Genotyping mutant lines
Tic22V Ex 6 fwd	GCAACGACGACGGGATGTTGTTGAC	Genotyping mutant lines
Tic22V Ex 8 rev	CTCCTGTTGAAATCCCTACCATTGTTATC	Genotyping mutant lines
Tic22V fwd BamH1	GATCGGATCCATGGGTTCCGCCGGA	Cloning in pSP65
Tic22V fwd SacI	GATCGAGCTCATGGGTTCCGCCGATAAGC	Cloning in pSP65
Tic22V rev HindIIIneu	GATCAAGCTTTTACTGGTCATCACCTCTAC	Cloning in pSP65
Tic22V RNAi fwd	CACCATGGGTTCCGCCGATAAGCAAC	Cloning in pENTRY (final: pOpoff)
Tic22V RNAi rev	CACAGGGCCATTCTCTCGCTCTTAG	Cloning in pENTRY (final: pOpoff)
Tic22VrevEcoRI900bpstop	GATCGAATTCCTATTCTTGAACCTCTGG	Cloning in pSP65
Trol Ex7 fwd NS	AATAGGAAAGGCTCTTCTCTCAATC	Genotyping mutant lines
Trol Ex8 rev NS	GGCTGCGATGGCATCGGAGAAGAT	Genotyping mutant lines
Trol fwd Finland	GAAGCTCTGAAAACCGCAAC	Genotyping mutant lines
Trol rev Finland	CAGGGATTTAGCAGGAGCTG	Genotyping mutant lines
TROL_3'UTR_rev	GTCCACTTATCTCAGATTCTG	Genotyping mutant lines
TROL_Ex7_fwd	CAGTTGCAGCTACAACAACC	Genotyping mutant lines
Trol LC fwd	CTGAGGACCGAAAGCA	Real-time PCR
Trol LC rev	GCAATCGGAGAAGATGG	Real-time PCR
Tic62 LC fwd	GGAGTGTGACTTGGAGAA	Real-time PCR
Tic62 LC rev	GCAAGAGTGAGATTATGAGTT	Real-time PCR
Tic22 III fwd	AACATTTTCCCAACATCG	Real-time PCR
Tic22 III rev	GGAAGTCCCTGAAACCAA	Real-time PCR
Tic22 IV fwd	AGTGTACCCGCTTCAG	Real-time PCR
Tic22 IV rev	GTAATGGGAACAACCTTCG	Real-time PCR
Tic22 V fwd	CGGGATGTTGTTGACG	Real-time PCR
Tic22 V rev	CTCTAAGTAGTGATGCGG	Real-time PCR
Tic22 V fwd neu	TGAAGAGAGAGATCCTCTATTG	Real-time PCR
Tic22 V rev neu	CTATTGAGAGCATGGGTG	Real-time PCR
pSSU fwd	CGGATTCGACAACACC	Real-time PCR
pSSU rev	TTGTAGCCGCATTGTC	Real-time PCR
NDPK2 fwd	GCCGAATCGGGAATCT	Real-time PCR
NDPK2 rev	GCTGTCACTACCATGC	Real-time PCR
OE17 fwd	GCCAAGCTCGGTTAAT	Real-time PCR
OE17 rev	TGATCACGAAGTTGGTGT	Real-time PCR
OE23 fwd	AAGGGAGCCAGGAAAT	Real-time PCR
OE23 rev	CTATAGCTTCTTTCTGAGTCAAT	Real-time PCR
OE33 fwd	GACAAAGAGCAAGCCG	Real-time PCR
OE33 rev	TTTACGATGAAGGACATGG	Real-time PCR
NDPK2 fwd neu	TACATGGCTAAGGGAGTGA	Real-time PCR
NDPK2 rev neu	CGTAGAACCAAATGCAGAT	Real-time PCR
NDH H fwd	AGTACGACTTAGCGAAATG	Real-time PCR
NDH H rev	TGCTACCGAGTATCGTCA	Real-time PCR
ATP A fwd	TATAGGACGCGCCAG	Real-time PCR
ATP A rev	AGGCAGTCATACTCCC	Real-time PCR
PSA A fwd	AGGAAACTTTGCACAGAG	Real-time PCR
PSA A rev	CCTACAGCACGTCCTT	Real-time PCR

PSB E fwd	ATGTCTGGAAGCACAGG	Real-time PCR
PSB E rev	TCGAGTTGTTCCAAAGG	Real-time PCR
RPL 20 fwd	GAGGCGTAGAACAAAAC	Real-time PCR
RPL 20 rev	CGAAATTGTATAAAGACAACCTCC	Real-time PCR
RPS 15 fwd	GAACAAAAGAAGAAAGCAGG	Real-time PCR
RPS 15 rev	ATTCCCGAATATTCAACTGAT	Real-time PCR
PSA C fwd	TACTCAATGTGTCCGAGC	Real-time PCR
PSA C rev	CTAGACCCATACTTCGAGTT	Real-time PCR
ACC 2 fwd	ACACAGAAACTGCTGAAT	Real-time PCR
ACC 2 rev	AGGAAGCCGTTCAAATC	Real-time PCR
NAD 4 fwd	TAGTGAGCACCATGCC	Real-time PCR
NAD 4 rev	CATCCGAACGAGTCCA	Real-time PCR

2.4 Vectors and constructs

All plasmid vectors used in this work are listed in table 2.

Table 2: Plasmid vectors used in this work

Plasmid vector	Application	Origin
pCR blunt	Subcloning, sequencing	Invitrogen
pENTR/D/TOPO	Entry vector for GATEWAY recombination	Invitrogen
pET14b	protein overexpression	Novagene, Merck
pET15b	protein overexpression	Novagene, Merck
pET21b	protein overexpression	Novagene, Merck
pET21d	protein overexpression	Novagene, Merck
pF3A	Entry vector	Promega
pGex-6-p1	protein overexpression	AG Wolf/MPI Martinsried
pHUE	protein overexpression	AG Wolf/MPI Martinsried
pOpOff	inducible RNAi vector	Wielopolska <i>et al.</i> , 2005
pRSetA	protein overexpression	Invitrogen
pSP65	translation vector	Promega

All constructs generated and used in this work can be found in table 3.

Table 3: Constructs used in this work

Gene	Plasmid vector	Application
mTic22 IV	pRSetA	Overexpression
mTic22 IV	pRSetA	Overexpression
mTic22 pea	pRSetA	Overexpression
mTic22 pea	pHUE	Overexpression
mTic22IV	pRSetA	Overexpression
mTic22pea	pGex-6-p1	Overexpression
mTic22syn	pET21a	Overexpression
peaTic22	pET21b	Overexpression
pTic22 IV	pCR blunt	Subcloning
synTic22	pRSetA	Overexpression
synTic22	pHUE	Overexpression
synTic22	pET14b	Overexpression
synTic22	pET21b	Overexpression
Tic22V 429bp	pENTRY	Subcloning
Tic22V 429bp	pOpOff	Inducible RNAi
Tic22V 900bp	pSP65	Translation for import assay
Trol -R+F	pET21d	Overexpression
Usp2	pET15b	Overexpression

2.5 Molecular weight markers and DNA standards

*Pst*I digested λ -Phage DNA (MBI Fermentas) was used as a molecular size marker for agarose gel electrophoresis.

For SDS-PAGE analysis the Low Molecular Weight Marker composed of Lactalbumin (14 kDa), Trypsin-Inhibitor (20 kDa), Trypsinogen (24 kDa), Carboanhydrase (29 kDa), Glyceraldehyd-3-Dehydrogenase (36 kDa), Ovalbumin (45 kDa) and Bovine Serum Albumin (66 kDa) from Sigma-Aldrich was used. The peqGOLD Protein Marker II from Peqlab was applied as well.

2.6 Antibodies

All antibodies used in this work were already available in the lab.

2.7 Strains

Cloning in *Escherichia coli* was performed using the following strains: DH5- α (Invitrogen, Karlsruhe, Germany) and TOP10 (Invitrogen). The strain BL21 (DE3) (Novagen/Merck, Darmstadt, Germany) was used for heterologous expression of proteins. The *Agrobacterium tumefaciens* GV3101::pMK90RK (Koncz and Schell, 1986) strain used for stabile transformation of *A. thaliana* was a kind gift of Dr. J. Meurer (Dept. Biologie I, Botany, LMU Munich).

2.8 Plant material

All experiments were performed on *A. thaliana* plants, ecotype Col-0 (Columbia 0 Lehle seeds, Round Rock, USA).

The T-DNA insertion lines used in this work were: GABI_387C03 (Tic22III, At3g23710), GABI_810F06 (Tic22IV, At4g33350), SALK_106217 (Tic22V, At5g62650), SAIL_124G04 (Tic62, At3g18890) and SAIL_27_B04 (Trol, At4g01050). All lines were purchased from NASC (University of Nottingham, UK) and GABI-KAT (MPI for Plant Breeding Research, Cologne, Germany).

Peas (*Pisum sativum*) var. "Arvica" were ordered from Bayerische Futtersaatbau (Ismaning, Germany).

3 Methods

3.1 Plant methods

3.1.1 Growth of *A. thaliana*

Seeds of *A. thaliana* were sown on MS media (0.215% MS, 0.05% (2-(N-morpholino) ethanesulfonic acid) MES, 0.3% gelrite (pH 5.8 with KOH), (Murashige and Skoog, 1962) or directly on soil. Before sowing on sterile media, the seeds were surface sterilized in 70% Ethanol containing 0,05% Triton X-100 for 10 minutes followed by five washing steps with 100% Ethanol. To synchronize germination the seeds were vernalized at +4°C in the dark for 24 hours. For selection of transformed plants, the seeds were grown on MS media containing the adequate antibiotic (25 µg/ml hygromycin, 100 µg/ml kanamycin). To induce RNAi expression, 10 µM dexamethason was added to the media, and the plants were transferred to soil after 2 to 3 weeks. In order to maintain the RNAi expression, the relevant plants were watered continuously with 10 µM dexamethason until the seeds could be harvested. Plants were grown in a 16 h light (+21°C; 100 µmol photons m⁻² s⁻¹) and 8 h dark (+16°C) cycle (long-day). Unit µmol photons m⁻² s⁻¹ \triangleq µmol in this work.

3.1.2 Cross fertilization of *A. thaliana*

For generating double mutants (Δ tic22IIIxIV and Δ tic62xtrol), both homozygous T-DNA insertion lines were crossed respectively (Table 4). For this purpose, flowers from the female parent were used before the anther dehiscence. For each flower the sepals, petals and each anther were removed leaving the carpel intact. For the male parent, flowers were chosen where pollen were visibly released. These flowers were removed and squeezed anthers separated. The convex surface of the anthers was brushed against the stigmatic surface of the exposed carpels on the female parent. The elongated siliques resulting from the crossing procedure were harvested after 2-3 weeks and dried at room temperature for 2 weeks before planting (Detlef and Glazebrook, 2002).

Table 4: Generating of double mutants

Name double mutant	Gene	T-DNA line
Δ tic22IIIxIV	Tic22 III (At3g23710)	GABI_387C03
	Tic22 IV (At4g33350)	GABI_810F06
Δ tic62xtrol	Tic62 (At3g18890)	SAIL_124G04
	Trol (At4g01050)	SAIL_27_B04

3.1.3 Stable transformation of *A. thaliana*

The stable transformation of *A. thaliana* plants was performed as published by Bechtold *et al.*, (1993). Three days before plant transformation, 10 ml of an *Agrobacterium tumefaciens* suspension harbouring the appropriate vector including the construct to be transformed was incubated in LB media at +28°C and 180 rpm. After two days, 500 ml of LB media (1% peptone, 0.5% yeast extract, 1% NaCl) were inoculated with 5 ml *Agrobacterium* culture and allowed to grow for one day under continuous shaking at +28°C. For transformation, the bacteria were harvested (6.000 x g, 10 min) and the pellet was resuspended in 400 ml infiltration medium (5% (w/v) sucrose, 0.215% MS, 0.05% (v/v) Silwet L-77). To prepare the plants for transformation, already formed siliques were removed and the plants were covered with a plastic bag to allow a maximum opening of the stomata one day before transformation. The plants were transformed by dipping them upside down into the infiltration media (Clough *et al.*, 1998). After the transformation, the plants were allowed to recover lying on a humid paper, and covered again with a plastic bag until the next day when they were rinsed with water and erected. The T1 seeds from the transformed plants were harvested and selected on MS media supplied with the appropriate antibiotics.

3.1.4 Chlorophyll fluorescence measurements of PSII

In vivo chlorophyll a fluorescence of single leaves was measured using a PAM 101/103 fluorometer (Walz, Effeltrich, Germany). Plants were dark adapted for 15 minutes and minimal fluorescence (F_0) was measured. Then pulses (0.8 sec) of saturating white light ($5000 \mu\text{mol photons m}^{-2} \text{s}^{-1}$) were applied to determine maximal fluorescence (F_m) and calculate the ration $F_v/F_m = (F_m - F_0)/F_m$ (max. quantum yield of PSII). Plants were illuminated with actinic light ($90 \mu\text{mol photons m}^{-2} \text{s}^{-1}$) and steady state fluorescence was measured (F_s). Supplying a further saturating light pulse resulted in the maximal fluorescence in the light (F_m') and the effective quantum yield pf PSII was calculated as $(F_m' - F_s)/F_m'$.

3.2 Microbiological methods

3.2.1 Media and growth

E. coli was cultivated in LB media (1% peptone, 0.5% yeast extract, 1% NaCl and if necessary 1.5% agar) at +37°C in either liquid culture or on agar plates supplemented with the appropriate antibiotics (ampicillin 100 $\mu\text{g/ml}$, kanamycin 50 $\mu\text{g/ml}$, streptomycin 50 $\mu\text{g/ml}$

and spectinomycin 100 µg/ml).

Agrobacterium was cultivated in LB media (liquid as well as on plates), at +28°C, supplemented with the appropriate antibiotics according to the resistance of the respective strain (50 µg/ml kanamycin (resistance strain GV3101), 100 µg/ml rifampicin (resistance Ti-plasmid)), and the resistance of the transformed vector.

3.2.2 Bacteria transformation

The preparation of chemical competent cells for transformation was carried out according to the protocol of Hanahan (1983). The transformation of the bacteria was performed using the heat shock method (Sambrook *et al.*, 1989).

For the preparation of competent *Agrobacterium* cells, 10 ml of liquid media supplied with the adequate antibiotic were inoculated with a single colony and incubated over night under continuous shaking at +28°C. The cells were harvested in 1 ml aliquots by centrifugation (5 min, 6.000 x g, +4°C), and the pellet was resuspended in 100 µl CaCl₂ (10 mM) at +4°C and centrifuged again (5 min, 6.000 x g at +4°C). Upon resuspending the pellet in 50 µl CaCl₂ (10 mM) at +4°C, it was snap frozen in liquid nitrogen. The competent cells were stored at -80°C before use. For transformation of the cells, 0.5 µg of DNA plasmid was carefully mixed with 50 µl of competent cells and snap frozen for 1 min in liquid nitrogen. Afterwards, the cells were incubated at +37°C for 5 min and chilled down on ice. After the addition of 400 µl LB media or SOC media (2% trypton, 0.5% yeast extract, 10 mM NaCl, 2.5 mM KCl, 10 mM MgCl₂, 10 mM MgSO₄, 20 mM glucose) cells were shaken for 2-4 h at +28°C. After centrifugation for 10 s at 16.000 x g, the pellet was resuspended in a minimal amount of media and spread on LB plates supplied with the appropriate antibiotics and incubated for 2 to 3 days at +28°C. The uptake of DNA was tested by colony PCR.

3.3 Molecular biology methods

3.3.1 Polymerase Chain reaction

DNA fragments for cloning into vectors and genotyping of plant mutant lines were amplified using Polymerase Chain Reaction (PCR) (Saiki *et al.*, 1988). The protocol was applied according to the manufacturer's recommendations. The BioTherm *Taq*-Polymerase (Diagonal), (Bioron) and the Tripel Master *Taq*-polymerase (Eppendorf) were used for PCR-genotyping. The *Phusion*-Polymerase (Finnzymes) was utilized in case of cloning a fragment into a destination vector.

3.3.2 Cloning strategies

General molecular biological methods like restriction digestion of vectors, DNA ligation, determination of DNA concentrations and agarose gel electrophoresis were performed as described in Sambrook *et al.*, (1989) as well as according to the manufacturer's instructions. For purification of DNA fragments from agarose gels or directly after PCR amplification the "Nucleospin Extract II Kit" from Macherey and Nagel (Düren, Germany) was used. LR-recombination using the GATEWAY system (Invitrogen) was performed according to the manufacturer's recommendations. The LR recombination reaction for the inducible pOpOff vector was incubated over night at 25°C.

3.3.3 Isolation of DNA plasmids from *Escherichia coli*

DNA plasmid preparation from transformed *E. coli* cells was performed by alkaline lysis with SDS and NaOH from 3-5 ml overnight cultures according to the protocol from Zhou *et al.*, (1990). For high yield DNA purification, the Nucleobond AX Plasmid Purification Midi („AX 100“) und Maxi („AX 500“) kits from Macherey and Nagel (Düren, Germany) according to the manufacture's recommendations were used.

3.3.4 Preparation of genomic DNA of *A. thaliana*

For genotyping of T-DNA insertion lines the following protocol was applied: 2-3 *A. thaliana* rosette leaves were supplied with 450 µl of extraction buffer (0.2 M Tris-HCl (pH 7.5), 0.25 M NaCl, 25 mM EDTA, 0.5% SDS, 100 µg/ml RNase) and disrupted using the Tissue Lyser from Retsch/Qiagen for 3 min. Afterwards, the samples were incubated at +37°C for 10 min and centrifuged for 10 min at 16.000 x g. The DNA present in the clear supernatant was precipitated with 300 µl of isopropanol for 5 min. After 5 min centrifugation at 16.000 x g at +4°C, the pellet was washed with 70% ethanol and resuspended in 50 µl H₂O. For one PCR reaction (25 µl), 1 µl of DNA was used.

3.3.5 Determination of DNA and RNA concentrations

The concentration of DNA and RNA was measured. For this purpose, the absorption of a diluted sample at 260 nm, 280 nm and 320 nm was determined and the concentration was calculated according to the following equations:

$$\text{DNA: } c [\mu\text{g}/\mu\text{l}] = (E_{260/280} - E_{320}) \times 0,05 \times f_{\text{dil}}$$

$$\text{RNA: } c [\mu\text{g}/\mu\text{l}] = (E_{260/280} - E_{320}) \times 0,04 \times f_{\text{dil}}$$

E denotes absorption of the sample at the given wavelength and f_{dil} denotes the dilution factor of the sample. Additionally, the absorption at 280 nm was measured as an indication of protein contamination. In pure nucleic acids, the relation E260/E280 corresponds to 1.8-2.

3.3.6 Characterization of plant T-DNA insertion lines

T-DNA insertion lines were genotyped by PCR analysis (see chapter 3.3.1). To identify mutants with the T-DNA insertion in both alleles (homozygous), a combination of gene-specific primers flanking the predicted T-DNA insertion sites and T-DNA-specific primers were used. Amplification using a T-DNA specific primer (LB or RB) in combination with a specific gene primer will only generate an amplification product in heterozygous and homozygous plants. On the other hand, amplification with only gene specific primers flanking the T-DNA insertion site will only generate an amplification product in wild-type and heterozygous plants under the PCR conditions applied. The combination of these two PCR results allows a clear discrimination between wild-type, heterozygous and homozygous plants for the T-DNA insertion (Table 1).

3.3.7 DNA sequencing

DNA sequencing was performed by the sequencing service of the Faculty of Biology, Genetics, Ludwig-Maximilians-Universität Munich.

3.3.8 RNA extraction and Real-Time RT-PCR (qRT-PCR)

Total RNA from *A. thaliana* and pea plants was isolated using the Plant RNeasy Extraction kit (Qiagen, Hilden, Germany). The residual DNA was digested with RNase-free DNase I (Qiagen) and the RNA was reverse transcribed into cDNA using MMLV Reverse transcriptase (Promega, Mannheim). For that purpose, a final volume of 10 μ l composed of 0.5-1.0 μ g RNA, 4 μ M oligo-dT-Primer, 0.5 mM dNTP and 2 units of MMLV was incubated at +42°C for 1.5 h (adapted from Clausen *et al.*, 2004). RNA extraction of small amounts of plant pieces (less than 5mg) was performed with the RNeasy Extraction micro kit (Qiagen, Hilden, Germany) and the following cDNA transcription was performed with the Omniscript RT Kit (Qiagen, Hilden, Germany) following manufacturer's instructions.

The resulting cDNA was diluted 1:20 and the Real-Time PCR was performed using the FastStart DNA Master SYBR-Green Plus Kit (Roche, Penzberg) according to the manufacturer's recommendations. The detection and quantification of transcripts were

performed using the LightCycler system (Roche, Penzberg). A total of 40 cycles composed of 1 s at +95°C (denaturation), 7 s at +49°C (annealing), 19 s at +72°C (elongation) and 5 s at +79°C (detection) were realized. The gene specific mRNA content was normalized to appropriate housekeeping gene molecules (18S, Actin). The relative amount of RNA was calculated using the following equation:

Relative amount of cDNA = $2^{[n(\text{housekeeping gene}) - n(\text{Gen})]}$ with n=threshold cycle of the respective PCR product.

3.3.9 Microarray analysis

60-75 mg plant powder of 14 days old WT Col-0, *tic22IV* single mutant plants and *tic22dm* plants were used for RNA isolation. RNA (200 ng) of four individual samples per plant line (n=4) was labelled using the “3’ IVT Express” kit (Affymetrix UK, High Wycombe, UK) and hybridized to Affymetrix “GeneChip *Arabidopsis* ATH1 Genome Arrays” according to manufacturer’s instructions. The statistical significance of gene regulation was calculated as described in Duy *et al.* (2011). The hybridization of the microarrays and statistical analysis of the data was performed by Karl Mayer and Dr. Katrin Philippar (Department Biologie I, Plant Biochemistry and Physiology, LMU Munich).

3.4 Biochemical methods

3.4.1 Determination of protein concentration

The protein concentration of the samples was determined with the Bradford (Bradford, 1976) (Bio-Rad Protein Assay, Bio-Rad, München, Germany) or-, BCA (bicinchoninic acid) method (Pierce BCA Protein Assay Kit, Thermo Scientific, Rockford, USA), or alternatively using the Nanophotometer (Implen, Munich, Germany).

3.4.2 Protein extraction of *A. thaliana*

For the protein extraction, plant leaves were harvested, placed immediately in liquid nitrogen and grounded thoroughly with a mortar and a pestle or directly mixed in the extraction buffer (50 mM Tris-HCl, (pH 8), 2% LDS (Lithium dodecyl sulphate), 0.1 mM PMSF) using the electro pistil. The powder was mixed with one sample volume extraction buffer and incubated on ice for 30 min. A centrifugation step followed (20 min at 16.000 x g at +4°C) to remove insoluble components. The protein concentration was determined using the BCA method (see chapter 3.4.1).

3.4.3 SDS-PAGE (polyacrylamide gelelectrophoresis)

The separation of proteins was performed according to Laemmli (1970) with an acrylamid concentration (relation of acrylamid to N,N'-methylenebisacrylamide 30:0.8) of 12.5 or 15% (as indicated) in the separating gel. For the stacking gel 0.5 M Tris-HCl (pH 6.8) and for the separating gel 1.5 M Tris-HCl (pH 8.8) was used. Prior to loading the samples on the gels, they were solubilized in Laemmli buffer (250 mM Tris-HCl (pH 6.8), 40% glycerine, 9% SDS, 20% β -mercaptoethanol, 0.1% bromophenol blue).

SDS gels were stained using 0.18% Coomassie Brilliant Blue R250 dissolved in 50% methanol and 7% acetic acid for 15 min. Destaining was performed using 40% methanol, 7% acetic acid and 3% glycerine. Afterwards the gels were incubated in water and dried under vacuum.

3.4.4 Immunodetection

The proteins separated by SDS-PAGE were transferred onto nitrocellulose (PROTRAN BA83, 0.2 μ m, Whatman/Schleicher & Schüll) or a PVDF membrane (Zefa Transfermembran Immobilon-P, 0.45 μ m, Zefa-Laborservice GmbH, Harthausen, Germany) by a semi-dry-blot equipment (Amersham Biosciences) (Kyhse-Andersen, 1984). For this purpose, paper, membrane and gel were soaked with Towbin buffer (25 mM Tris (pH 8.2-8.4), 192 mM glycine, 0.1% SDS, 20% methanol). The transfer was conducted for 1 to 1.5h at 0.8 mA per cm² membrane surface. To visualize the proteins including the size marker, the membrane was stained with Ponceau S (0.5% Ponceau, 1% HAc) solution afterwards.

Labelling with protein-specific primary antibodies was carried out with polyclonal antibodies, and bound antibodies were visualized either with alkaline phosphatase (AP)-conjugated secondary antibodies (goat anti-rabbit IgG (whole molecule)-AP conjugated, Sigma-Aldrich Chemie GmbH, Taufkirchen) or using a chemiluminescence detection system (ECL, see below) in combination with a horseradish peroxidase-conjugated secondary antibody (goat anti-rabbit (whole molecule)-peroxidase conjugated, Sigma). For this purpose, the membrane was incubated three times in skimmed-milk buffer (1-3% milk powder, 0.03% BSA, 1x TBS) for 10 min each, and incubated with a dilution of the primary antibody (1:250-1:2.000) in this buffer at room temperature for two hours or overnight at +4°C. The membrane was washed in skimmed-milk buffer three times for 10 min and the secondary antibody (1:10.000) was added for 1 h. The membrane was once more washed in skimmed-milk buffer three times for 10 min. Detection of AP signals was performed in a buffer containing 66 μ l/10 ml NBT (nitro blue tetrazolium chloride, 50 mg/ml in 70% N,N-

dimethylformamide) and 132 μ l/10 ml BCIP (5-bromo-4-chloro-3-indolyl phosphate, 12.5 mg/ml in 100% N,N-dimethylformamide) in 100 mM Tris-HCl (pH 9.5), 100 mM NaCl, 5 mM MgCl₂ buffer. To stop the reaction the membrane was incubated in water.

To detect signals with the Enhanced Chemiluminescence (ECL) method, the Pierce ECL Western Blotting Substrate Kit (Thermo Fisher Scientific Inc., Rockford, USA) was used after manufacture's recommendations. The following protocol was also used: solution 1 (100 mM Tris-HCl (pH 8.5), 1% (w/v) luminol, 0.44% (w/v) coomarcic acid) and solution 2 (100 mM Tris-HCl (pH 8.5), 0.018% (v/v) H₂O₂) were mixed in a 1:1 ratio and added onto the blot membrane (1-2 ml per small gel). After incubation for 1 min at RT, the solution was removed and luminescence was detected with a film (Kodak Biomax MR, PerkinElmer, Rodgau, Germany), which was placed onto the membrane for distinct time periods (30 seconds up to 30 minutes, dependent on the signal intensity).

3.4.5 Blue Native PAGE

BN-PAGE analysis for two-dimensional separation of proteins and protein complexes was performed as described previously (Rokka *et al.*, 2005; Sirpiö *et al.*, 2007) with certain modifications: Thylakoid membranes were resuspended in 25BTH20G buffer (25 mM BisTris/HCl (pH 7.0), 20% (w/v) glycerol and 0.25 mg/ml Pefabloc) to a final chlorophyll concentration of 1 mg/ml. An equal volume of 2% n-dodecyl- β -D-maltoside was added and the thylakoids were solubilized on ice for 3 min. Traces of unsolubilized material were removed by centrifugation at 18.000 x g at 4°C for 20 min. The supernatant was supplemented with 1/10 volume of 100 mM BisTris/HCl (pH 7.0), 0.5 M ϵ -amino-*n*-hexanoic-acid, 30% (w/v) sucrose and 50 mg/ml Coomassie Blue G. Proteins were loaded on BN-PAGE in amounts corresponding to 3 mg of chlorophyll per well. Electrophoresis (Hoefer Mighty Small, Amersham Pharmacia Biotech, Uppsala, Sweden) was performed at 4°C by gradually increasing the voltages as follows: 75 V for 30 min, 125 V for 30 min, 150 V for 60 min, 175 V for 30 min, and 200 V for 45-60 min, or until the staining solution reached the bottom of the gel. After electrophoresis, proteins were electroblotted onto PVDF membrane and detected by specific antibodies.

3.4.6 *In vitro* transcription and translation

Transcription of linearized plasmid was performed as previously described (Firlej-Kwoka *et al.*, 2008). Translation was carried out using either the Flexi Rabbit Reticulocyte Lysate

System or Wheat Germ Extract System from Promega (Madison, USA) following the manufacturer's protocol in presence of [³⁵S]-methionine for radioactive labeling.

3.4.7 *A. thaliana* chloroplast isolation

Chloroplasts were isolated from 21 days old *A. thaliana* plants, grown on ½ MS-glass-plates without sucrose, according to the protocol by Aronsson and Jarvis (2002) with following exceptions: the buffers were supplied with 0.3 M sorbitol, and NaHCO₃ as well as gluconic acid were added. An import reaction (chloroplasts equivalent to 10 µg chlorophyll) was subsequently carried out in 100 µl volume containing 3 mM ATP and maximal 10% (v/v) [³⁵S]-labeled translation product. Import reactions were performed for the indicated time at 25°C and terminated by the addition of 2 volumes ice-cold washing buffer (0.3 M sorbitol, 50 mM Hepes-KOH (pH 8.0), 3 mM MgSO₄). Chloroplasts were washed twice in washing buffer and finally resuspended in Laemmli buffer (50 mM Tris-HCl (pH 6.8), 100 mM β-ME, 2% (w/v) SDS, 0.1% (w/v) bromphenol blue, 10% (v/v) glycerol).

3.4.8 *A. thaliana* chloroplast isolation and fractionation

Intact chloroplast were prepared from approximately 200 g fresh weight leaf material of 3-week-old plants directly after the dark period (8 h dark) essentially as described by Seigneurin-Berny *et al.* (2008). Chloroplasts were subsequently resuspended in 15 ml of 10 mM HEPES-KOH (pH 7.6), 5 mM MgCl₂ and lysed using 50 strokes in a 15 ml-Dounce homogenizer (Wheaton). Further separation of stroma, thylakoids and envelopes was done according to Li *et al.* (1991). 20 µg of the fractions were separated by a 12.5% SDS PAGE and immunoblotted with distinct antibodies.

3.4.9 *Pisum sativum* chloroplast isolation and protein import

Chloroplasts were isolated from 10 days old pea plants according to the protocol of Schindler *et al.* (1987). 5 µl of the intact chloroplasts were resolved in 5 ml 80% acetone and the chlorophyll concentration was estimated by measuring the optical density at three wavelengths (645 nm, 663 nm, 750 nm) using the solvent as reference (Arnon, 1949).

[³⁵S]-labelled precursor proteins were mixed with freshly prepared intact chloroplasts in the presence of 3 mM ATP in a final volume of 100 µl and incubated at 25°C for 5-20 minutes (Waegemann and Soll, 1995). Import products were separated by SDS-PAGE and analyzed by a phosphorimager or by exposure on autoradiography films (Kodak Biomax-MR).

3.4.10 Protein expression, purification and crystallization

For heterologous soluble protein expression, constructs were transformed in *E. coli* BL21 (DE3) cells (Novagen/Merck) and grown at +37°C in LB media in the presence of an appropriate antibiotic to an OD₆₀₀ of 0.4-0.6. Expression was induced by addition of 1 mM IPTG (isopropyl β-D-1-thiogalactopyranoside). Subsequently, cells were grown at 37°C for 3h or at 12°C over night and harvested at 5.000 x g for 15 min at 4°C. The bacteria were resuspended in lysis buffer (50 mM Tris pH 8.0, 150 mM NaCl). Depending on the protein properties, the pH as well as the salt concentration and the ion composition has been varied as indicated until an optimal purification was reached, and cells were broken using the Microfluidizer-Processor from Microfluidics (Newton, USA). Afterwards the samples were sonified to destroy the DNA and finally centrifuged at 30.000 x g for 30 min at 4°C.

The supernatant containing soluble protein was purified by its C-terminal polyhistidine tag using Ni-NTA-Sepharose (GE Healthcare, Munich, Germany) and subsequent batch purification and chromatography techniques (size exclusion chromatography SEC, hydrophobic interaction chromatography HIC, ion exchange chromatography IEX) using the ÄKTA system (GE Healthcare) in the buffer utilized for initial purification steps and, if necessary, raising imidazole (batch purification), decreasing (HIC chromatography) or increasing (IEX chromatography) salt concentrations.

The crystallization process of the purified protein (synTic22, see chapter 4.1.11) was performed by Ira Schmalen (Group Eva Wolf, MPI Martinsried, Germany) by utilizing following crystallization screens: Hampton Research Index, Qiagen JSCG+, Qiagen Classics, Qiagen pH Clear I and II and Morpheus. Hampton Research and Qiagen screens including exact buffer compositions and crystallization conditions are summarized on the webpage http://xray.bmc.uu.se/markh/php/xtalscreens.php?func=lookup&screen_name=Expand+List. The Morpheus screen is described in Gorrec, 2009.

3.5 Metabolite analysis

Plants for metabolite analysis were grown on MS plates without sugar under different light exposure (50 and 100 μmol) under longday conditions (16h h light/8 h dark). After 12 days the seedlings were frozen in liquid nitrogen after 16 h light, 8 h dark and 8 h light. This was performed with 4 replica per plant line and time point.

For metabolite analysis and enzyme tests, the plants were harvested as described above and pestled in liquid nitrogen before the plant powder was further analyzed by Ina Thormählen,

AG Geigenberger (LMU Munich, Germany). Starch contents were determined as described in Thormählen *et al.* (2013). For determination of the NAD(P)(H) ratios, extraction of plant material was done as described in Kolbe *et al.* (2005) and photometric measurements were performed according to Gibon *et al.* (2004). The isolation of AGPase and determination of the activation state was done as described in Hendriks *et al.* (2003).

3.6 Microscopy

Cotyledones and the third primordial leaf from 2-3 individual *A. thaliana* plants at the age of 10 to 20 days were harvested in the morning prior to illumination. Samples were prefixed in glutaraldehyde 2.5% (w/v) in 75 mM cacodylate buffer (pH 7.0), subsequently rinsed in cacodylate buffer and fixed in 1% (w/v) osmium tetroxide in the same buffer for at least 2.5 h at room temperature. The samples were stained with uranyl acetate 1% (w/v) in 20% acetone, dehydrated in a graded acetone series and embedded in Spurr's low viscosity epoxy resin (Spurr, 1969). Further steps and microscopic investigation were performed by Dr. Irene Gügel (Department Biologie I, Plant Biochemistry and Physiology, LMU Munich).

3.7 Computational analysis

To analyze the prediction of protein structures and transit peptides, expression profiles of proteins, gene and protein sequences and to create *in silico* DNA constructs, computational databases and programs were used (Table 5).

Table 5 Computational databases and programs used in this work

Following computational databases were used to analyze genomic structures of *A.th.* genes, to predict amino acid composition of proteins and their transit peptides and to generate *in silico* constructs.

Name	Reference	URL
BLAST (Databank GenBank)	Altschul <i>et al.</i> , 1997	http://www.ncbi.nlm.nih.gov/BLAST
Vector NTI	Invitrogen	
ARAMEMNON version 3.2	Schwacke <i>et al.</i> , 2003	http://aramemnon.botanik.uni-koeln.de
TAIR (The Arabidopsis Information Resource)	Lamesch <i>et al.</i> , 2011	http://www.arabidopsis.org
ChloroP 1.1	Emmanuelsson <i>et al.</i> , 1999	http://www.cbs.dtu.dk/services/ChloroP/
TargetP 1.1	Emmanuelsson <i>et al.</i> , 2000	http://www.cbs.dtu.dk/services/TargetP/
ExpASy	Gasteiger <i>et al.</i> , 2003	http://www.expasy.org/
Genedoc	Nicholas and Nicholas, 1997	http://www.psc.edu/biomed/genedoc
ClustalX	Thompson <i>et al.</i> , 1997	
MEGA5	Tamura <i>et al.</i> , 2011	http://www.megasoftware.net/

4 Results

4.1 Characterization of Tic22 in *A. thaliana*

4.1.1 The Tic22 protein family in *A. thaliana*

Tic22 was originally identified as a component of the Tic complex, which facilitates the import of preproteins across the inner envelope into chloroplasts via the general import pathway (Kouranov *et al.*, 1997). It was described to be localized in the intermembrane space, being weakly attached to the inner envelope and to function as a guiding protein, which targets incoming preproteins to the TIC core complex that subsequently transports precursor proteins into the chloroplast stroma (Kouranov *et al.*, 1998). The detailed structural and functional analysis of Tic22 in *A. thaliana* is the focus of the present study.

In *A. thaliana*, two different isoforms are present: Tic22III (At3g23710), Tic22IV (At4g33350) and a third protein is thought to belong to the Tic22 family, but not yet identified as an isoform (Tic22V; At5g62650). The mature form of the Tic22III protein has a molecular weight of 24.6 kDa, Tic22IV has 23.5 kDa and Tic22V has a predicted size of 50.2 kDa (<http://aramemnon.botanik.uni-koeln.de/>, <http://www.cbs.dtu.dk/services/ChloroP/>), thus it is twice as large as the other two isoforms. Beside these differences concerning the molecular weight, the proteins additionally differ from each other in their expression profiles:

Tic22III and Tic22IV possess a similar expression pattern in *A. thaliana*, showing a consistent expression in almost every plant tissue (Figure 4, analyzed with Arabidopsis eFP browser: <http://bar.utoronto.ca/efp/cgi-bin/efpWeb.cgi>). The *A. thaliana* eFP viewer provides a schematic representation of the abundance of individual mRNAs associated with ribosomes (translatomes) and total cellular mRNA (transcriptomes). With this tool, it was found that Tic22III is highly expressed in dry and imbibed seeds, in the shoot apex, as well as in the vegetative rosette and the seeds in the later silique developmental stages (Figure 4 A). Tic22IV shows a higher expression level in all plant tissues, but the highest RNA expression can be found again in dry and imbibed seeds, in nearly all flower stages, leaves, the shoot apex and finally in all seeds developing in the siliques (Figure 4 B). Since Tic22IV is more

abundant in all plant tissues, it is conceivable that it represents the main isoform of Tic22 in *A. thaliana*. In contrast to the expression profiles of Tic22III and Tic22IV, Tic22V is strongly expressed in dry seeds, but shows lower expression levels in other plant tissues (Figure 4 C). Hence, this expression profile suggests that Tic22V might be required predominantly during seed development. Despite these differences, all three isoforms depict a remarkably low expression level in the first node, in the stamen during flower stage 12 in the hypocotyl, the roots and in the mature pollen.

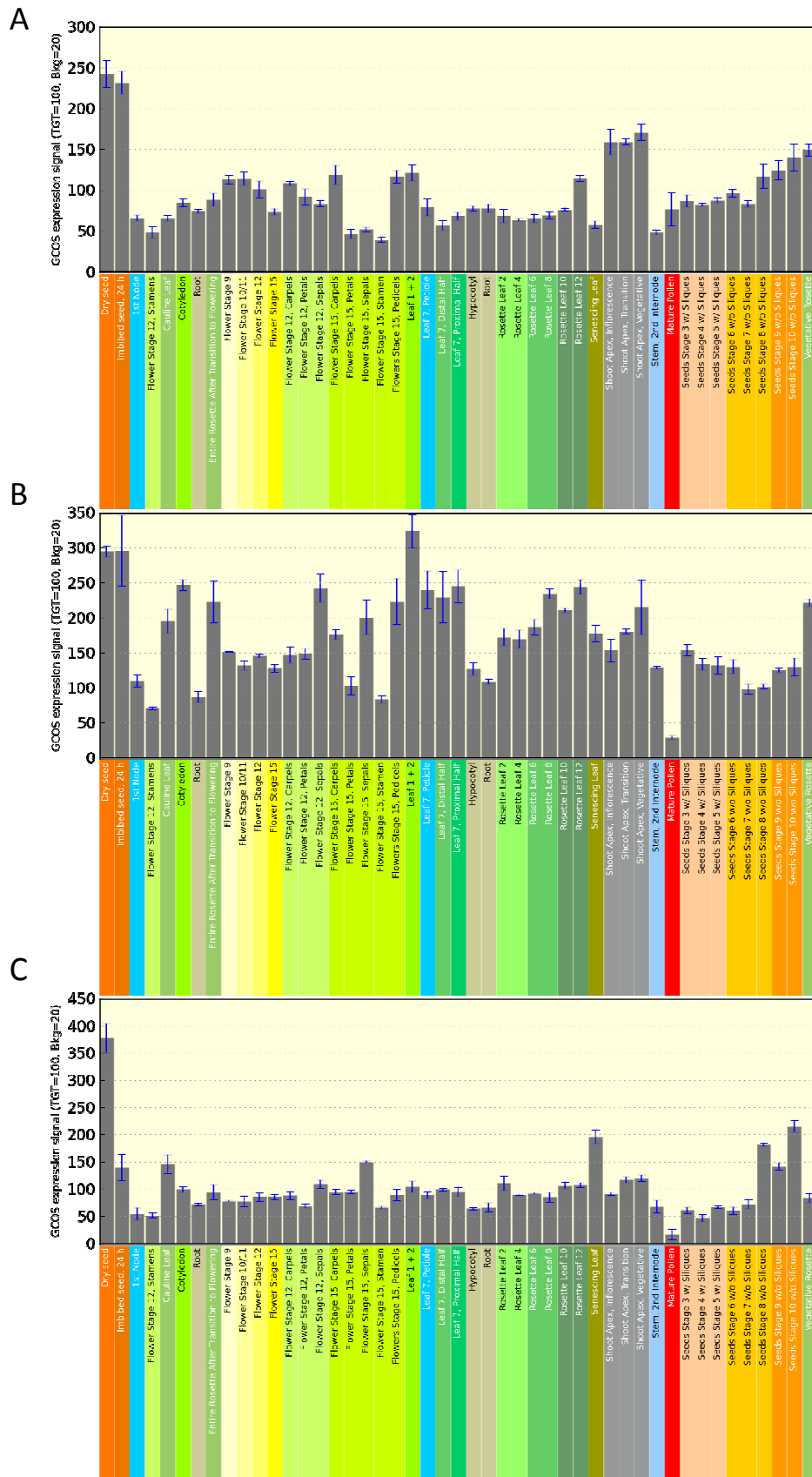


Figure 4 Expression pattern of the Tic22 isoforms in *A. thaliana*

Overview of the expression pattern of Tic22III (A), Tic22IV (B) and Tic22V (C) during plant development. The data derived from Microarray-analysis of the AtGenExpress consortium (Schmid *et al.*, 2005), and was visualized by the eFP Browser Programm (<http://bar.utoronto.ca/efp/cgi-bin/efpWeb.cgi>).

The precursor proteins of the three Tic22 isoforms were further analyzed by sequence alignment on amino acid level (Figure 5, <http://www.ebi.ac.uk/Tools/msa/clustalw2/>), demonstrating that Tic22III and Tic22IV show the highest similarity with an amino acid identity of 35% and a similarity of 61%, whereas Tic22IV and Tic22V possess 22% identity and 46% similarity, respectively. These data are in line with the expression profiles, proposing a similar or overlapping function of Tic22III and Tic22 IV, whereas Tic22V seems to play a different/more specialized role. Since Tic22V depicted a weak homology with the sequences of Tic22III and Tic22IV, the sequence alignment of all three isoforms was not successful, due to an altered illustration aligning all three amino acid sequences.

However, all isoforms feature a conserved amino acid motif “GVPVF” (Figure 5, green line), which seems to be conserved, although no function has been assigned to this motif so far.

```

A
At3g23710 MNSMIFPPSKQQMELNMIQQSFNLSQCSNLLLNVSQTLMLPNANTNMKPMIFSALN 60
At4g33350 MESSVKP-----NPLFSFSSFIHHQCTRFSSDLSARI----- 32
*:*: * * : . * : * : * : * : * : * :

At3g23710 SFPDQAKQALDSRISRFNSGKAPVMARISDDGGARAQVTVPIRSGKGLSADAIEERLA 120
At4g33350 --EDTKRFAETLATRRFSLPTPPFASVQSQKSGTPTTT-----LSPSLVAKALA 80
. * : * ** . . * : * : * : . * : . * : * : * :

At3g23710 GVPVYALSNMEEFVLVSGTSSGKSLGLLFCKEEDAETLLKEMKSMDFRMRKESKVVVAL 180
At4g33350 GTSVFTVSNNTNNEFVLISDPTGGKSIIGLLCFRQEDAEAFLAQAR-LRRRELKTNKVVPI 139
* . * : * : * : * : * : * : * : * : * : * : * : * : * : * : * : * :

At3g23710 ALSKVFLKLVNGVAFRLIPESTQVKNAKERTAGIDDDDFHGVVVFQSKSLILRSEMMS 240
At4g33350 TLDQVYLLKVEGISFRFLPDPPIQIKNALELKSSG--MRNGFDGVPVFQSELLVVRKKNRR 197
* . * : * : * : * : * : * : * : * : * : * : * : * : * : * : * : * :

At3g23710 YRPVFRKEDLEKSLIRASSQQNRLNLPALPGDIOQVAVFEDIVKGMRES-TTSMDDIVF 299
At4g33350 YCPVYFSKEDIERELSKYTRASR-----GDQQIMVGSLEDVLRKMEMSEKNSGWEDVIF 251
* * : * * : * : * : * : * : * : * : * : * : * : * : * : * : * : * :

At3g23710 IPPGFEVSTEQTE--- 313
At4g33350 IPPGRSYAQHMQLIKE 268
**** . . :

B
At4g33350 MESSVKPNPFLFSFSSFIHHQCTRFSSDLSARIEDTKRFAETLATRRFSLP--TPPPFASV 58
At5g62650 MGSPPKQHRRHVAEFLHSAVTSSISSIIPFPKTAAPSRLPLRFSVDDVSSPFEST 60
* * . * : . : * : * : * : * : * : * : * : * : * : * : * : * :

At4g33350 SQSKSGTPTTTLSPSLVAKALACTSVFTVSNNTNNEFVLISDPTGGKSIIGL----LCFRQ 113
At5g62650 VKSTSSASSSCLNSTRVRISSLSDDGKRGPAFVGQVFSMCDLTGTGLMAVSTHFDIPFIS 120
: * . * : : * : : * : * : * : * : * : * : * : * : * : * :

At4g33350 EDAAEFLAQAARLRRELKTNKVVPIITLDQ----VYLLKVEGIS----- 153
At5g62650 KRTPEWLKMFSTITKSERNGPVFRFMDLGDVAVYVKKLNIPSGVVGACRLDLAYEHFK 180
: : * : : * : * : * : * : * : * : * : * : * : * : * : * :

At4g33350 ----FRFLPDPPIQIKNALELKSSGKNGK----FDGVPVFQSELLVVRKKNRR----YCP 200
At5g62650 EKPHLQFVPNERQVKAANKLLKSMPOKQKTKQVGVVFGAQNLDIAVATADGIKMYTP 240
* : * : * : * : * : * : * : * : * : * : * : * : * : * : * :

At4g33350 VYFS-----KEDIERELSKYTRASRGDQQIMVGSLED 232
At5g62650 YFFDKAVLDNILEESVDQHFTLIQTRHVQRDRVDDSLASEVMEEMGDSMLEPPEVQEQ 300
: * : * : * : * : * : * : * : * : * : * : * : * : * : * :

At4g33350 VLRKMEMS----- 240
At5g62650 AMEEIGTSGIPLSVVAKAAEIQLLYAVDRVLLGSRWFRKATGIQPKLPYLVDSEFRRSAF 360
. : : : *

At4g33350 --EKNSG-----WEDVIFIPP----- 254
At5g62650 SIQRASGSATRCLGDSVEADTSASLLRVEDDPSSEAEKRQQLWFFPGDWISHSVSRKEH 420
: : * : * : * : * : * : * : * : * : * : * : * : * :

At4g33350 ----GRSYAQHMQLIKE----- 268
At5g62650 THHGSGSDQRDMESREREMLRSPFLPKITMVGISTGEEAQAQMSKANLKKTMEDLTEDLEQS 480
* * . : * : * :

At4g33350 ----- 529
At5g62650 DEGNDHGSKRYDSLKIEERDPLFVAVVGYYSGLARAGSARLSRRGDDQ 529

```

Figure 5 Alignment of the amino acid sequences of the Tic22 isoforms in *A. thaliana*

The protein sequences of Tic22III and Tic22IV (A) and Tic22IV and Tic22V (B) were aligned using Clustal W2 (<http://www.ebi.ac.uk/Tools/msa/clustalw2/>). The green bars mark an amino acid sequence conserved in all isoforms (GVPVF).

4.1.2 Generation of Tic22 mutants in *A. thaliana*

To investigate the physiological function of Tic22III and Tic22IV in more detail, T-DNA insertion lines of both genes were analyzed. For this purpose seeds of the respective T-DNA insertion lines (Tic22III: GABI_387C03, Tic22IV: GABI_810F06) were ordered and first analyzed on DNA level. At this time point, no T-DNA insertion line was available for Tic22V. In both Tic22III and Tic22IV lines the T-DNA insertion was annotated to be localized in the first exon and should hence lead to the complete knock-out of the gene (Figure 6). To verify the T-DNA insertion on DNA level, PCR screenings were also performed with further oligonucleotide combinations (see material, Table 1) than shown in Figure 3, and this analysis resulted in the identification of a homozygous single mutant for the *tic22III* gene (line 66-1) as well as for the *tic22IV* gene (line 57-4). These lines were further analyzed in regard to their phenotypes.

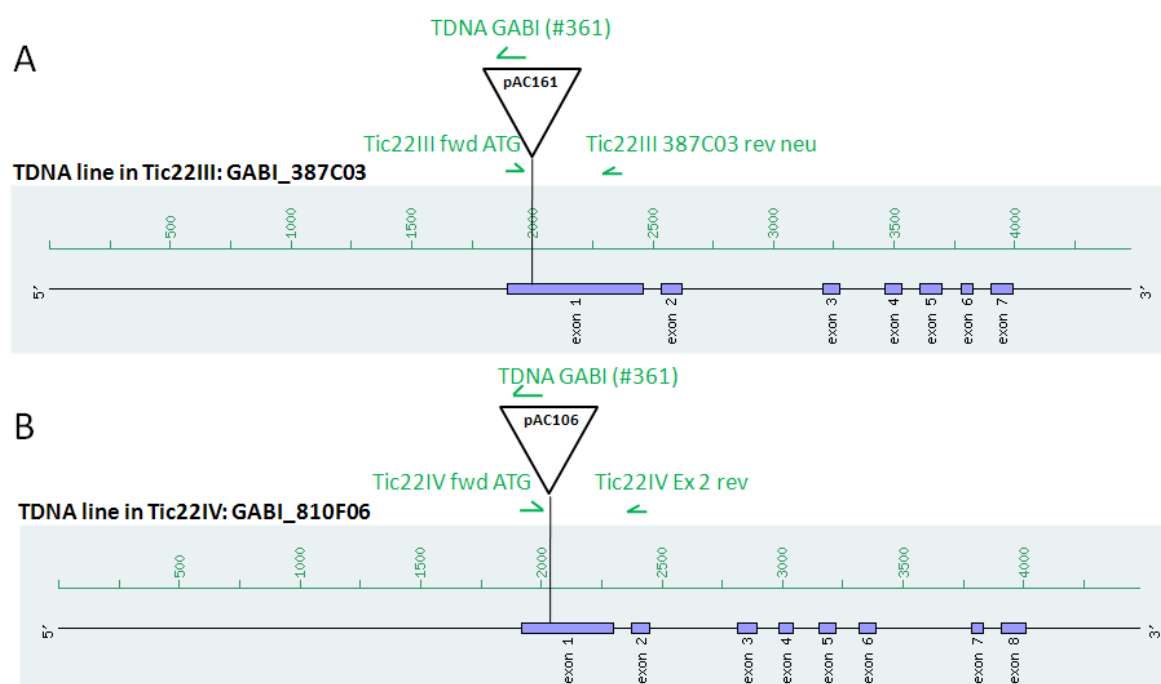


Figure 6 Schematic representation of the genomic DNA of Tic22III and Tic22IV including the T-DNA insertions
 Prediction of the genomic DNA pattern of Tic22III (**A**) and Tic22IV (**B**) according to <http://aramemnon.botanik.uni-koeln.de/>. The T-DNA insertion in Tic22III (vector pAC161, line: GABI_387C03) was localized in the first exon. The molecular characterization was performed with the oligonucleotides Tic22III fwd ATG and Tic22III 387C03 rev neu to screen for WT lines and Tic22III fwd ATG and T-DNA GABI (#361) to screen for mutant lines (**A**). The T-DNA insertion in Tic22IV (vector pAC106, line: GABI_810F06) was localized in the first exon and was detected by PCR with the oligonucleotides Tic22IV fwd ATG and T-DNA GABI (#361). The Tic22IV lines lacking the T-DNA insertion were verified by PCR with the oligonucleotides Tic22IV fwd ATG and Tic22IV Ex 2 rev (**B**).

The single mutant lines were analyzed under long day conditions (16h light/8h dark and 100 μmol light intensity) regarding their growth and appearance compared to WT plants. Since no obvious differences could be detected in the homozygous single mutants under normal growth conditions, homozygous double mutants were generated. For this purpose the homozygous single mutants were used for cross fertilization in order to obtain $\Delta\text{Tic22IIIxIV}$ double mutant plants (*tic22dm*).

The verification of the double knockout on DNA level was performed by PCR analysis using oligonucleotides which amplified the respective gene in WT plants, but not in the mutant plants and vice versa with oligonucleotides of which one of them was specific for the T-DNA, thus exclusively amplifying the sequence of the mutant plants (Figure 7 A). This screening procedure resulted in the identification of three independent homozygous double mutant lines, named *tic22IIIxIV* #1, #214 and #221 as well as an “outcrossed” WT line, which was further used as WT control in all experiments. The presence of both T-DNA insertions in the double mutant was additionally verified by sequencing the DNA, which was obtained by PCR, using the genomic DNA as a template and performed with the T-DNA oligonucleotides *Tic22III* ATG fwd and T-DNA GABI (#361) for *TIC22III* and *Tic22IV* ATG fwd and T-DNA GABI (#361) for *TIC22IV* (Sequencing Service, Department of Genetics, LMU Munich).

To exclude the existence of remaining RNA transcripts, RT-PCR was performed (Figure 7 B). For this purpose, RNA was isolated from WT-, *tic22IV* single mutant (*tic22IVsm*)- and *tic22IIIxIV* double mutant plants (*tic22dm*) and reverse transcribed to cDNA, which was used as the template for RT-PCR. The oligonucleotides utilized in this PCR analysis amplify either *TIC22III* or *TIC22IV* and should not lead to a gene product if the T-DNA insertion prevented the synthesis of RNA and therefore the transcription of cDNA. The PCR products were analyzed by agarose gel electrophoresis and clearly showed gene products in WT plant as well in the *TIC22IV* single mutants but not in the double mutant using oligonucleotides which amplified the *TIC22III* gene (Figure 7 B). Moreover, no gene products were detected in the *TIC22IV* single mutant and the double mutant using oligonucleotides amplifying parts of *TIC22IV*, whereas the respective band was clearly visible in WT used as a positive control. These results demonstrate that the double mutant did not contain any residual transcript, thus suggesting that functional *Tic22III/Tic22IV* proteins can no longer be synthesized in

tic22dm.

To verify that indeed no Tic22III and Tic22IV protein is detected in the double mutants, immunoblots with different plant tissues were performed using an antibody generated against Tic22IV, which should recognize both Tic22III and Tic22 IV isoforms in *A. thaliana*. However, the antibody did not recognize any Tic22 protein in WT plants, neither in whole leaf extract nor in whole chloroplasts or envelope fractions under different conditions, varying the amount of protein loaded on the gel (10- 225 µg of whole protein extract, 1-20 µg protein in whole chloroplasts), various blocking buffers with different blocking strength (0.3-1% milk powder, with and without 0.03% BSA), different dilutions of the antibody (1:250-1:1.000) and several incubation periods (4h at 4°C-over night 4°C) (data not shown). Nevertheless, since RT-PCR data clearly demonstrated the absence of residual TIC22III and TIC22IV transcripts, it was concluded that generation of *tic22dm* was successful and the plants were used for further analyses.

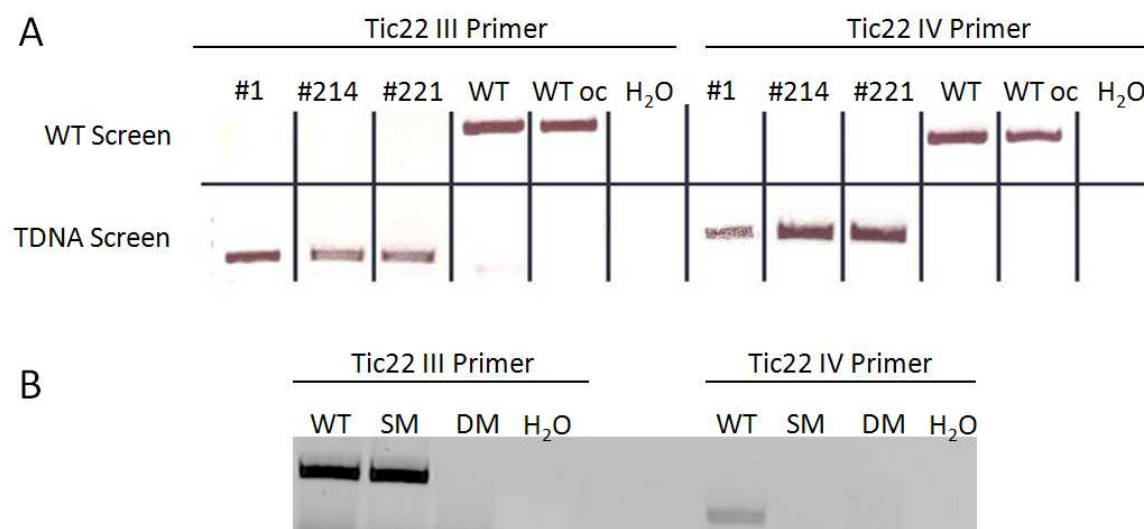


Figure 7 Molecular confirmation of *tic22dm*

A) 1µl of genomic DNA was used for PCR (35 cycles) with oligonucleotides amplifying *tic22III* WT (Tic22III ATG fwd, Tic22III 387C03 rev neu) and mutant (Tic22III ATG fwd, T-DNA GABI #361), as well as *tic22IV* WT (Tic22IV ATG fwd, Tic22IV Ex2 rev neu) and mutant (Tic22IV ATG fwd, T-DNA GABI #361). Positive controls are WT and “outcrossed” WT (WT oc). **B)** RT-PCR experiment (35 cycles) using cDNA (0,5 µl) of WT, *tic22IVsm* and *tic22dm* plants performed with *tic22III* (Tic22III ATG fwd, Tic22III 387C03 rev neu) and *tic22IV* WT primers (Tic22IV ATG fwd, Tic22IV Ex2 rev neu).

4.1.3 Phenotypic characterization of the *tic22III/IV* double mutant

First, phenotypic analysis of all three lines was performed by monitoring the plant’s growth on MS plates with and without sucrose as well as on soil under different light conditions

(long day 16h light/8h dark with 100 μ mol and 50 μ mol, respectively, short day 8h light/16h dark, constant light). The growth of the mutant plants did not show obvious differences compared to WT. However, closer inspection of the leaves and flowers revealed alterations of the leaf at distinct developmental stages:

Although the cotyledons had WT appearance (Figure 8, red box), the primary leaves of all three lines showed certain differences in the intensity of green (Figure 8, red arrows), which were further analyzed using a binocular (see below).



Figure 8 Phenotypic analysis of *tic22dm*

WT and *tic22dm* #221 were grown on MS plates without sucrose and analyzed after 12 days. The cotyledons (red box) and the primary leaves (red arrows) of *tic22dm* were compared to WT.

The analysis using a binocular or the transmission electron microscope (TEM) was performed for all homozygous *tic22dm* lines #1, #214 and #221. Depicted are exclusively the plants which showed the most severe phenotype.

With a magnification of 10 x, pale to almost chlorotic parts at the margins and leafbase of the third primordial leaf (PM 3, approximately 6-8 days old) were detected in *tic22dm* (Figure 9 A). Observing PM 3 with a magnification of 50 x, this chlorotic appearance seemed to be restricted to a certain zone of the leafbase (Figure 9 B, red dotted lines), whereas the area around the midvein did not differ from WT leaves. Additionally, a boundary separating green and chlorotic parts was revealed (Figure 9 C, red arrows). The green part seemed to surround the midvein of the leaf from the leaf tip to the leafbase in *tic22dm* as well as in WT. Furthermore, this phenotype was found to be most prominent during the first 12 to 14 days of plant growth after sowing and vernalisation procedure and disappeared during later

stages of leaf growth. Moreover, this difference was found at the margin of the whole leaf during early developmental stages, whereas it was restricted to the bottom of the leaf in later stages. In addition, during initial development, the leaves were smaller in the mutant compared to WT (Figure 8), however, after approximately 14 days of development, the leaf size was equal compared to WT. The observed phenotype occurred in every new emerging leaf, until the plant started to develop flowers.

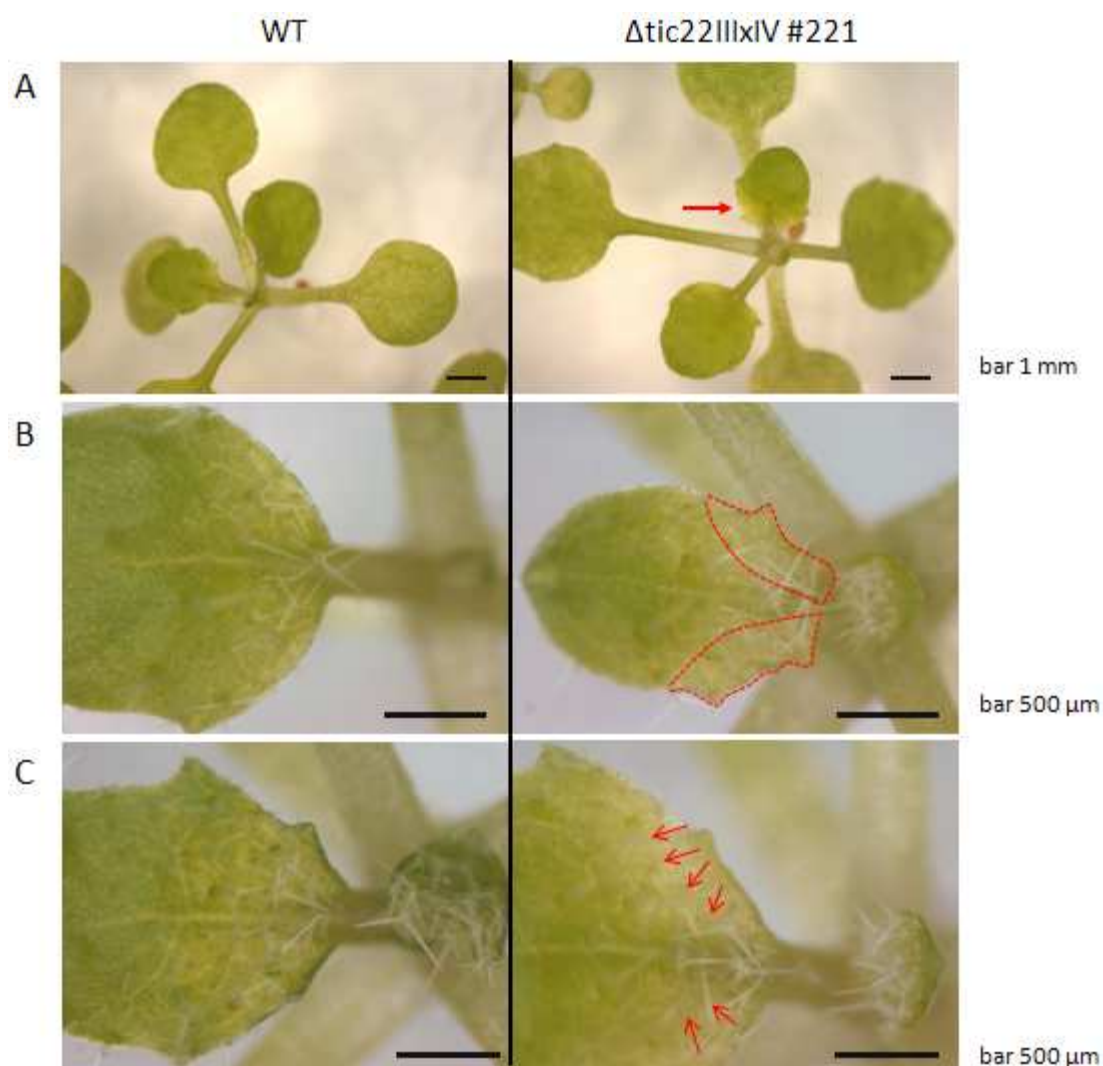


Figure 9 Detailed phenotypic analysis using the binocular

The third primordial leaf of 12 days (growth time in climate chamber) old seedlings, grown on MS plates without sugar (long day, 100 μmol) were analyzed with 10 x magnification (A, scale bar: 1 mm) and 50 x magnification (B-C, third leaf, scale bar: 500 μm) using a binocular. The red arrow (A) and dotted lines (B) depicted the chlorotic area at the leafbase of *tic22dm* and red arrows (C) demonstrate the boundary between chlorotic and green parts compared to WT.

The alteration in leaf color might be an indication for decreased chlorophyll content. To test this assumption, chlorophyll measurements of the primary leaves were performed. For this purpose, the chlorophyll of one single primary leaf (4 replica, equal leaf weight) of WT and

tic22dm was extracted with 80 % acetone, and chlorophyll a and b were subsequently measured and their amount calculated (Porra *et al*, 1989, done by Dr. Ulrike Oster). However, no differences in chlorophyll content of whole leaves between WT and *tic22dm* were observed (data not shown). This might be due to the fact that the parts of the leaves which displayed the phenotype become underrepresented when whole leaves were used for the analysis, including large parts which did not show the chlorotic phenotype. Current measurement of the chlorophyll content using exclusively the chlorotic parts of the leaf revealed a 50% decrease of the chlorophyll content compared to the green parts of the leaf (personal communication Dr. Bettina Bölter).

Next, chloroplast ultrastructure was analyzed by transmission electron microscopy (TEM) of ultra-thin sections of the chlorotic parts of the leaves. For this purpose, a leaf-area representing exclusively the chlorotic parts of *tic22dm* was chosen (Figure 10, red box). To ensure direct comparison, the respective areas of WT leaves were analyzed as well. Leaves for sample preparation were between 10 and 14 days old, since younger leaves were too small to ensure separation of chlorotic and green parts, and older leaves did not exhibit clear borders between the respective areas any longer.

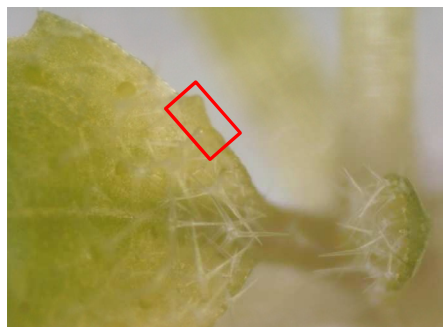


Figure 10 Leaf area used for electron microscopy

An area of the third *tic22dm* leaf, exclusively representing the chlorotic area (red box) was cut with a razor blade, fixed in 2.5% glutaraldehyde and prepared for TEM microscopy (done by Dr. Irene Gügel).

When analyzing the sections with a magnification of 1.800 x to obtain an overview of the cellular ultrastructure, the cells of *tic22dm* appear remarkably smaller compared to WT (Figure 11). The number of chloroplasts per cell did not differ from WT (Figure 8). Furthermore, some of the cells were even found to be completely filled with chloroplasts, which made the cells appear to be swollen (Figure 11, red arrows).

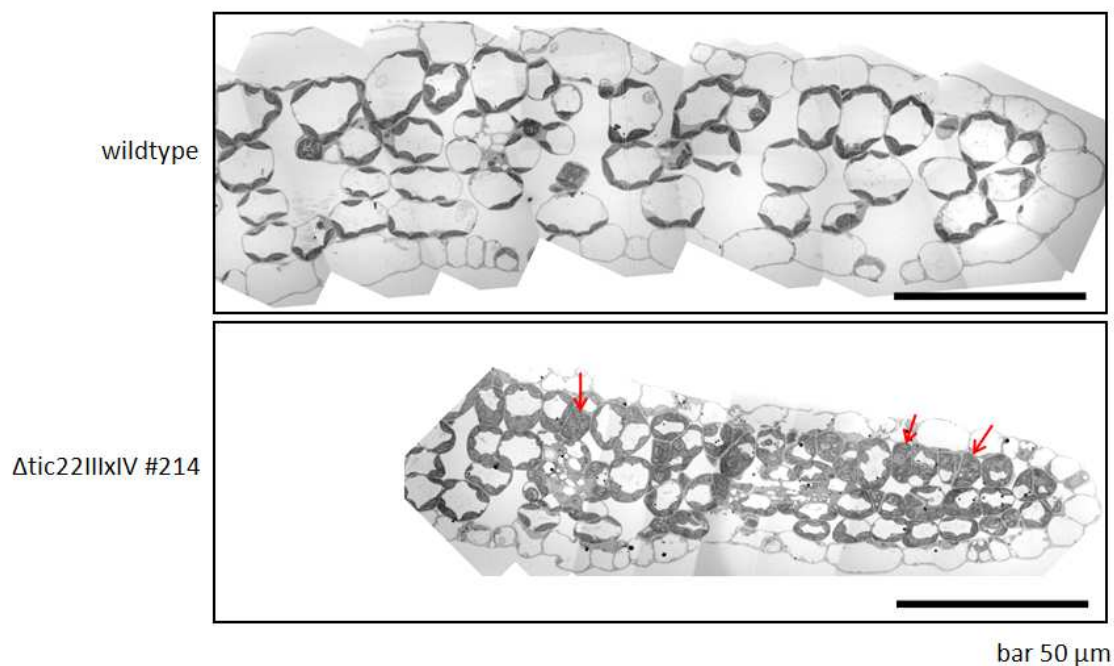


Figure 11 Overview of the ultrastructural cell composition of WT and *tic22dm* using TEM

Primary leaves of 14 days old *A. thaliana* WT (upper panel) and *tic22dm* (lower panel) plants grown under standard longday conditions on 1/2 MS plates without sucrose were prepared for transmission electron microscopy (TEM) as described in chapter 3.6. The 1.800 x magnification gives an overview of the cell architecture and content. Red arrows depict cells which were completely filled with chloroplasts. Scale bar: 50 μm .

Further detailed analysis of the chloroplast's ultrastructure using a magnification of 7.100 x revealed that the thylakoids in the mutant seem to be exclusively composed of stromal lamellae lacking grana stacks (Figure 12). This difference was observed in the palisade parenchyma (Figure 12 A) as well as in the sponge parenchyma (Figure 12 B), which might indicate that the differences in thylakoid composition are not dependent on tissue type. Moreover, the chloroplast size of *tic22dm* plants was decreased. Interestingly, this ultrastructural phenotype was still observed after 30 days of development, though the differences in leaf color disappeared within the first 14 days of development.

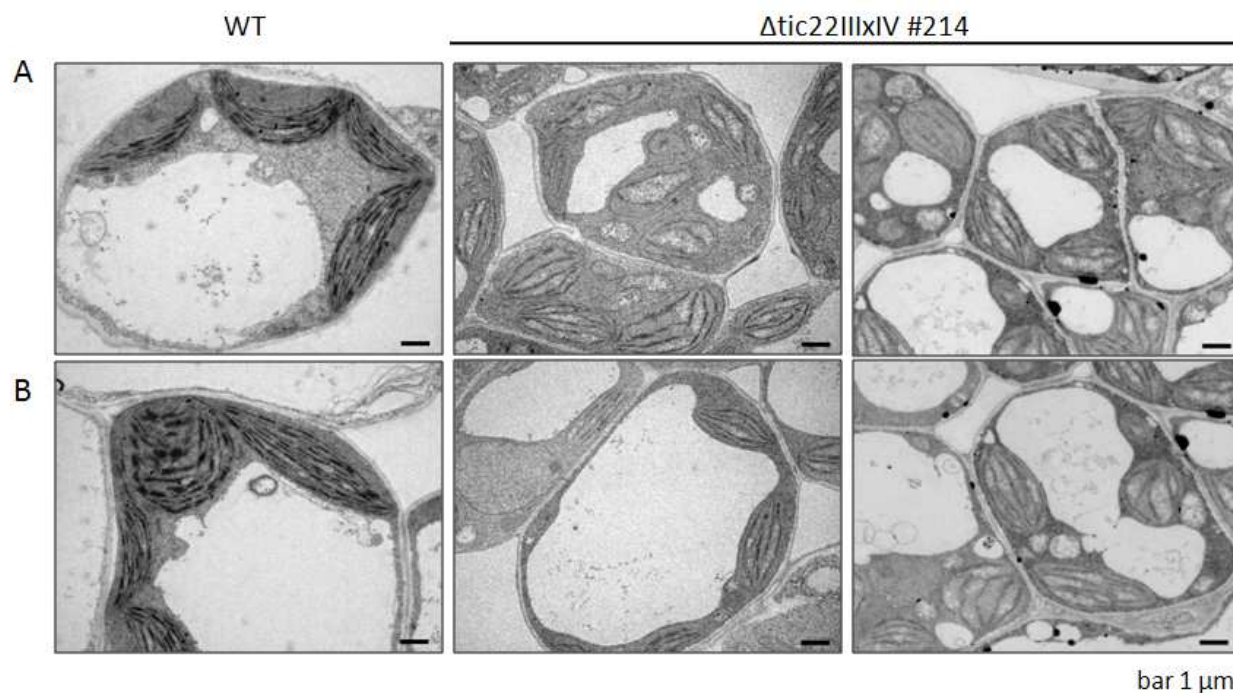


Figure 12 Ultrastructural analysis of *tic22dm* using TEM

Photographs taken with a 7.100 x magnification using transmission electron microscopy (TEM) provide a detailed view of two representative chloroplast sections of WT (left panels) and *tic22dm* (right panels), separated in palisade (A) and sponge (B) parenchyma. The bar indicates 1 μm .

4.1.4 Photosynthetic performance of WT and *tic22dm* plants

To test possible effects on photosynthetic performance in the different leaf areas, Pulse-Amplitude-Measurements (PAM) were performed using a Mini-PAM-Fluorometer (Walz, Effeltrich, Germany). This method enables the reliable measurement of the effective quantum yield of photochemical energy conversion in photosynthesis calculated referred to a certain leaf area. To compare the distinct leaf areas, the light pulse (growth light 90 $\mu\text{mol photons m}^{-2} \text{sec}^{-1}$) was adjusted to the leaf tip and the margin of the sixth leaf of five weeks old *tic22dm* and WT plants. Since the observed phenotype disappeared during later developmental stages, the primary leaf, which did not obviously contain chlorotic parts anymore, was additionally measured (Figure 13 A). Before starting the measurements, the plants were kept in the dark for 15 minutes. The Mini-PAM-Fluorometer automatically measured the fluorescence yield (F) and the maximal yield (F_m), which were used to calculate the photosynthesis yield ($Y = \Delta F / F_m$). The fluorescence was calculated referred to the respective area which was exposed by the light pulse. However, no difference in the values of the PSII maximum efficiency could be detected (Figure 13 B), which was not expected due to the appearance of the chlorotic phenotype.

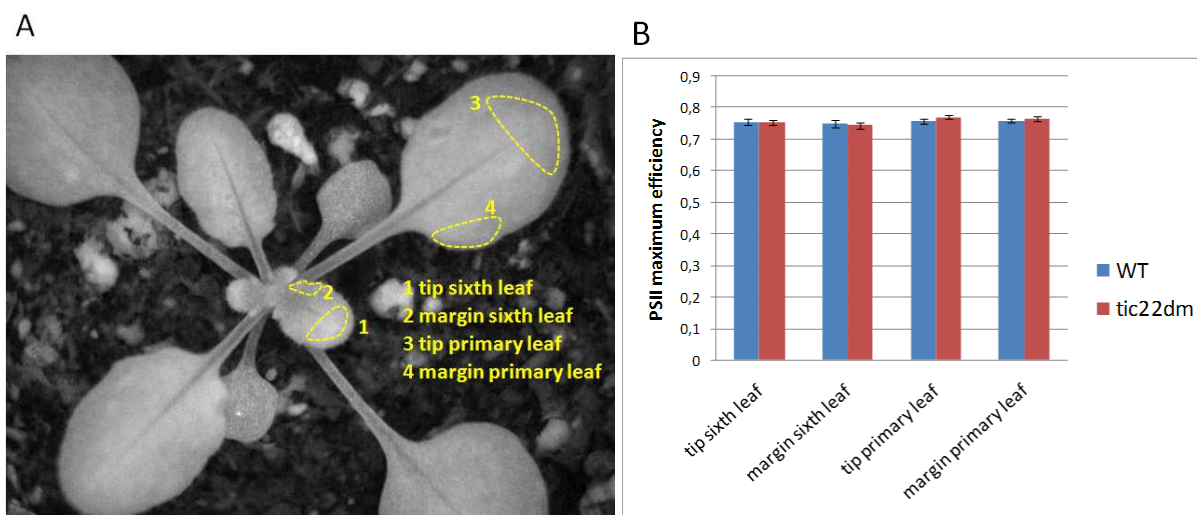


Figure 13 Pulse-Amplitude-Measurements (PAM) of *tic22dm* and WT

A) WT and *tic22dm* plants were grown under long day conditions on soil for five weeks. The light pulse, given by the Mini-PAM-Fluorometer (Walz, Effeltrich, Germany) to dark-adapted plants was adjusted to the tip of the primary and sixth leaf, as well as to the margins of the primary and sixth leaf, depicted by the yellow lines. **B)** Values of the PSII maximum efficiency were directly calculated by the Mini-PAM-Fluorometer. The experiment was performed in quintuplicate.

4.1.5 Molecular analysis of separated leaf parts

To determine whether the observations regarding thylakoid morphology caused the detected changes in leaf color, the protein composition of the appropriate leaf areas was investigated in detail. Particular attention was paid to the photosynthetic proteins, especially of photosystem II, which is localized in the grana stacks. To investigate these differences on a molecular level, leaves of WT and mutant plants were cut into specific sections (Figure 14 A). For determination of potential differences in biological processes like RNA transcription and protein synthesis in the distinct leaf areas, the chlorotic parts were cut independently from the green parts in liquid nitrogen and collected until an appropriate amount of material was obtained (~50 leaves per RNA isolation or protein extraction). The cutting process was performed under visual control using a binocular, and to ensure separation of the chlorotic and green parts, exclusively the leaf tip was used to represent the green area (Figure 14 B).



Figure 14 Cutting pattern of the distinct leaf areas

The third leaf of 14 days old plants grown under longday conditions on $\frac{1}{2}$ MS plates without sugar were cut into sections with a razor blade under the binocular with a magnification of 50 x (A). Approximately 50 leaves were cut to obtain an appropriate amount of leaf tip (B) and side (chlorotic) areas (C). 1 represents the leaf tip, 3a the left side of the midvein at the leafground and 3b the right side of the midvein at the leafground. The indicated bar represents 500 μm .

As shown in Figure 14 A, the sections labeled with 1 represent the leaf tip, which correspond to the green parts of the leaf, whereas 3a and 3b include the chlorotic areas at the boundary of the lower leaf-half. The lines depict the cutting pattern applied to separate both areas for further analysis. Direct comparison of the cut sections under the light microscope clearly illustrates that the observed difference is restricted to the area 3a/b (Figure 14 C), which appear paler in *tic22dm* compared to WT, whereas no changes were detected for the leaf tip (Figure 14 B, area 1).

In a first step for a more detailed molecular characterization of the respective leaf sections, the expression of specific genes was investigated. For this purpose, expression of genes encoding for chloroplast proteins, particularly located in the thylakoids was monitored by qRT-PCR. The following genes were analyzed in the RT-PCR approach: OE17, OE23, OE33, LHCB1.3, LHCB4.1, LHCB5, LHCB6, ATPaseC, ATPaseD, ATPaseG. Lhcb proteins are part of the

light-harvesting complex of photosystem II. The oxygen evolving complex proteins (Oe17, Oe23 and Oe33) are associated with photosystem II and the ATP synthase genes C, D and G encode for subunits of the CF₀CF₁ ATP synthase. However, due to the low amount of leaf material available and the resulting difficulty of RNA isolation in a reproducible manner, only for a subset of genes reliable results could be evaluated (Figure 15, Table 6).

The most prominent difference between *tic22dm* and WT was found in the *tic22dm* leaf tip: This section showed a higher expression of all genes compared to both WT leaf sections and *tic22dm* side area. The LHCb expression was reduced in the *tic22dm* side areas compared to WT side areas, whereas the expression of the ATP genes and OE23 in the margins of *tic22dm* did not differ from the margins of the WT plants.

Table 6 Gene regulation in leaf sections of *tic22dm* and WT

Numerical evaluation of gene expression of LHCb, ATPases and OE23 is depicted by comparing WT and *tic22dm* (WT→DM) and the sections within WT and *tic22dm* (DM): Bold letters show the perspective from which the gene regulation is depicted (the expression of LHCb1.3 was decreased 5.0-fold in the WT leaf tip compared to *tic22dm* (DM) leaf tip and was enhanced 2.6-fold in the WT side area compared to *tic22dm*).

	LHCb 1.3	LHCb 4.1	LHCb 6	ATP C1	ATP D	ATP G	OE 23
WT → DM leaf tip	5.0-fold ↓	18.5-fold ↓	4-fold ↓	2.1-fold ↓	6.3-fold ↓	4.5-fold ↓	5.6-fold ↓
WT → DM side area	2.6-fold ↑	1.9-fold ↑	2.9-fold ↑	1.9-fold ↑	equal	equal	equal
WT leaf tip → side area	equal	3.9-fold ↑	1.5-fold ↓	8.8-fold ↑	3.3-fold ↑	3.8-fold ↑	2.4-fold ↑
DM leaf tip → side area	15.4-fold ↑	9.2-fold ↑	7.5-fold ↑	10-fold ↑	15.9-fold ↑	13-fold ↑	11.7-fold ↑

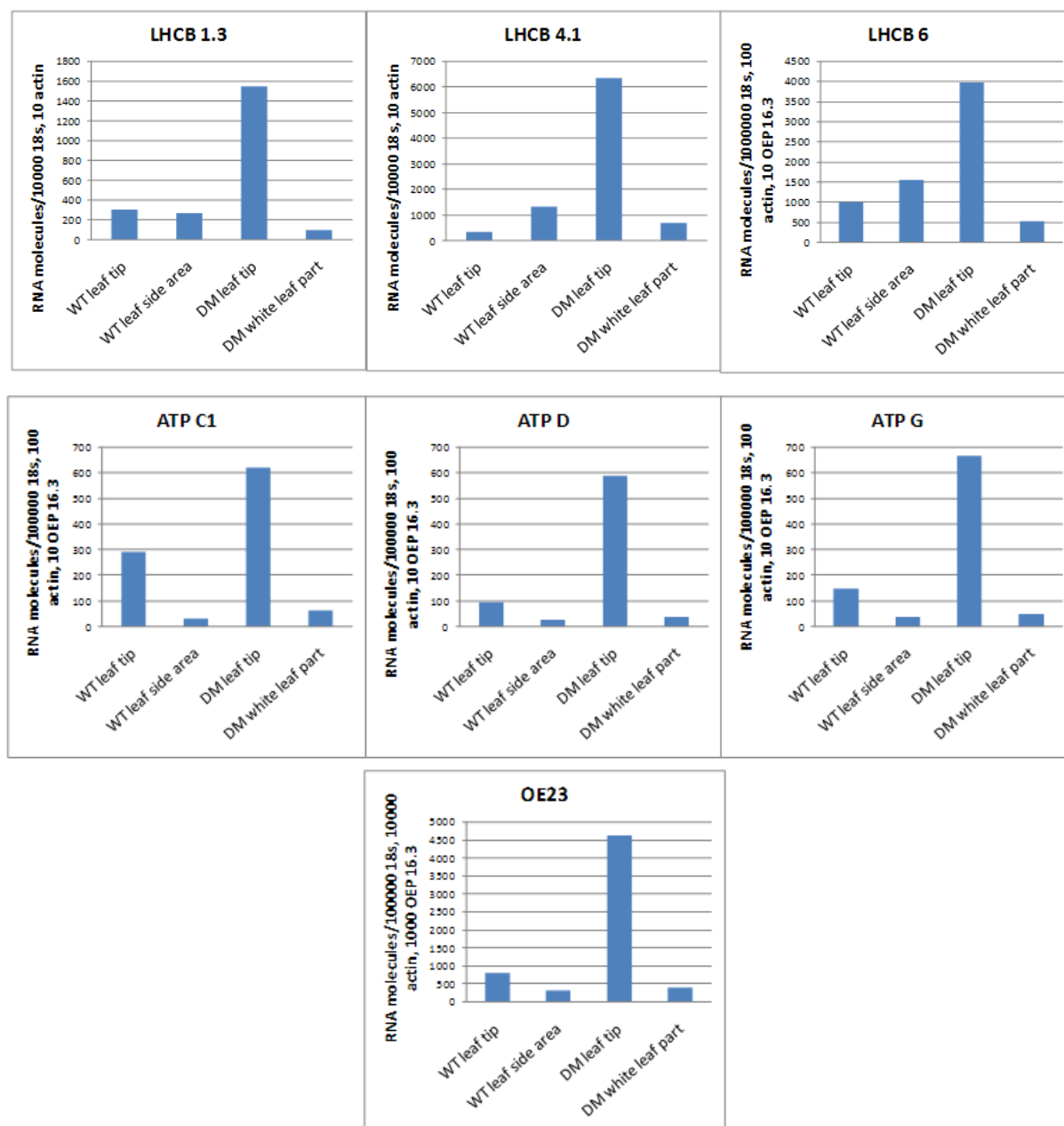


Figure 15 LHC-, ATP- and OE23 transcript levels in *tic22dm* and WT

Quantification of the mRNA levels of LHC1.3, LHC4, LHC6, ATPC1, ATPD, ATPG and OE23 using qRT-PCR. RNA was isolated from leaf tip and side areas of 12 days old seedlings and 100 μ g RNA was subsequently reverse transcribed into cDNA. The cDNA was diluted 1:20 and used for light cycler RT-PCR as described in methods. qRT-PCR contained 40 cycles. The mRNA amount (arbitrary units, $n=2$) was normalized to appropriate transcripts of actin, 18S and OEP 16.3 per PCR run.

To summarize these results, the gene expression of all LHCs was lower in the *tic22dm* side area compared to the respective section of the WT, whereas the expression of all ATPase genes as well as of OE23 was similar or even slightly increased in the side areas of *tic22dm*. In all cases, the most striking difference was the drastically enhanced gene expression of all genes in the leaf tip of the *tic22dm* compared to every other plant area of the WT and the *tic22dm*, including the leaf tip of the WT.

In the next experiment, differences between the above analyzed leaf parts were determined on protein level. For this purpose, specific antibodies were chosen: α OE23, α OE33, ATPase subunit α and β (α ATPase α/β), α PorB, α D1, α D2, α Lhca 2, α Lhcb 6, α NDH a and α NDH j/h were used for the decoration of membranes, containing 10 μ g of total protein extract per lane. Due to low protein amount, most of the antibodies failed to detect the proteins, especially in the side areas of WT and *tic22dm*. Only incubation with α OE33 resulted in a clear signal. Whereas OE33 was detected in WT and *tic22dm* leaf tip, as well as in the WT side area in comparable amounts, the protein was found to be clearly reduced in the *tic22dm* side area (Figure 16).



Figure 16 Immunoblot of OE 33 in particular leaf areas

10 μ g of whole protein extract isolated from leaf pieces of approximately 50 leaves per line was separated on a 12.5 % SDS page and blotted on a nitrocellulose membrane. The proteins were detected with an antibody against OE 33.

As mentioned before, most of the antibodies utilized for detection of the proteins in the leaf sections failed to recognize the protein in the side area of WT and *tic22dm*, while the proteins could be detected in the leaf tip of WT and *tic22dm* (data not shown).

4.1.6 Immunoblot of Lhc proteins in *A. thaliana* WT and *tic22dm* chloroplasts

To analyze the protein content of nuclear encoded photosynthesis proteins in *tic22dm*, immunoblots of WT and *tic22dm* chloroplasts were performed (Figure 17 A). For this purpose, chloroplast proteins were separated by SDS-PAGE and after transfer onto a membrane the blot was decorated with antibodies against LHCA and Lhcb proteins. The loading control (Figure 17 B) verified that equal protein amounts (5 μ g Chl) were loaded. In this experiment, no differences in protein amount were detected between WT and *tic22dm* chloroplasts.

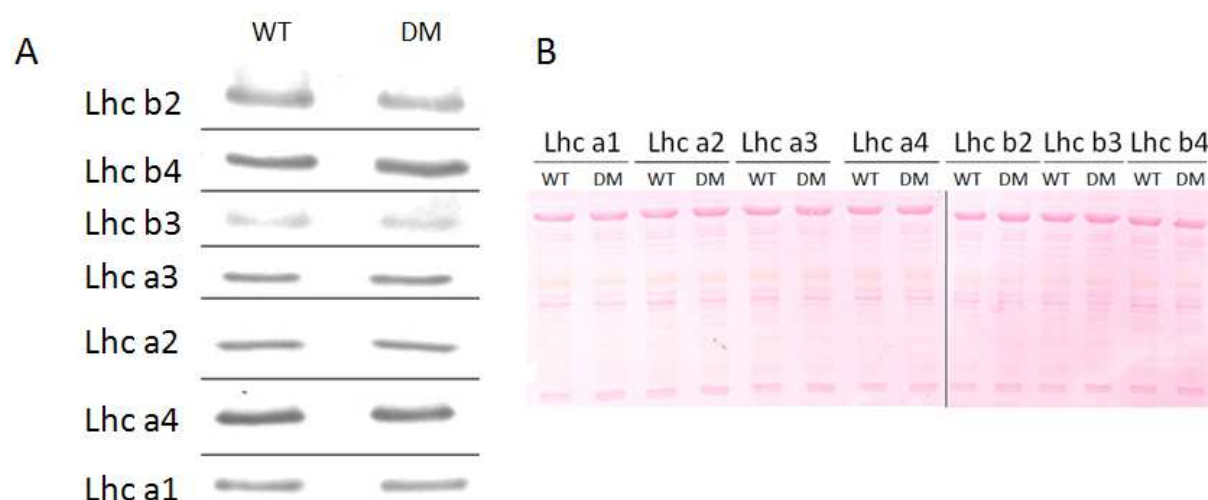


Figure 17 Immunoblot of Lhc precursor proteins in *A. thaliana* WT and *tic22dm* chloroplasts

(A) Whole chloroplasts (5 μ g Chl) isolated from WT and *tic22dm* plants were loaded on a 12.5 % SDS page and blotted against Lhc proteins. (B) Ponceau staining (loading control)

4.1.7 Analysis of the gene regulation in WT and *tic22dm* by DNA-Microarray analysis

The phenotype observed in distinct areas in *tic22dm* indicates a possible regulation of genes in the mutant. To detect genes, which are up- or down regulated, a DNA-Microarray analysis was performed (Affymetrix ATH1 Gene chip). For this purpose, WT, *tic22dm* and the *tic22IVsm* were grown on MS plates lacking sucrose under long day conditions and 100 μ mol light intensity for 14 days in four replicas. Afterwards, RNA was isolated from whole leaves, reverse transcribed into cDNA and used for the Microarray. The evaluation contained the comparison between WT and *tic22dm* as well as *tic22dm* and *tic22IVsm*. Finally, 927 genes were found to be regulated in *tic22dm* compared to the single mutant, whereof 477 were down regulated and 450 were up regulated. The comparison between *tic22dm* and WT revealed in total 4927 regulated genes in the double mutant. Of these, 2802 genes were repressed in *tic22dm*, whereas 2125 were upregulated in the double mutant. To get an overview, which gene families showed the most frequent regulation, the genes were first ordered with regard to their functional characterization of the respective proteins (BIN codes, <http://bioinfoserver.rsbs.anu.edu.au/utills/GeneBins/>). The analysis revealed that many genes which were down regulated in *tic22dm* are involved in photosynthesis, more precisely in the light reactions, i.e. encoding for subunits of photosystem I (PSI) or II (PSII). To narrow down the high number of genes, only genes were chosen which showed the highest fold change (fc), indicating the highest regulation in *tic22dm* and, in addition, genes, which were plastid encoded.

The plastid encoded genes, which exhibited the most prominent down regulation, were: NDHH, ATPA, PSAA and PSBE. NDHH is a NAD(P)H dehydrogenase subunit H (49 kDa), a protein involved in photochemical electron transfer at PSI as well as chlororespiration. ATPA encodes the ATPase alpha subunit, which is a subunit of ATP synthase and part of the CF1 subcomplex which catalyzes the conversion of ADP to ATP using the proton motive force. This complex is located in the thylakoid membrane of chloroplasts. PsaA constitutes the reaction center of PSI (together with PsaB protein) and PsbE represents the PSII cytochrome b559, which is thought to function as an electron acceptor or donor under conditions when electron flow through PSII is not optimal.

Furthermore, four plastid encoded genes were found to be up regulated and which showed the highest fold change: RPL20, RPS15, PSAC and ACC2. RPL20 encodes the chloroplast ribosomal protein L20, which is a constituent of the large subunit of the ribosomal complex and involved in translation. RPS15 also encodes a chloroplast ribosomal protein (S15), which is a constituent of the small subunit of the ribosomal complex and it is also involved in translation. PSAC encodes a subunit of PS I and is therefore involved in photosynthesis, and ACC2 encodes for the acetyl-CoA carboxylase, which plays a role in fatty acid .

In addition to these plastid encoded genes, the NAD4 gene was also chosen for further investigation. It codes for the NAD(H) dehydrogenase subunit 4 and is involved in the cell respiration in the mitochondria. Since NAD4 showed a high degree of regulation in *tic22dm*, it was analyzed as an example for possible retrograde signaling, where changes in the plastid gene expression influences mitochondrial gene expression (for an overview, see Table 7).

To test the results of the DNA-Microarray, a quantitative RT-PCR was performed. For this purpose, the RNA which was isolated for the DNA-Microarray was used for reverse transcription into cDNA, which was then used as template for qRT-PCR (Figure 18). The repression of NDHH, ATPA, PSAA and PSBE (Figure 18 A) could be verified: NDHH was found to be downregulated in the *tic22IVsm* (2-fold) and in *tic22dm* (5-fold) and ATPA showed a repression of 1.7-fold in the *tic22IVsm* and 3-fold in *tic22dm*. PSAA showed a stronger repression in the single mutant (2.7-fold) and especially in *tic22dm* (34-fold), not being in line with the hierarchy achieved with the DNA-Microarray, where NDHH and ATPA were shown to be stronger regulated in *tic22dm* (see Table 7, fold change). The gene expression

of PSBE was almost equal between WT and *tic22IVsm*, whereas it is 1.4-fold down regulated in *tic22dm* compared to WT.

In contrast, the up regulation of the genes (Figure 18 B), observed by the DNA-Microarray experiment could not be verified by the qRT-PCR approach: RPL20 seemed to be slightly up regulated in the *tic22IVsm* (1.2-fold), whereas the expression in *tic22dm* was comparable to WT, but showed a slight repression (0.8-fold). Furthermore, the expression of RPS15 was slightly increased in *tic22IVsm* and *tic22dm* (1.2 x), whereas the expression of PSAC was 1.4-fold higher in the *tic22IVsm* compared to WT, but 0.7-fold decreased in *tic22dm*, which was not in line with the results of the DNA-Microarray, where PSAC was up regulated in *tic22dm* compared to WT. The gene expression of ACC2 and NAD4 was slightly increased in the *tic22IVsm* (ACC2: 1.2-fold, NAD4: 1.03-fold) and clearly increased in *tic22dm* compared to WT (ACC2: 2.1-fold, NAD4: 1.2 fold).

An overview of the analyzed genes and the results of the DNA-Microarray analysis as well as the quantitative qRT-PCR are shown in Table 7. It contains the gene number, the function, fold-change and the regulation of the genes in *tic22dm* and *tic22IVsm* compared to WT.

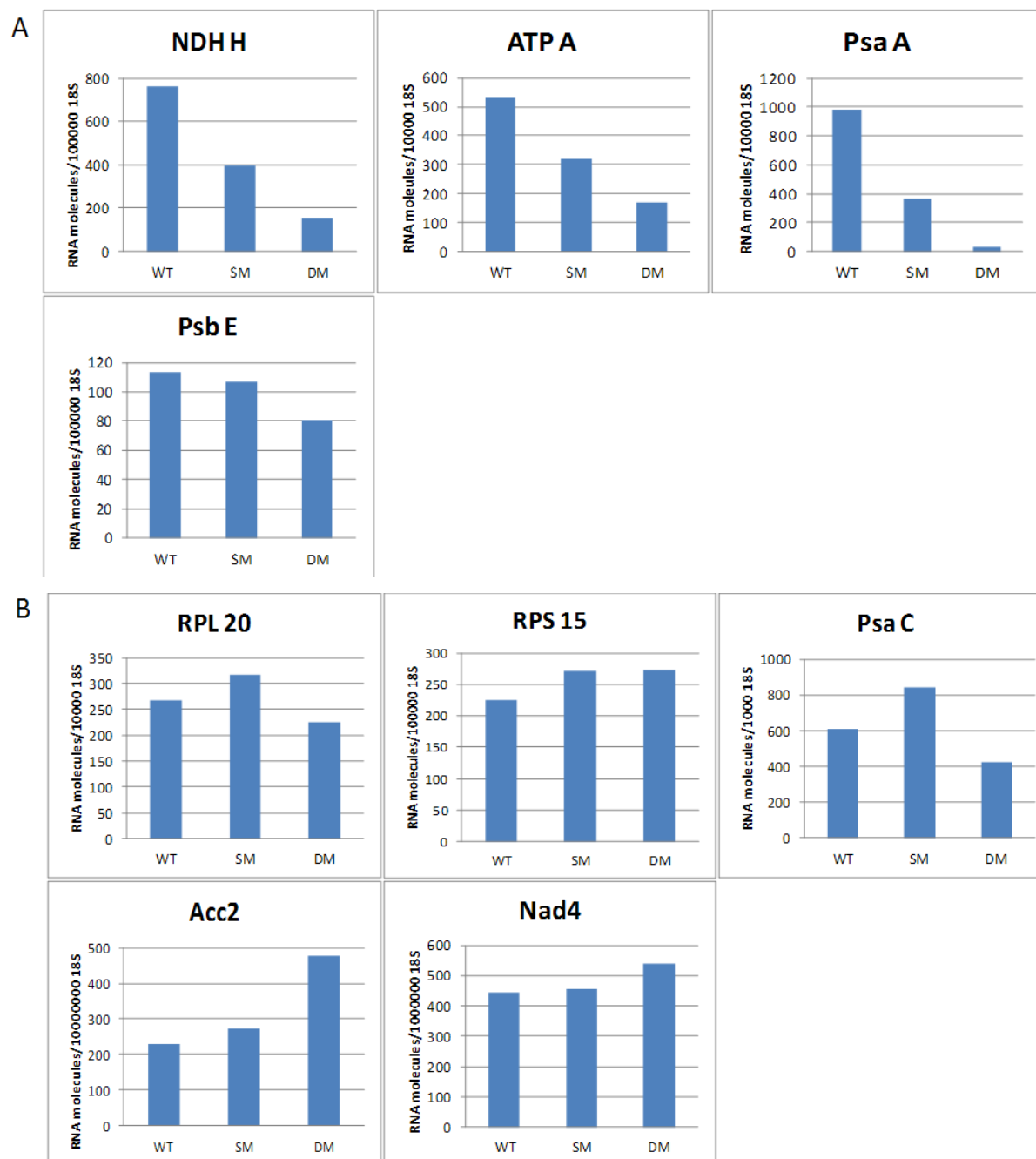


Figure 18 Relative transcript levels of regulated genes in *tic22IVsm* and *tic22dm*

Quantification of the gene expression of down (**A**) and up (**B**) regulated genes in the *tic22IVsm* (SM) and *tic22dm* (DM) using RT-PCR. RNA of 14 days old seedlings was isolated and 100 μ g RNA was reverse transcribed into cDNA as described in Methods. The cDNA was diluted 1:20 and used for light cycler RT-PCR as described in methods. The qRT-PCR contained 49 cycles. The mRNA amount (arbitrary units, n=1) was normalized to appropriate transcripts of 18S.

Table 7 Overview of regulated genes in *tic22dm* compared to WT

Depicted are the genes, which are down- or upregulated in *tic22dm*. The fold change represents the potency of the regulation in *tic22dm* compared to WT. The end of the table shows the results of the qRT-PCR, where the gene expression of the respective genes in *tic22IVsm* (SM) and *tic22dm* (DM) was compared to the gene expression in WT.

downregulated			Microarray	RT-PCR	
Name	ATG number	function	fold change	regulation in SM	regulation in DM
NDH H	Atcg01110	photosynthetic electron transport	8,9	2-fold	5-fold
ATP A	Atcg00120	conversion of ADP to ATP	5,5	1.7-fold	3-fold
PSA A	Atcg00350	reaction center for PSI	5,2	2.7-fold	34-fold
PSB E	Atcg00580	electron donor/acceptor	4,8	equal	1.7-fold
upregulated					
RPL 20	Atcg00660	ribosomal protein, translation	6	1.2-fold	0.8-fold
RPS 15	Atcg01120	ribosomal protein, translation	4,9	1.2-fold	1.2-fold
PSA C	Atcg01060	photosynthesis	4,1	1.4-fold	0.7-fold
ACC 2	At1g36180	fatty acid synthesis, metabolism	3,1	1.2-fold	2.1-fold
NAD 4	Atmg00580	cellular respiration	3	1.03-fold	1.2-fold

To summarize the results, the characterization of *tic22dm* revealed that the knock-out of both genes, TIC22III and TIC22IV, led to a chlorotic phenotype at the side areas of the leaves. Though no differences in photosynthetic activity between WT and *tic22dm* could be detected, several thylakoidal genes were found to be up- and down regulated in *tic22dm* compared to WT. Furthermore, *tic22dm* showed an enhanced gene expression of LHCB, ATPase and OE23 genes in the leaf tip compared to the side areas, which showed the pale leaf color. An explanation for these divergent results could be that the altered thylakoid composition in the chlorotic leaf parts might also influence the gene expression in the leaf tip by certain still unknown cell signaling pathways.

4.1.8 Gene silencing of TIC22V by RNAi

The third protein, which is thought to belong to the Tic22 family, Tic22V (At5g62650), possesses properties which differ from TIC22III and TIC22IV as described in chapter 4.1.1. The mature protein has a molecular weight of 50.2 kDa, which is as twice as large as the other two forms and – in contrast to the two other isoforms - it has not been characterized as an import component so far (Jarvis, 2008).

For characterization of Tic22V, one single T-DNA line (N614348) was available, which had already been analyzed in our group before (done by Dr. Elisabeth Ankele). However, since no homozygous mutants were found in spite of screening of more than 300 plants, indicating that the knock-out of Tic22V might be lethal. Therefore, another experimental approach was selected to characterize the function of the protein. For this purpose, RNA interference (RNAi) lines were generated by cloning the first 429 bp of TIC22V into the pOpOff2 plasmid vector (Wielopolska *et al.*, 2005). This vector allows dexamethason-induced repression of

RNA of plant genes, which leads to the silencing of the target genes. The construct was stably transformed into Col-0 and in a *tic22dm* line (#221) and transformed plants were selected on MS media supplied with the selection antibiotic hygromycin. Three lines which contained the RNAi vector were recovered and first analyzed regarding their phenotypes. Thereby, the influence of the TIC22V silencing on the one hand in WT and on the other hand in *tic22dm* was investigated. The induction of TIC22V silencing with dexamethason showed a retarded growth of *tic22dm* plants containing the induced RNAi-construct (*tic22dmRNAi*) in the first 10 days of development (Figure 19). Additionally, the *tic22dmRNAi* seedlings showed violet cotyledones (Figure 19 A), whereas WT seedlings showed no phenotypic alteration. The phenotype disappeared after approximately 10 days (Figure 19 B), which might indicate that this observation was due to stress caused by dexamethason and not induced by the gene silencing of TIC22V. After transferring the plants onto soil and stringent watering with dexamethason, no differences between RNAi induced WT and *tic22dm* were detected compared to non-induced WT and *tic22dm* (data not shown).



Figure 19 Inducible RNAi of TIC22V

A) Four days old F2 generation of Col-0 and *tic22dm* #221 plants grown on 1/2 MS + 1% sucrose, without (-dex) and with 10 μM dexamethason (+dex) **B)** 14 days old F2 generation of Col-0 and *tic22dm* #221 plants transformed with the inducible RNAi system TIC22V/pOpOff2 grown on 1/2 MS + 1% sucrose supplied with 10 μM dexamethason. The plants were grown under long day conditions.

To ensure that the RNA synthesis was successfully silenced due to active RNAi, qRT-PCR of WT and *tic22dm* plants, which were either non-induced or induced, was performed (Figure 20). However, the expression of Tic22V was not reduced in the induced WT, but showed a slightly higher expression after RNAi induction with dexamethason (Figure 20, WT +dex). In contrast, the expression of TIC22V was reduced in both induced *tic22dm* lines, indicating

TIC22V silencing in these plants. Since there was residual RNA transcript left, it had to be assumed that the RNAi silencing approach was not completely successful and that the Tic22V protein was still synthesized. The expression of TIC22V was 4-fold lower in the *tic22dmRNAi* #221 line than compared to *tic22dmRNAi* #1 (0.7-fold) by comparing both lines to the respective non-induced lines, which was in line with the phenotype observed in Figure 19 A. Although the phenotype disappeared in seedlings older than four days, the expression of TIC22V seemed to be repressed in 14 days old plants, indicating that the TIC22V silencing did not have any impact on the development of the plant.

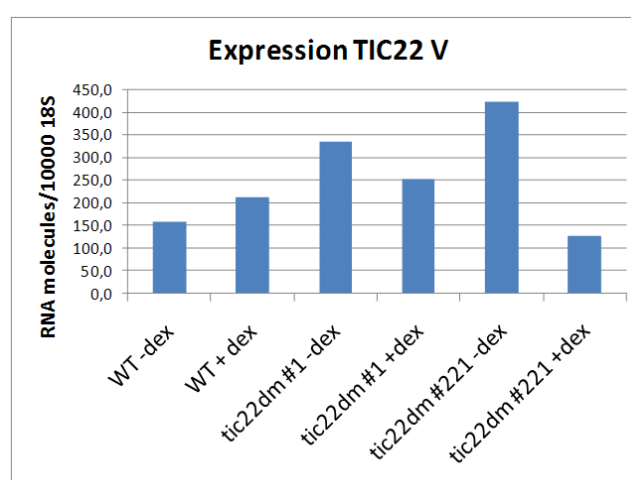


Figure 20 TIC22V transcript levels in RNAi-induced and non-induced WT and *tic22dm* plants

Quantification of the TIC22V mRNA level using qRT-PCR. RNA was prepared of 14-days old seedlings of RNAi-induced and non-induced WT and the *tic22dm* plant lines #1 and #221. Depicted are the results obtained from dexamethason uninduced (-dex) and induced (+dex) plants. The RNA amount was normalized to 10000 18S transcripts.

Furthermore, the influence of TIC22V RNAi on seed development was investigated. For this approach, the seeds of 10 siliques per line were counted (Figure 21). It turned out that the number of seeds of non-induced plants was equal in WT and *tic22dm* (average: 40 seeds per silique), whereas the number of the seeds was slightly although not significantly decreased upon induction of the RNAi system by dexamethasone treatment. Furthermore, less seeds were present in the induced *tic22dm* (average: 24 seeds per silique) compared to the induced WT (average 29 seeds per silique), indicating that the silencing of TIC22V might influence the seed development stronger in *tic22dm* than in the WT. This result indicated that the TIC22V silencing might be successful during seed development, especially in the WT, since the Tic22V silencing in mature induced WT leaves could not be shown (Figure 20).

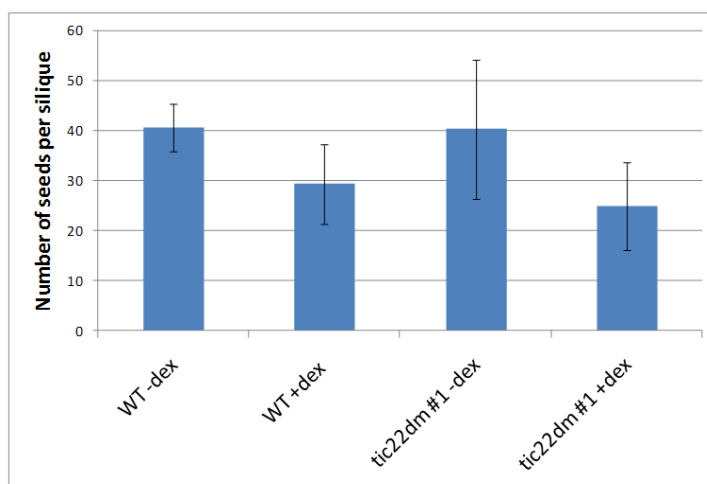


Figure 21 Number of seeds per silique in dexamethason induced plants

Plants of WT and *tic22dm* #1 were grown under normal longday conditions on ½ MS plates with and without 10 µM dexamethason. After 14 days, plants were transferred onto soil and watered with and without dexamethason until the plants developed seed containing siliques. 10 siliques per line were harvested and the comprised seeds were counted.

4.1.9 Isolation of TIC22V knock-out mutants

Silencing of TIC22V using RNAi method gave no clear information about the function of Tic22V in *A. thaliana* plants. Moreover, at a later time point of the present thesis, a T-DNA line of the TIC22V gene (Salk_106217) became available. Thus, the aim was to identify homozygous mutant plants. For this purpose, seedlings were screened for the presence of potential T-DNA insertion in exon 7 with oligonucleotides either amplifying a part of the WT gene sequence or, if existent, a part of the T-DNA sequence (Figure 22 A). This screening procedure resulted in two lines, which were found to be heterozygous for TIC22V (lines #13 and #114, Figure 22 B). Selfing of the parental lines produced exclusively heterozygous and WT progeny, whereas no homozygous loss of function plants were found. The screening of the plant line *tic22V* #114 depicted a weak band using oligonucleotides for the WT sequence and an intense band using oligonucleotides, which amplified the T-DNA, whereas plant line *tic22V* #13 showed an intense band upon performing the WT screen, whereas the resulting band after the T-DNA screen was weak. These lines were used for further analysis as they were expected to be heterozygous for the T-DNA insertion.

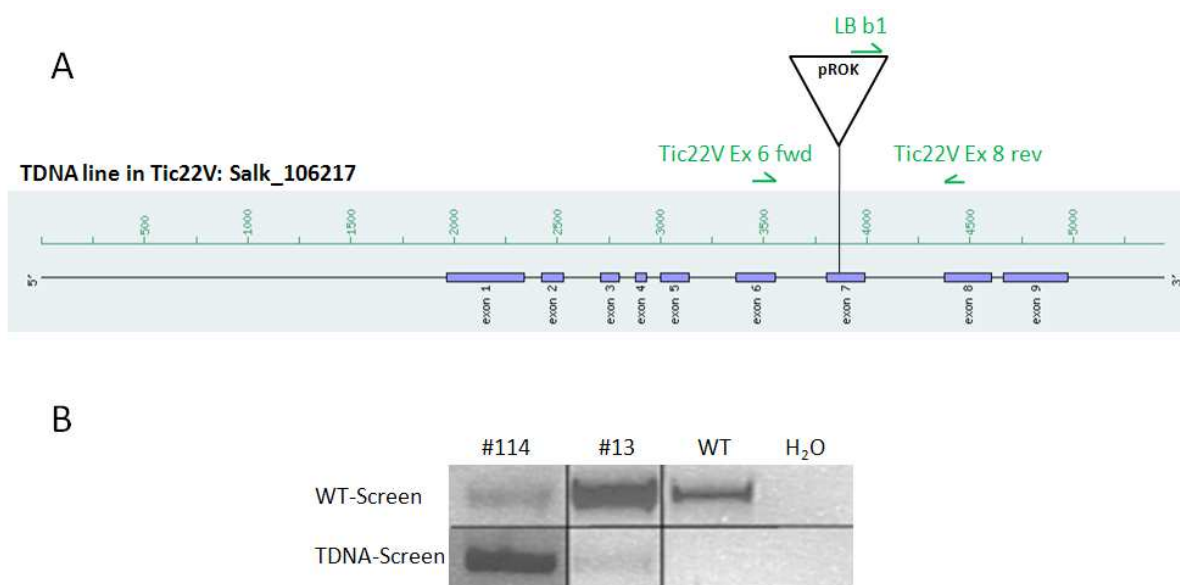


Figure 22 Schematic representation of the genomic DNA of TIC22V including the T-DNA insertion

A) Prediction of the genomic DNA sequence of TIC22V comprising 9 exons and the T-DNA insertion Salk_106217 in exon 7 (black triangle). Oligonucleotides used for screening procedures are shown in green. **B)** Agarose gel containing PCR products (Oligonucleotides: WT-Screen: Tic22Ex6fwd and Tic22Ex8rev, T-DNA-Screen: LBb1 and Tic22Ex8rev). WT- and T-DNA screenings of *tic22V* #114 and *tic22V* #13 as well as a control (WT) for WT and T-DNA is shown.

Initial analysis of selfed Tic22V heterozygous plants did not reveal homozygous mutants. Thus, siliques were investigated with regard to potentially aborted seeds. As shown in Figure 23 A no underdeveloped or aborted seeds were present in WT or mutant siliques, indicating that seed development is not disturbed in the heterozygous mutant. Subsequent germination test did also not reveal any differences between WT and mutant seeds, which leads to the conclusion that the failure to produce homozygous plants could be due to pollen sterility. Further substantiation for this notice could come from analyzing segregation behavior of the progeny – a ration of 50/50 WT/heterozygous is a strong hint at a defect in the male gametophyte. This investigation has to be performed in future experiments.

To investigate, if the T-DNA insertion in TIC22V had impact on the embryo development, 500 seeds were weighed. Interestingly, the seeds of the selfed *tic22V* plants were slightly heavier than WT plant seeds, indicating potential differences during embryo development (Figure 23 B). However, the standard deviations in both lines showed that the differences in seed weight were not substantial.

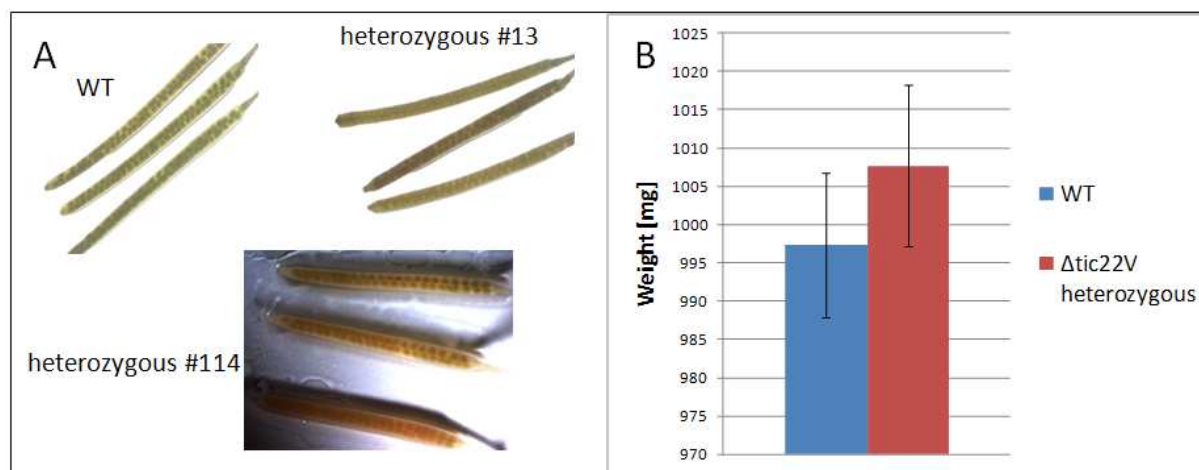


Figure 23 Analysis of siliques and seeds of WT and selfed *tic22V*

A) Whole siliques of WT and the two heterozygous *tic22V* lines #13 and #114 were bleached in 100% ethanol for seven days and analyzed using a binocular. **B)** Average weight of 500 seeds per WT and selfed *tic22V* #114 (in [g]).

4.1.10 Localization of Tic22V

In the next step, the exact localization of mature Tic22V was to be determined. For this purpose, the gene sequence of the full length TIC22V was cloned into a translation vector (pSP65), *in vitro* synthesized and the translation product was incubated with isolated pea chloroplasts to follow the import pathway of the protein (Figure 24). The import without subsequent fractionation (lane 2, 3) showed one protein band, which could represent the mature (m) size of the Tic22V protein (Figure 24, m, 50.7 kDa). However, this band remained present after digestion with thermolysin, but also the protein band representing the precursor protein (p) was still detectable after protease treatment, either indicating that the protease concentration was too low or that Tic22V was not completely imported into the chloroplasts, but remained attached to the TOC translocon, exposing the main precursor part to the thermolysin accessible outer envelope of the organelle. The separation into soluble (S) and membrane (M) fractions (lanes 4-7) was achieved by lysis of the chloroplasts (10 mM HEPES-KOH for 30 min of ice) and subsequent ultracentrifugation (256.000 x g for 10 min). Without protease treatment, the precursor protein could be found in a soluble form in low amounts and more abundant in the membrane fractions, whereas the protease treatment did not lead to the complete degradation of Tic22V bound to the accessible outer membrane (+Thl, M). The results suggested an exclusively membrane-associated localization of Tic22V (Figure 24, red box), indicating that it might represent a membrane integrated or – associated protein.

The control protein FNR was successfully imported into the chloroplasts, since the mature

band was not removed after protease treatment (FNR, m). Furthermore, the FNR showed the expected distribution of membrane- bound and soluble forms (Benz *et al.*, 2008).

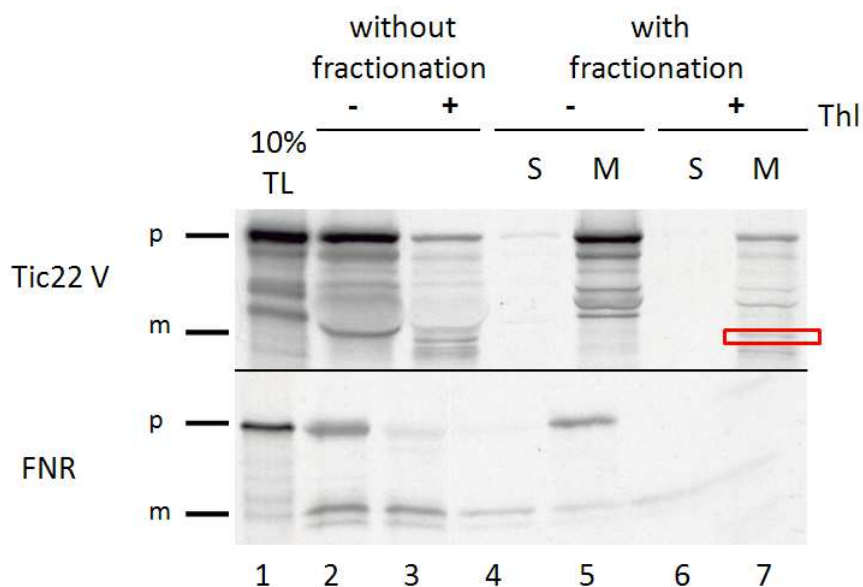


Figure 24 Import of Tic22V into pea chloroplasts

Tic22V and FNR (control protein) were in vitro translated in presence of [³⁵S]-methionine in Wheat Germ lysate and imported into isolated pea chloroplasts at 25°C for 15 min in a standard import reaction containing 3 mM ATP. After import, samples were directly treated with thermolysin (Thl, lane 3) or additionally lysed in 10 mM HEPES-KOH (pH 7.6) and fractionated in stromal (S) and membrane (M) fractions using ultracentrifugation at 256.000 x g for 10 min (lane 4-7). Precursor (p) and mature (m) proteins were visualized by autoradiography films after separating the proteins on a 12.5% SDS-PAGE.

4.1.11 Structural analysis of *Synechocystis sp.* Tic22 by X-Ray crystallography

In addition to the functional characterization of *A.thaliana* Tic22, it was aimed to determine the three-dimensional structure of the protein by X-ray crystallography. By using the Tic22 proteins from *A. thaliana*, *Pisum sativum*, *Plasmodium falciparum*, *Toxoplasma gondii* and *Synechocystis sp.* (expression and purification of *Plasmodium f.* and *Toxoplasma g.* by Dr. Bettina Bölter), the aim was to obtain expression of one of these homologues in a soluble form in high amounts in order to determine conditions for the crystallization of the protein.

The expression of Tic22 from *A. thaliana* and from *Pisum sativum* exclusively yields non-soluble protein, by expressing the protein in *E.coli* (BL21) cells with the pET21d vector system for three hours at 37°C. The following gives a detailed description of the successful expression and purification of Tic22 of *Synechocystis sp.* PCC 6803 (slr0924), while the expression and purification of the other homologues is still in progress.

Tic22 of *Synechocystis sp.* PCC 6803 (slr0924) further named synTic22, was used to express the protein for subsequent applications. The cloning of synTic22 (amino acid MK – PK, beginning with the second methionine as starting point) into the expression vector pET21d

was kindly performed by Dr. Ingo Wolf. Former expression assays using the full-length protein revealed two protein bands, which could not be separated from each other, whereas the expression of the shorter protein led to a single band, which was used for further approaches (Figure 25).

```

1  MPWLQTFSFRRSPFSLARRHLKKNKIFVKIKSIFLLSLLFEATATMKSLLRIGATLGLIGTTAIGTWL
68  GTTLQALALPTEEVVKILQGVVPVFTIVDAQQGAPLVAVGNDNEKVTGVFISQQEANGFLQELKK
131 QKPDVGSQVSVQPVSLGEVVKIAQANANQTDPLGFAYVPIPAQVQAAQQMPNSEYQGGVP
191 LRVARGGEDQGYLTIQQENEQIIPFFLEASQIQQMVERFKQEQPAMADSIVIDVIAMENVISTL
254 QTSDDAMLKQIRIVPTQEAIQFIRLSLAQQPK

```

Figure 25 Putative protein sequence of synTic22

Green bars depict two potential start methionines resulting in a 32 kDa and a 26 kDa protein. Underlined is a putative Sec signal peptide as predicted by PRED-TAT algorithm (Bagos *et al.*, 2010). The second methionine served as starting point for translation.

Expression trials with synTic22/pET21d under several expression conditions (12°C over night, 18°C over night, 28°C 3h and 37°C 3h) did not succeed in sufficient amount (3.87 µg/µl in total 40 µl, Figure 26 A, Con.), independent on the culture volume which was used (1 to 3 liters). Therefore, synTic22 was cloned into other expression vectors (pRSetA, pHue and pET21b), in order to obtain sufficient protein amounts for crystallization purposes. Overexpressing the protein in pRSetA, comprising a polyhistidine tag (Invitrogen, Karlsruhe, Germany) and pHue, comprising a histagged ubiquitin tag (Catanzariti *et al.*, 2004), which have been published to be suitable for high-level expression and easy purification of recombinant proteins, did not lead to suitable protein amount: Using the vector pRSetA as an expression system, no protein was achieved after induction with 1 mM IPTG (Figure 26 B). The gel shows the expression in a one-liter-culture for 3h at 37°C, but the expression conditions were also varied (12°C over night, 18°C over night, increasing the IPTG concentration up to 10 mM and using different culture volumes from 30 ml to 3 liters), not leading to a protein expression under any given condition.

The protein expression with the ubiquitin tag system (vector pHue) led to a successful synTic22 expression after induction with 1 mM IPTG (Figure 26 C). Again, the construct was transformed in E.coli BL21(DE3) cells and grown in a one-liter-culture. After induction of the protein expression with 1 mM IPTG, the culture was incubated at 37°C for 3h and the protein was separated in soluble and membrane forms by centrifuging the disrupted bacterial cells at 30.000 x g for 30 min. The supernatant, which contained the soluble protein, was then purified by Ni²⁺-NTA affinity chromatography. Afterwards, the protease Usp2 cut the protein at a specific recognition side between synTic22 and ubiquitin, resulting in a soluble form of

synTic22 which did not comprise the tag anymore. Remaining ubiquitin in the solution was removed by the addition of further Ni-NTA beads, binding the tag via its polyhistidine tag. The unbound protein was then concentrated to a final volume of 50 μ l (Figure 26 C, Con.) and protein amount was determined. Under each expression condition, the protein amount was not sufficient to continue with crystallization trials (\sim 50 μ g in total). Thus, the gene sequence of synTic22 was cloned into another vector (pET21b), which was available in our lab and comprised well expression properties before (personal communication).

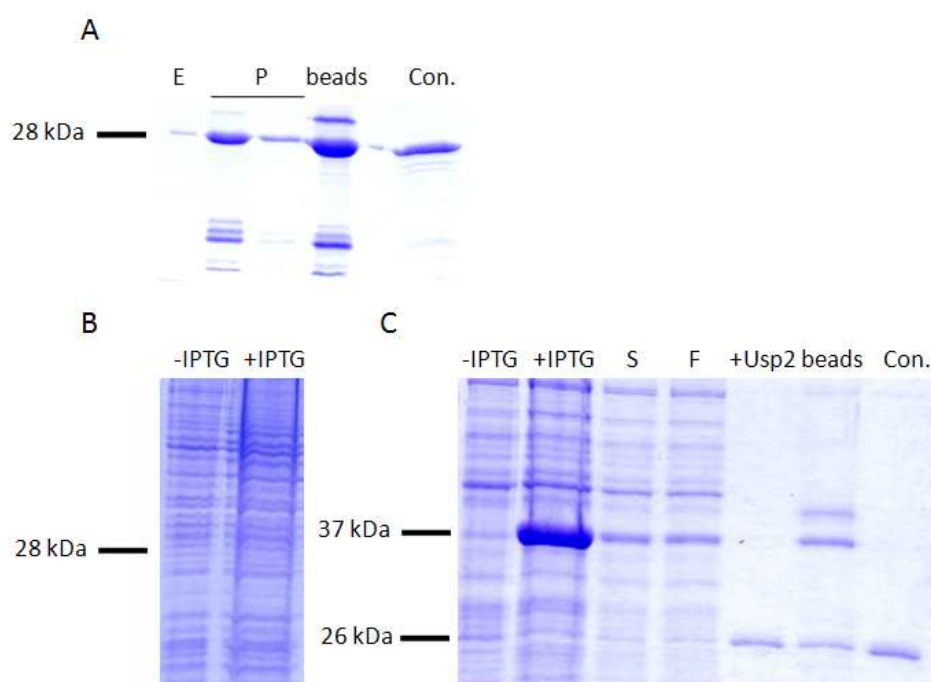


Figure 26 Expression trials of synTic22 with different expression systems

synTic22 was expressed in the vectors pET21d (A), pRSetA (B) and pHue (C). The depicted gels show exemplarily the expression performed in a one-litre-culture with BL21(DE3) E.coli cells. Induction of protein expression was performed with 1 mM IPTG. All samples were loaded on a 12.5% SGS-PAGE (A) The purification of synTic22/pET21d was achieved by binding the soluble protein to Ni-NTA agarose via its polyhistidine tag and incubation for 3h at 4°C. The suspension was subsequently eluted with 100 mM imidazole and centrifuged at 50.000 x g for 20 min. 5 μ l of the 20 ml elution (E) and the pellet fractions (P), as well as the Ni-NTA beads after eluting the protein and 4 μ l of the concentrated protein (40 μ l) were loaded on a 12.5% SDS-PAGE. The protein concentration was 3.87 μ g/ μ l. (B) No protein expression was achieved by expression synTic22 in pRSetA using the conditions described above. (C) The protein expression using the pHue system was achieved in high amounts after induction with 1 mM IPTG (+IPTG). 10 % of the supernatant (S), obtained after separating the cells in soluble and membrane parts, and 10% of the TCA precipitation was loaded on the gel as well. The soluble protein was bound to Ni-NTA for 3h at 4°C and the protease Usp2 was added to the column. Soluble protein without containing the tag was obtained (+Usp). The beads were loaded on the gel as well to control the remaining protein. 10% of the concentrated protein (Con.) was also loaded on the gel.

Overexpression of synTic22 in pET21b at 37°C for 3h offered optimal conditions to produce sufficient amounts of soluble protein (Figure 27 A). For purification, the soluble protein was first enriched by Ni²⁺-NTA (Figure 27 B), and purified further by ion exchange chromatography. After binding the soluble synTic22 to the Ni-NTA (affinity binding for 3h), it

was first eluted with 50 mM imidazole, which resulted in pure protein, although in low amounts. Therefore, synTic22 was subsequently eluted with 100 mM imidazole (Figure 27 B), separating the protein from the agarose beads more efficiently, and additionally resulting in a high protein amount. As unspecific bound proteins were eluted as well, additional purification steps became necessary.

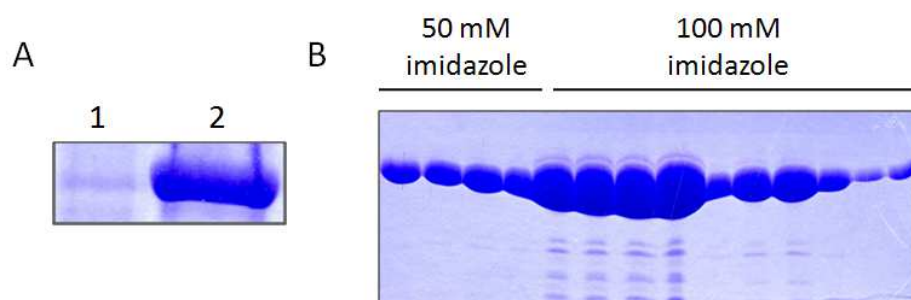


Figure 27 Overexpression and purification of *Synechocystis* sp. Tic22

synTic22/pet15b was transformed and overexpressed as described in Methods. The overexpression was performed for 3 h at 37°C after induction with 1 mM IPTG. **A)** 1 ml cell culture was centrifuged and the cell pellet resuspended in solubilization buffer before (1) and after (2) induction with 1 mM IPTG and 3h of overexpression at 37°C. **B)** After affinity chromatography (Ni-NTA) the protein was eluted 4 times with 50 mM imidazole and 10 times with 100 mM imidazole. The fractions were combined and concentrated to an appropriate volume for further chromatography steps (1 ml for IEC, see below).

For subsequent purification of synTic22, anion exchange chromatography was performed (Figure 28 A). Since the pI of synTic22 is comparatively acidic (pI 5.08), this method seemed to be promising to remove unspecific proteins. For this purpose, the elution fractions obtained by Ni-NTA chromatography were concentrated to a final volume of 1 ml using a centrifugal filter (Amicon, Millipore). During this procedure, the salt concentration in the sample was minimized by dilution (150 mM NaCl to 10 mM NaCl), simultaneously enriching the protein. The sample was subsequently passed over a HiTrapQFF column under low salt conditions (50 mM Tris, 10 mM NaCl, pH 8.0) and the protein was eluted by a linear gradient, where the salt concentration was slowly increased (0-1 M NaCl). Unbound protein was detected in fractions prior to ion exchange (Figure 28 A, red arrows), whereas synTic22 was eluted by increasing amount of NaCl (Figure 28 A, green arrow). Analysis of further peak fractions by SDS-PAGE verified that Tic22 was further enriched (Figure 28 A, SDS-PAGE).

The resulting fractions (Figure 28 A, B 10-15) were combined, concentrated and purified using size exclusion chromatography (Figure 28 B) on Superdex75 matrix (GEHealthcare, Uppsala, Sweden). High molecular weight oligomers or aggregates eluted in the void volume (Figure 28 B, red arrow), while synTic22 was detected in later fractions (Figure 28 B, green

arrow). The fractions B 1-3 were combined and concentrated to a final volume of 50 μ l. Aggregates (Figure 28 C, 2) were removed by centrifugation (20.000 x g, 20 min) and the soluble protein (Figure 28 C, 1) was subjected to crystallization trials (Ira Schmalen, group of Eva Wolf, MPI Martinsried). The protein was exposed to 6 screens (Hampton Research Index, Qiagen JSCG+, Qiagen Classics, Qiagen pH Clear I and II, Morpheus, see Methods 3.4.10), which represent the standard crystallization screens, but synTic22 did not form crystals at any given buffer composition and crystallization condition.

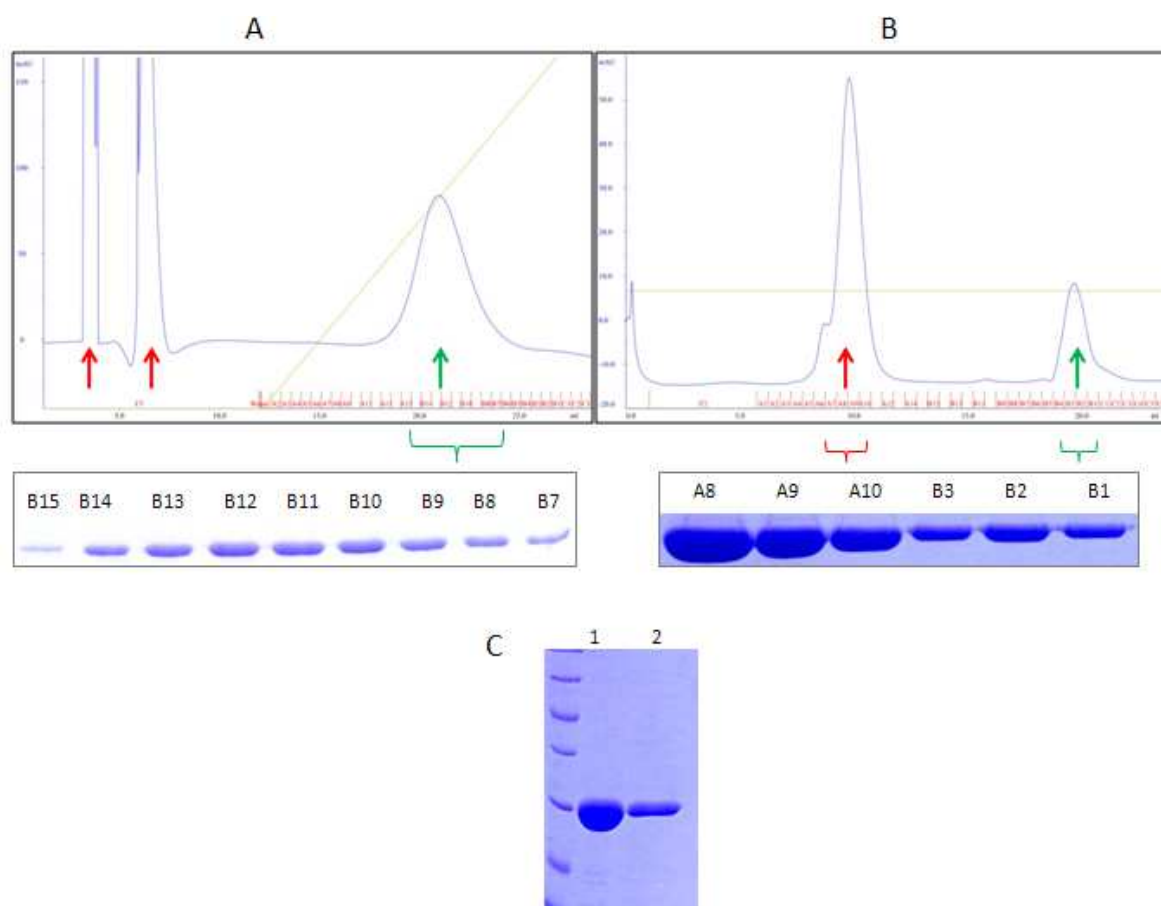


Figure 28 Anion Exchange Chromatography and Size Exclusion Chromatography of synTic22

A) Ni-NTA purified synTic22 (see Figure 24 B) was further purified by Anion Exchange Chromatography. Red arrows depict proteins, which were not bound to the column. The green arrow shows the eluted synTic22. 5 μ l of the 250 μ l elution fractions were loaded on a 12.5% SDS page (B 10-B 15, Coomassie staining). The fractions were combined, concentrated using an Amicon Ultra centrifuge filter (Millipore, Darmstadt, Germany) and purified by Size Exclusion chromatography (**B**). Red arrow depicts the aggregate fractions (A 8-A 10), green arrows shows the eluted synTic22 (B 1-B 3). The fractions B 1-B3 were combined and concentrated to a final volume of 50 μ l. Centrifugation at 20.000 x g for 20 min separated soluble (**C**, 1) and aggregated (**C**, 2) protein. The soluble protein (final concentration: 30 μ g/ μ l) was used for crystallization procedure (performed by Ira Schmalen, MPI Martinsried, Germany).

4.2 Characterization of Tic62/Trol and their relation to FNR

In the second part of this work, two further chloroplast proteins - Tic62 and Trol - were characterized in more detail as both proteins are known to play a distinct role in photosynthetic processes.

Previous studies revealed that Tic62 interacts with the ferredoxin-NADPH-oxidoreductase (FNR), which is responsible for the electron transfer from ferredoxin to NADP^+ , representing the last step of the light electron transfer chain (Benz *et al.*, 2009). Furthermore, it has been shown that the localization of Tic62 changes between IE, stroma and thylakoids, dependent on the day and night cycle: At night, FNR accumulates at the thylakoids associated with Tic62, whereas at the beginning of the day, when the electron transfer at the thylakoids starts, FNR dissociates from the membrane (Benz *et al.*, 2009).

Additionally, the thylakoid rhodanese like protein (Trol) was shown to represent a second docking station for FNR, tethering the protein to the thylakoid membrane (Juric *et al.*, 2009). A direct interaction between Tic62 and Trol has not been demonstrated so far, indicating that the proteins act independently from each other.

4.2.1 Generating *tic62trol* double mutants

To investigate a possible relation between the two interaction partners Tic62 and Trol and to analyze potential effects on attachment of the soluble FNR to the thylakoids, double mutants lacking *tic62* as well as *trol* were generated and the influence on photosynthetic activity was analyzed. Homozygous single mutants had already been generated by Dr. Philipp Benz in our laboratory. The T-DNA SAIL_124G04 is located in exon 6 of TIC62 (Figure 29 A) and the T-DNA SAIL_27B04 is inserted in intron 7 of the TROL gene (Figure 29 B). Homozygous single mutants of *tic62* and *trol* plants were crossed (see chapter 3.1.2) and subsequently screened for both T-DNA insertions. As shown in Figure 29 C, a PCR reaction using oligonucleotides amplifying the WT gene sequence of TIC62 (*tic62* In4 fwd, *tic62* Ex6/8 rev, Figure 29 A) did not amplify the gene in the lines 2-8 6 and 2-1 18, whereas a gene product was obtained in the line 13-5 1, which was in further experiments used as a heterozygous plant line, still containing the functional TIC62 gene. The PCR carried out for the detection of the T-DNA, which was performed with oligonucleotides amplifying a T-DNA fragment (*tic62* In4 fwd, LB1, Figure 29 A), resulted in PCR products in all three lines, indicating the presence of the T-DNA in the respective gene sequence. The WT-PCR with oligonucleotides amplifying a part of the TROL gene sequence (*trol* Ex7 fwd, *trol* 3' UTR rev,

Figure 29 B) was not successful in all three plant lines, whereas a gene product was obtained in WT plants, confirming the insertion of the T-DNA within TROL, whereas the PCR with the oligonucleotide trol 3' UTR rev and the specific T-DNA oligonucleotide LB1 showed PCR products in all lines, demonstrating the existence of the T-DNA in all three lines. To verify the PCR result, two plants were tested per line (1 and 2).

The homozygous plant lines 2-6 8 and 2-1 18, containing both T-DNA insertions, were used for further experiments.

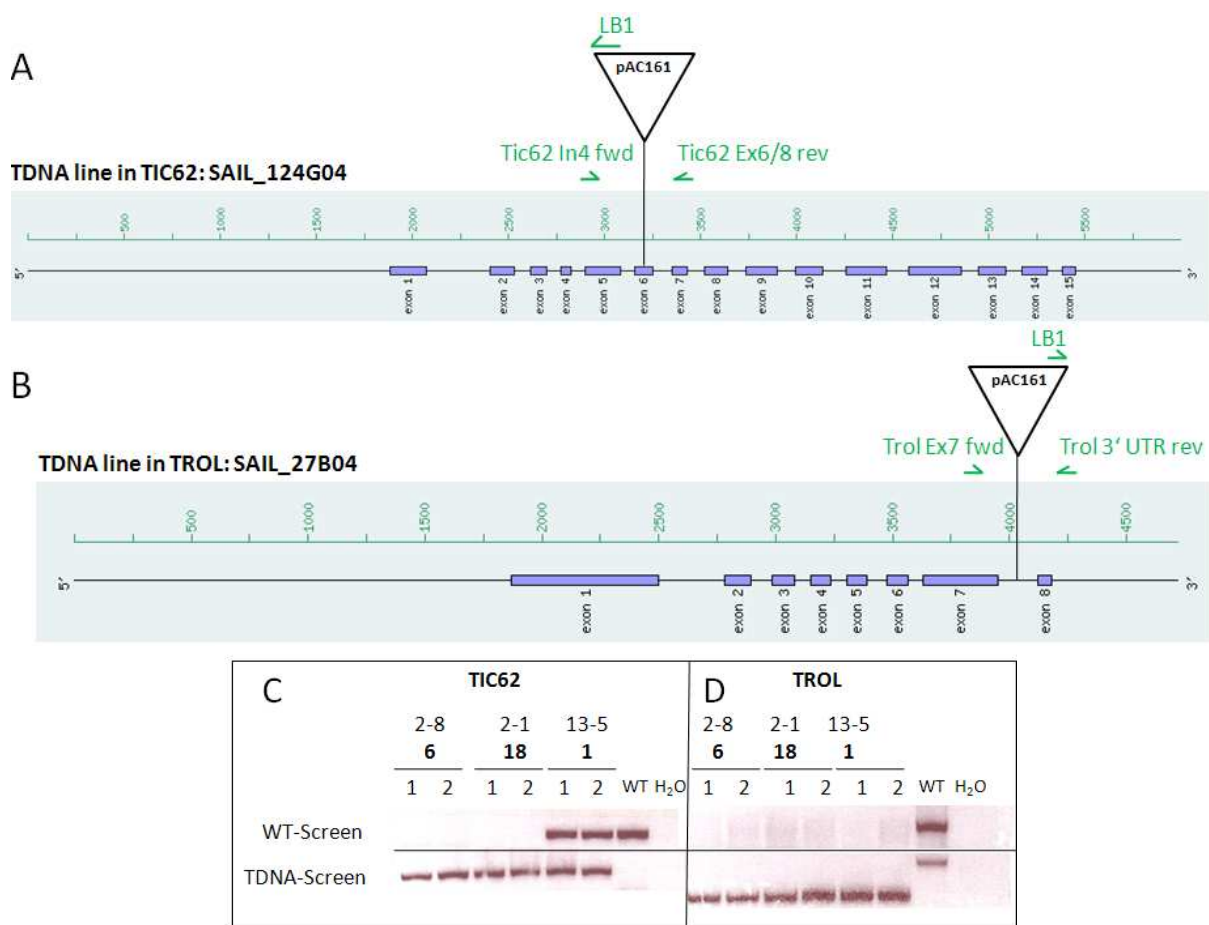


Figure 29 Schematic representation of the genomic DNA of TIC62 and TROL including screening for T-DNA insertions via PCR.

Prediction of the genomic DNA pattern of TIC62 (**A**) and TROL (**B**) according to <http://aramemnon.botanik.uni-koeln.de/>. The T-DNA insertion in TIC62 (vector pAC161, line: SAIL_124G04) was localized in the sixth exon. The molecular characterization was performed with the oligonucleotides Tic62 In4 fwd and Tic62 Ex6/8 rev to screen for WT lines and Tic62 In4 fwd and LB1 to screen for mutant lines (**A**). The T-DNA insertion in TROL (vector pAC161, line: SAIL_27B04) was localized in intron 7 and was detected by PCR with the oligonucleotides Trol 3' UTR rev and LB1. The Trol lines lacking the T-DNA insertion were verified by PCR with the oligonucleotides Trol Ex7 fwd and Trol 3' UTR rev (**B**). Screening of the genomic DNA of three lines 2-8 6, 2-1 18 and 13-5 1 was performed with TIC62 oligonucleotides (**C**) and TROL oligonucleotides (**D**).

To verify that the T-DNA insertions in TIC62 and TROL were true knock outs, RT-PCR analysis was performed. As shown in Figure 30, the RT-PCR performed with tic62 WT (lane 1)- and T-DNA oligonucleotides (lane 2) did not result in PCR products at appropriate size (see lane 3,

WT), indicating that no mRNA is synthesized due to T-DNA insertion. The cDNA of WT (positive control) still contained TIC62 (lane 3), whereas the PCR with T-DNA-oligonucleotides did not result in PCR products (lane 4). The control lanes (lane 5, 6) exclusively showed oligonucleotide bands, since the size of the TIC62 fragment is larger (lane 3). On the contrary, the RT-PCR using TROL oligonucleotides revealed remaining transcripts using WT (lane 7) and T-DNA (lane 8)-TROL oligonucleotides, indicating that RNA is still synthesized despite T-DNA insertion. Subsequent sequencing of appropriate fragments revealed parts of the TROL sequence.

The RT-PCR using WT-cDNA resulted in a PCR product using WT-oligonucleotides (lane 9) and no product using T-DNA-oligonucleotides (lane 10). The control RT-PCR using trol-oligonucleotides for WT (lane 11) and T-DNA (lane 12) depicted no PCR products. WT cDNA (13) and genomic WT DNA (14) was applied in a standard control reaction, where actin-oligonucleotides were used to control the performance of the PCR reaction. In both PCR reactions, the control revealed pure PCR products, which showed that the cDNA was suitable for RT-PCR and that the PCR reaction was successfully performed.

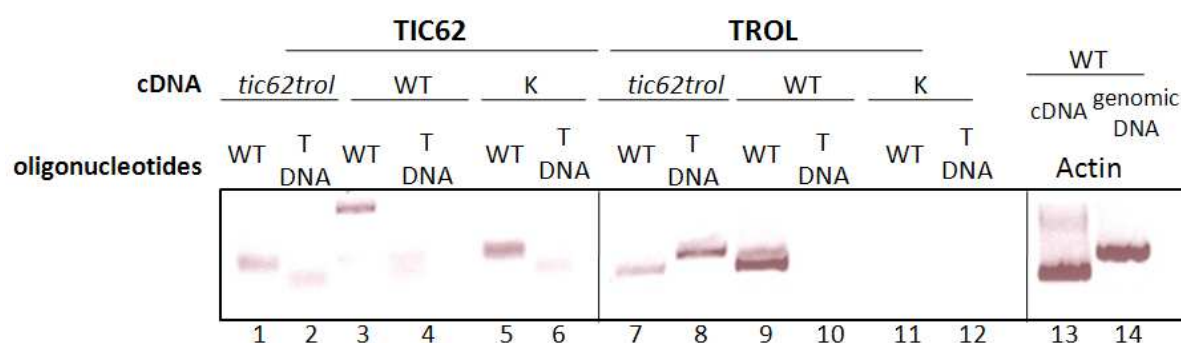


Figure 30 RT-PCR of WT and *tic62trol* cDNA

RT-PCR performed with cDNA of WT and *tic62trol* plants. *Tic62trol* cDNA (1, 2) and WT cDNA (3, 4) was analyzed with TIC62 WT oligonucleotides (1, 3) and TIC62 T-DNA oligonucleotides (2, 4). Lane 5 and lane 6 contain the water controls either with TIC62 WT oligonucleotides (5) or T-DNA oligonucleotides (6). *Tic62trol* cDNA (7, 8) was used for RT-PCR with TROL WT (7) and T-DNA (8) oligonucleotides and the same was performed with WT cDNA (9, 10). Water control lanes do not contain PCR product (11, 12). cDNA quality control was performed with actin oligonucleotides on WT cDNA (13) and genomic WT DNA (14).

However, immunoblotting of *tic62trol* plants (see Figure 31; performed by Minna Lintala, University of Turku) did not reveal any Trol protein in the mutant plants. Thus it can be noted, that despite synthesis of partial mRNA, there is no functional and full length Trol protein present in *tic62trol*. Furthermore, the soluble pool of FNR was increased in *tic62* and *tic62trol* plants, whereas the thylakoidal pool of FNR was reduced in *tic62* plants and totally missing from *tic62trol* thylakoids. In addition, the total FNR content was markedly decreased

in *tic62trol* plants (Figure 31).

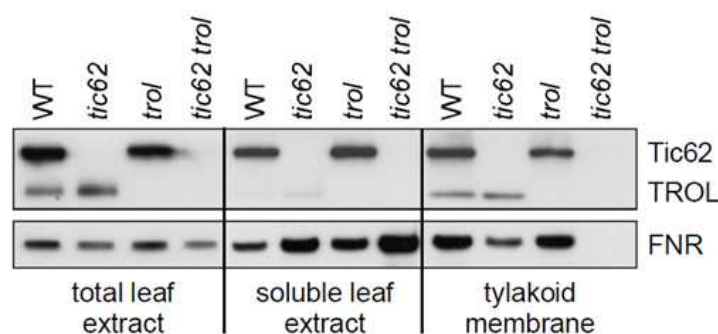


Figure 31 Tic62, Trol and FNR protein content in WT, *tic62*, *trol* and *tic62trol* plants (performed by Minna Lintala, University of Turku).

10 µg of protein was loaded on a SDS PAGE of the WT, *tic62*, *trol* and *tic62trol* total leaf extract, soluble leaf extract and thylakoid membranes. Proteins were immunodetected with Tic62 and FNR antibodies.

4.2.2 Localization of FNR in *tic62trol*

Earlier studies revealed that the FNR interaction with Tic62 and Trol results in thylakoid attachment (Benz *et al.*, 2009; Juric *et al.*, 2009). The current hypothesis that FNR is not only attached to the thylakoid membrane to stabilize it during time periods, where no or less FNR for electron transfer is needed, but to bring it in closer relation to PSI, where the last step of electron transfer occurs, is under debate. Investigating the knock-out mutants lacking both docking proteins for FNR should answer the question where the FNR was located and how this effect might influence photosynthesis.

In a first step, *A. thaliana* chloroplasts were isolated from 3-weeks-old plants and subsequently fractionated into stroma, thylakoids and envelope fractions. Polypeptides were separated by SDS-PAGE and afterwards an immunoblot was performed using antibodies against Tic62, FPBase, FNR, Oe23 and Oep21 (Figure 32). Tic62 was exclusively detected at the envelopes and thylakoids in the WT, whereas it was completely missing in the stroma, whereas in *tic62trol* no protein was found as expected. The FPBase-antibody used as stromal marker recognized the protein in WT and *tic62trol* in equal amounts. Residual FPBase was localized in envelope fractions, indicating a stromal contamination.

The FNR was detected in stromal fractions of WT and *tic62trol*, as well as at the thylakoids of the WT, but was completely lacking at the *tic62trol* thylakoids. The protein was also found in envelope fractions but as expected in lower amounts. Most importantly FNR was almost exclusively present in the stroma. Oe23 was used as thylakoid marker and was detected in both, WT and much less in *tic62trol*, and also in minor amounts in the stroma since it

represents a soluble luminal protein. Finally, the Oep21 protein, used as envelope marker, was detected in WT and *tic62trol* envelope fractions.

The verification that FNR is absent from the thylakoids in *tic62trol* led to the assumption that photosynthetic processes and/or metabolic pathways might be altered in *tic62trol*. This hypothesis was investigated in detail in further experiments.

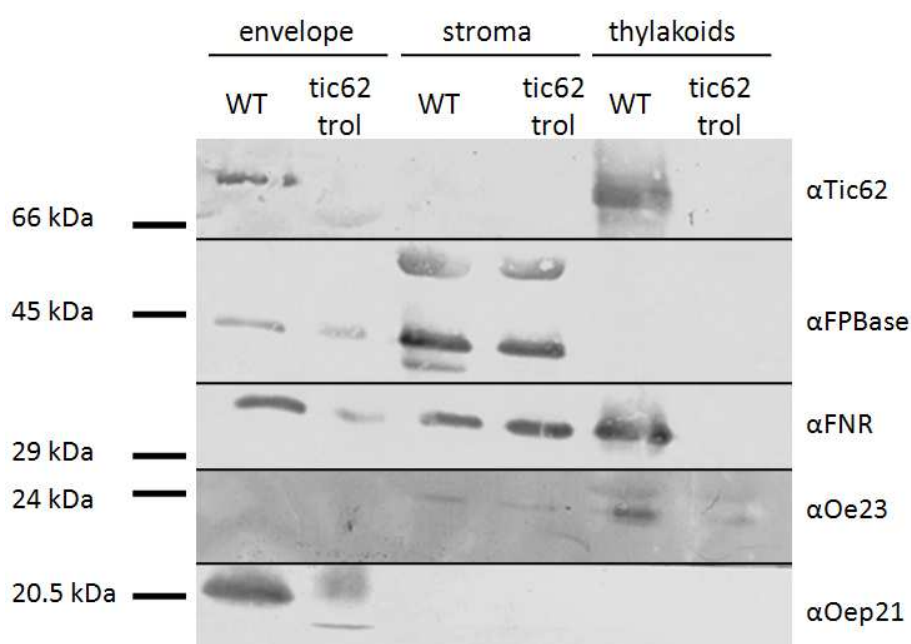


Figure 32 Immunoblot of stroma, thylakoid and envelope proteins isolated from *A. thaliana* chloroplasts

A. thaliana chloroplasts were isolated from 3-weeks-old plants and subsequently fractionated into stroma, thylakoids and envelopes. 20 μ g of each fraction were separated by a 12.5% SDS-PAGE and immunoblotted with antibodies recognizing Tic62, FPBase, FNR, Oe23 and Oep21 proteins.

4.2.3 Thylakoid complex composition in *tic62trol*

Blue-Native (BN)-PAGE was performed to determine possible differences in the composition of photosynthetic complexes in *tic62trol* (done with Minna Lintala, University of Turku, Finland). For this purpose, thylakoids were isolated of *A. thaliana* WT-, *tic62* single mutant-, *trol* single mutant and *tic62trol* double mutant plants, separated by a BN-PAGE (Figure 33 A) and immunodecorated with antibodies recognizing FNR, Tic62 and Trol (Figure 33 B).

In line with previous studies (Benz *et al.*, 2009, Juric *et al.*, 2009) the analysis of thylakoid protein complexes showed that the large protein complexes composed of FNR and Tic62 are completely missing in *tic62* single mutant plants, whereas FNR together with Trol was exclusively present in one protein complex of approximately 140 kDa in WT and *tic62* single mutant plants (Figure 33 B). Additionally, Trol was found to be present in at least one complex independently from FNR in WT and *tic62* plants. Neither with FNR nor with Tic62

antibodies the proteins could be detected in *tic62trol* thylakoid fractions, indicating an exclusive attachment of FNR to the thylakoid membrane via Tic62 and Trol. Furthermore, also the free FNR which is not associated with Tic62 and Trol in protein complexes is completely missing from *tic62trol* thylakoids.

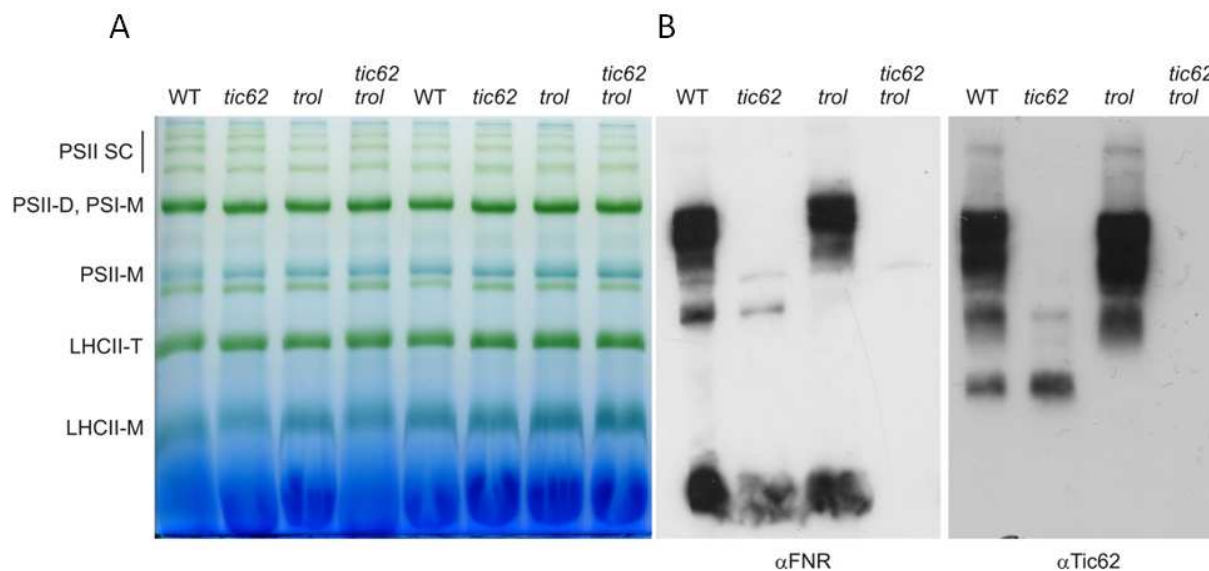


Figure 33 First dimension of Blue Native (BN)-PAGE of WT, *tic62*, *trol* and *tic62trol* thylakoids

A) High molecular weight complexes of thylakoids (5 μ g Chl) isolated from WT, *tic62*, *trol* and *tic62trol* plants are separated by BN-PAGE (5 to 13.5%). The experiment was performed together with Minna Lintala at the University of Turku in Finland. **B)** The BN-PAGE was used for performing immunoblots applying antibodies against FNR (left panel) and against Tic62 (right panel), which detects several large protein complexes of Tic62/FNR in WT and *trol* single mutant, one Trol/FNR complex at 140 kDa in WT and *tic62* single mutant and Trol complexes independent from FNR in WT and *tic62* single mutants.

The immunoblot and the first dimension of the BN-PAGE showed that the FNR was not able to bind to the thylakoid membrane in *tic62trol*, since Tic62 as well as Trol were missing. To investigate potential differences in the composition of thylakoid protein complexes in the mutant plants, a second dimension BN-PAGE was performed (Figure 34, done with Minna Lintala, University of Turku, Finland). To this end, high molecular weight complexes separated in the first dimension were further separated by SDS-PAGE and analyzed for differences in protein composition by silver staining. The only difference between WT and *tic62trol* thylakoids was a reduction of the NDH-PSI supercomplex in *tic62trol* (Figure 34, red box). However, this could not be repeated in additional experiments, indicating that the observed effect was due to preparatory artifacts. No further differences in thylakoid complex composition were detected.

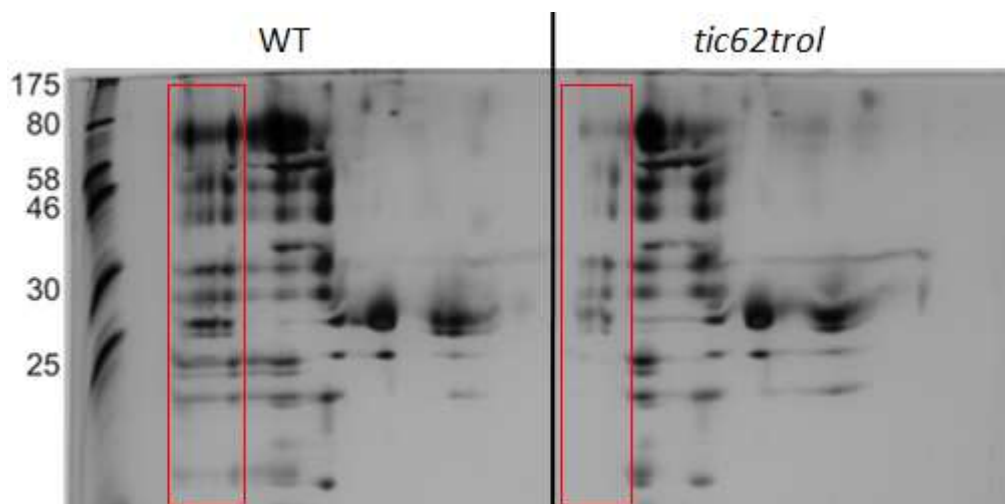


Figure 34 BN-PAGE second dimension of WT and *tic62trol* thylakoids

High molecular weight complexes separated by the first dimension were further separated by SDS-PAGE and visible by silver staining. The red frames depict differences in protein composition in NDH-PSI-supercomplex in WT (left panel) and *tic62trol* (right panel).

4.2.4 Phenotypic and photosynthetic analysis of *tic62trol*

The fact that FNR was not detected at the thylakoid membrane in *tic62trol* raised the question, whether and in which way the photosynthetic capacity is affected. Thus, the phenotype of the double mutant plants as well as the photosynthetic performance was further investigated. To analyze the phenotype of *tic62trol* compared to WT plants, seeds were grown under different light and growth conditions on soil. This analysis was performed by Minna Lintala (University of Turku, Finland). However, no phenotypic differences were observed, insubstantial if the plants were grown at long day, short day or continuous day-conditions or with 50 μmol , 100 μmol or 500 μmol light intensity (data not shown). Since the phenotypic analysis showed no effect of the *tic62trol* knockout on the plants, PAM measurements, determining the activity of PSI and PSII were performed (done by Minna Lintala, University of Turku, Finland). Again, no alterations in electron transfer were detected between *tic62trol* and WT plants, indicating that photosynthesis was not influenced, although the FNR was not tethered to the membrane.

4.2.5 Metabolic pathways influenced in *tic62trol* plants

Since no differences in photosynthetic activity were detected in *tic62trol* plants, metabolic effects were analyzed in order to investigate potential differences between *tic62trol* and WT. *A. thaliana* seeds were grown on MS plates without sucrose and harvested after 20 days at three time points. To cover the day/night cycle, plants were harvested at the end of the day (16 h light), at the end of the night (8 h dark) and in the middle of the day (after 8 h light)

by directly freezing the whole plant without roots in liquid nitrogen. The investigation of starch content, the AGPase activation state as well as the NADPH/NADP⁺ redox state was performed in cooperation with the group of Prof. Geigenberger (LMU Munich).

First, the starch content was analyzed in *tic62trol* and WT (Figure 35). Both plant lines showed typical starch amounts over the day and night course: At the end of the day, extensive amounts of starch have been synthesized, whereas during night, the starch content decreased in both plant lines (Figure 35 A and B). Exposing the plants to 100 μmol light intensity, no difference was detected between *tic62trol* and WT (Figure 35 A), whereas the light intensity of 50 μmol led to an increased starch content in *tic62trol* at the end of the night (Figure 35 B). The comparison between 50 μmol and 100 μmol light intensity, when exposing the plants for 10 minutes to light after the dark period, revealed an increased starch content in *tic62trol* under both growth conditions, however the effect was more pronounced upon exposure to 100 μmol light intensity (Figure 35 C).

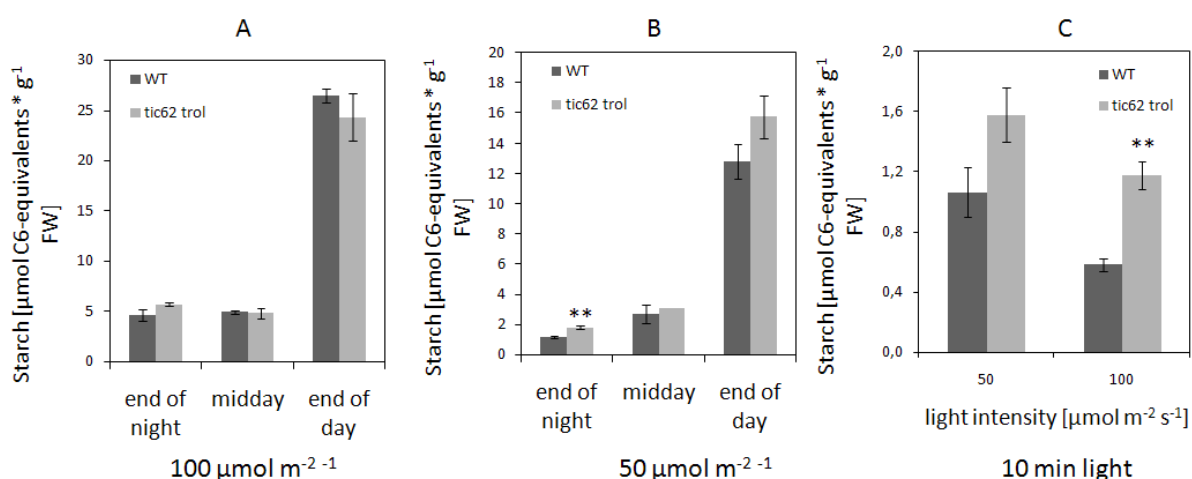


Figure 35 Starch content in *tic62trol* and WT at different time points and light intensities

A. *thaliana* plants were grown on MS plates without sucrose at (A) 100 μmol light intensity (n=4, no significant difference, SE) and (B) 50 μmol light intensity (n=3, **:p \leq 0.01, SE) for 20 days and subsequently harvested in liquid nitrogen after 8 h dark (end of night), after 8 h light exposure (midday) and 16 h light exposure (end of day) and (C) after 10 minutes light exposure after the dark period (50 μmol and 100 μmol light intensity, n=3, **:p \leq 0.01, SE). Metabolic analysis was performed by Ina Thormälen (AG Geigenberger, LMU Munich).

In order to investigate further metabolic components, which are influenced by the double knock-out of Tic62 and Trol, the activation status of ADP-glucose pyrophosphorylase (AGPase) was analyzed (Figure 36). This enzyme catalyzes the first step in starch biosynthesis by generating the sugar nucleotide ADP-glucose and inorganic pyrophosphate (P_i) from glucose-1-phosphate and ATP (reviewed in Orzechowsky, 2008). The increase of starch accumulation and/or synthesis as shown in Figure 35 could represent an effect of an altered

activation status of AGPase.

Differences in the enzyme activation status are usually determined by the APS1 (small subunit of AGPase) monomerization, indicating alterations during starch biosynthesis. As shown in Figure 36 A, *tic62trol* plants contained clearly increased AGPase activity at the end of the night in plants grown in 50 μmol light intensity. The activation status was not influenced in *tic62trol* plants when being exposed to 50 μmol and 100 μmol light intensity for 10 minutes after dark period (Figure 36 B). This correlates with the increased starch amount observed in *tic62trol* at the end of the night.

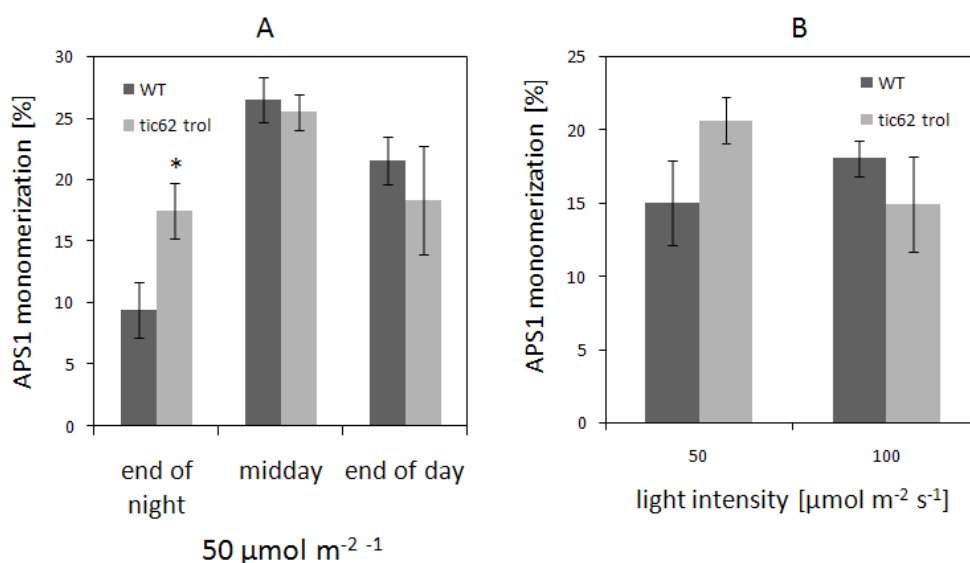


Figure 36 AGPase activation state in *tic62trol* and WT plants

A. *thaliana* plants were grown on MS plates without sucrose at (A) 50 μmol light intensity ($n=4$, *: $p \leq 0.05$, SE) for 20 days and subsequently harvested in liquid nitrogen after 8 h dark (end of night), after 8 h light exposure (midday) and 16 h light exposure (end of day), as well as (B) after 10 minutes light exposure after the dark period (50 μmol and 100 μmol light intensity, $n=3$, no significant difference, SE). Metabolic analysis was performed by Ina Thormälen (AG Geigenberger, LMU Munich).

Next, the ratios of $\text{NADPH}/\text{NADP}^+$ and NADH/NAD^+ in WT and *tic62trol* plants were analyzed. The $\text{NADPH}/\text{NAD}^+$ ratio represent basically the redox state in the plastid, whereas the NADH/NAD^+ ratio mainly reflects the situation in the cytosol (reviewed in Taniguchi and Miyake, 2012). As depicted in Figure 37 A, the $\text{NADPH}/\text{NADP}^+$ ratio was strongly reduced in *tic62trol* after 8 h light (midday) as well as after 16 h light (end of day). This suggests that at these two time points, the amount of NADPH in the chloroplast was extensively reduced compared to WT, which showed nearly equal amounts of the reduction equivalents at all three time points. By contrast, the NADH/NAD^+ ratio was exclusively altered at the end of the night (Figure 37 B): In *tic62trol*, the NADH/NAD^+ ratio was significantly increased, indicating the presence of more NADH in relation to NAD^+ in the cell, whereas there was no

difference detectable at midday and at the end of the day between WT and *tic62trol*.

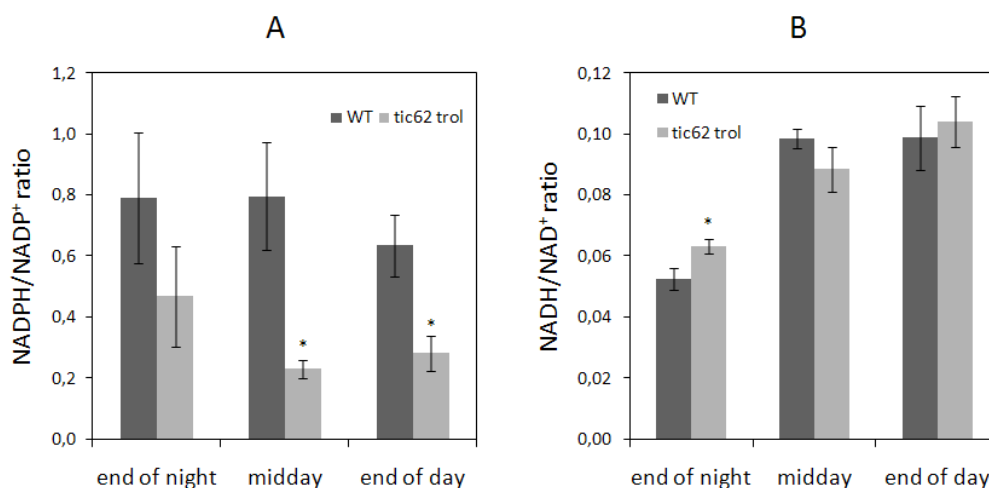


Figure 37 NADPH/NADP⁺ and NADH/NAD⁺ ratio in *tic62trol* and WT plants

A. thaliana plants were grown on MS plates without sucrose at 50 μ mol light intensity for 20 days and subsequently harvested in liquid nitrogen after 8 h dark (end of night), after 8 h light exposure (midday) and 16 h light exposure (end of day) in order to measure the NADPH/NADP⁺ ratio (A) and NADH/NAD⁺ ratio (B). Metabolic analysis was performed by Ina Thormälen (AG Geigenberger, LMU Munich). (N=4, *: p ≤ 0.05, SE)

In this study, initial metabolic targets were discovered, which seem to be influenced by the *tic62trol* knockout (starch, AGPase and the reduction equivalents NADPH and NADH). Further analysis, including the investigation of other metabolites, have to be performed in the future to complete the puzzle of the correlation and regulation of photosynthesis related proteins like FNR, Tic62 and Trol.

5 Discussion

5.1 Characterization of Tic22 in *A. thaliana*

Tic22 was originally discovered as a component of the import machinery of chloroplasts of *P. sativum* (Kouranov and Schnell, 1997). Since Tic22 was shown to be localized in the intermembrane space of chloroplasts, it was thought to act as a guiding protein, which facilitates the transport of incoming preproteins from the TOC to the TIC complex (Kouranov *et al.*, 1998). The results of this work give further information about the role of the two isoforms and the third potential member of Tic22 in *A. thaliana*.

5.1.1 General properties of the Tic22 isoforms in *A. thaliana*

For further investigation of the function and potential interplay of the two Tic22 isoforms in *A. thaliana*—namely Tic22III, Tic22IV—analysis of the respective expression pattern were used. Tic22III and Tic22IV show a similar expression pattern in *A. thaliana* (Figure 4 A, B), although the expression of Tic22IV is slightly higher in most of the plant tissues (Figure 4 B). Thus, it can be concluded that these Tic22 isoforms might fulfill similar or overlapping functions. Tic22V, representing a potential member of the Tic22 family in *A. thaliana*, differs clearly from the general sequence properties of Tic22III and Tic22IV, since it is twice as large as the other two isoforms and shows a lower expression in all plant tissues (Figure 4 C). Since Tic22V is mainly expressed in seeds, it was first proposed to play a role in seed- or embryo development (see chapter 5.1.2).

Further analysis of the amino acid sequence by alignments of Tic22 isoforms in *A. thaliana* revealed a common amino acid motif “GVPVFQS”, which is also present in other Tic22 forms of vascular plants (Figure 38 A). This motif has not been described in the literature so far. Furthermore, this sequence pattern seems to be unique for Tic22 in vascular plants, since it is not present in other Tic22 orthologues such as Apicomplexa or cyanobacteria. Interestingly, some species contain an additional serine and an alanine and a conserved asparagine instead of serine (Figure 38 A, green box). Furthermore, a single leucine is conserved in all vascular plants, indicating that this amino acid might also belong to the motif. The investigation whether the mutations within the motif appear at a certain evolutionary point did not reveal a specific pattern and it is present in different plant species of mono- and eudicots (Figure 38 B). Thus, it can be speculated that the conserved motif

Investigation of the growth and developmental phenotype (Figure 19) revealed that in the first 10 days of plant development, the induced *tic22dmRNAi* plants depicted a retarded growth and violet cotyledons compared to WT plants, which showed normal growth even upon RNAi induction. Interestingly, this phenotype is exclusively found in *tic22dm* background, indicating that Tic22III and Tic22IV are partially able to complement this function. Thus, the next step will be to generate triple mutants, lacking all three Tic22 isoforms in order to analyze the plant development.

To test the successful gene silencing in the plants, qRT-PCR was performed, revealing an increased TIC22V gene expression in the WT background and a decreased gene expression in *tic22dm* background, which could explain the divergent phenotype in young seedlings (Figure 19). The silencing of the TIC22V gene expression was also analyzed in seeds by qRT-PCR and an increased expression was detected in induced WT and *tic22dm* seeds (data not shown), which had, however, no impact on germination as it was analyzed by continuous dexamethasone treatment until the plants reached their adult size. It is well known that RISC (RNA-induced silencing complex)-based knock-downs might lead to the modulation of off-target proteins, which might potentially occur in the RNAi-TIC22V plants and which would explain unexpected gene expression in induced RNAi plants (Ossowski *et al.*, 2008; Chang *et al.*, 2012).

At this time point, a new T-DNA line became available for TIC22V and the characterization of heterozygous mutants thereof was continued (Figure 22). Again no homozygous mutants were found. Neither by weighing the seeds to detect a disordered seed development, nor by investigating the siliques with respect to potential gaps in the siliques, indicating malfunction of seed development, revealed differences between WT and *tic22V* (Figure 23). Additionally, germination tests showed no differences between WT and mutant, indicating that embryo development is not influenced. The failure to produce homozygous progeny might be due to pollen sterility. This will need to be tested in the future.

5.1.3 The knock-out of Tic22III and Tic22IV leads to a chlorotic phenotype and altered thylakoid composition

First analysis of the Tic22III/Tic22IV double knock-out (Figure 6) did not reveal visible differences in plant growth under a variety of conditions tested. However, the leaves of the *tic22IIIxIVdm* possess chlorotic areas at the margins/side areas, which is most prominent in the first 14 days of plant development (Figure 9). Previous data described several relations

between knock-outs of translocation machinery components of chloroplasts and pale or albino phenotypes, like Toc159 and Toc34/33. A strong correlation exists between the protein import of precursor proteins into chloroplasts and plastid biogenesis, including assembly of the photosynthetic apparatus at the thylakoids. Malfunctions in these processes might thus lead to a pale or albino phenotype due to a defective assembly of photosynthetic components. Tic22III/IV seems also to fall into this category of proteins, as the observed plastid phenotype is most prominent in the first 14 days of development. Hence, it is conceivable that the import of proteins is altered in *tic22dm*, although no differences were detected in Lhcb protein amount between WT and *tic22dm* (Figure 17). Other data reveal a threefold reduced import rate of the SSU precursor into *A. thaliana* chloroplasts of *tic22dm* compared to WT (Rudolf *et al.*, 2012).

TEM-analysis showed an altered thylakoid ultrastructure in the chlorotic leaf areas of *tic22dm*. The thylakoids are lacking grana stacks and are exclusively composed of stromal lamellae (Figure 11, 12). Interestingly, a similar phenotype has been published for *attic40* mutant plants, which comprise less grana stacks and a pale phenotype (Chou *et al.*, 2003). During rapid chloroplast differentiation and thylakoid biosynthesis *tic22dm* plants most likely have lower protein import capacity which leads to retarded photosystem assembly. This is supported by our observation that the chlorotic margins of *tic22dm* contain 50% less chlorophyll compared to the same areas of WT.

5.1.4 *Tic22dm* reveals an altered gene expression

The analysis of the gene expression of the light harvesting complex genes LHCB1.3, LHCB 4.1 and LHCB6, as well as the ATPase genes ATPC1, ATPD and ATPG and the oxygen evolving complex gene OE23 showed a markedly higher expression in the leaf tip of the *tic22dm* compared to all other plant parts in WT and *tic22dm* (Figure 15), whereas the gene expression in the chlorotic margins is equal compared to WT. This observation is surprising, as differences in the gene expression were expected to occur in the chlorotic parts, since the assembly of the photosynthetic apparatus was thought to be disordered in these areas, leading to the chlorotic phenotype. This could be explained by a potential retrograde signaling, enhancing the gene expression of photosynthetic genes in the leaf tip and thus compensating the dysfunction caused by the disordered thylakoid structure in the margins of the leaf. It has been described that specific plastid signals are able to regulate nuclear gene expression (retrograde signaling): These signals have been shown to be related to (i)

tetrapyrrole biosynthesis (Larkin *et al.*, 2003), (ii) to redox signals (Pfalz *et al.*, 2012), (iii) the production of reactive oxygen species (ROS) (Tikkanen *et al.*, 2012), (iv) to plastid gene expression, which is required for nuclear gene expression of LHCB genes (Woodsen *et al.*, 2012) and (v) to defects in protein import (Bauer *et al.*, 2000). It is believed that further plastid signals exist, but these are unknown to date.

5.1.5 *Tic22dm* reveals a reduced OE33 content in the margins

For analyzing potential differences in the amount of photosynthetic proteins in the distinct leaf areas, Oe23, Oe33 α ATPase α/β , PorB, D1, D2, α Lhca 2, Lhcb 6, Ndh a and Ndh j/h were chosen for detection in the leaf tip and margins of WT as well as *tic22dm* by immunoblot. However, due to the low protein amount obtained by protein extraction of the leaf tip and margins of WT and *tic22dm*, only Oe33 was successfully detected (Figure 16). The protein amount of Oe33 is reduced in the margins of *tic22dm*, which corresponds to the observation that the thylakoidal protein composition is altered due to lacking grana stacks. The enhanced gene expression of OE33 in the leaf tip of *tic22dm* could reflect on the other hand the effect of cell signaling, being provoked by alterations during photosystem assembly.

5.1.6 *Tic22dm* plants contain an altered plastid gene expression

Beside the differences in nuclear gene expression of photosynthetic genes in distinct plant areas, whole genome expression was investigated by DNA microarray analysis. The data showed an overall down regulation in *tic22dm* of genes involved in photosynthesis, whereas an increased gene expression was found concerning genes related to diverse processes in the cell including cell cycle related genes as well as translation corresponding genes (see appendix). In both cases, the genes, which depicted I) the highest fold change and II) which were found to be plastid encoded were examined in more detail (see table 7). The analysis was performed with whole leaves and not distinct cell types, since it was not possible to isolate sufficient amounts of the distinct leaf areas (margins and leaf tip). Beside the above-mentioned alterations in nuclear gene expression, several plastid encoded genes were found to be regulated in *tic22dm* compared to WT (Figure 18).

The most prominent gene repression in *tic22IVsm* as well as *tic22dm* was observed for NDHH, which represents the NAD(P)H dehydrogenase (NDH) subunit H (49 kDa). NDH reduces plastochinones in thylakoid membranes and is involved in cyclic electron flow in PSI and in photorespiration. Similar results were obtained for ATPA, PSAA and PSBE: ATPA and

PSAA are less expressed in *tic22IVsm* and expression is drastically reduced in *tic22dm*, whereas the expression of PSBE is not significantly decreased in *tic22IVsm* and just slightly repressed, compared to NDHH, ATPA and PSAA, in *tic22dm*. Since NDHH and ATPA both are connected to cyclic electron transport (CEF), the repression of both genes might be due to an altered CEF in *tic22dm*.

Moreover, all genes that were found to be down regulated encode for components of the thylakoid-located photosynthetic machineries: ATPA is part of the ATPase, PSAA encodes for the reaction center of PSI along with Psa B protein and PSBE encodes for cytochrome b559, a component of PSII complex. Although whole leaves were used for DNA Microarray analysis, a clear correlation between Tic22 knockout and the expression of photosynthetic genes was observed.

The observed up regulation of the genes RPL20, RPS15, PSAC, ACC2 and NAD4 was not always more pronounced in *tic22dm* compared to WT and *tic22sm* as detected for the down regulated genes: Moreover, only ACC2, a gene which is involved in fatty acid synthesis and other metabolic processes, shows a strong up regulation in the *tic22dm* compared to WT, potentially balancing defects of further involved genes due to the knock-out of Tic22. Single gene analysis by qRT-PCR gave controversial results in case of up regulated genes. These divergent data are difficult to reconcile and need to be further investigated.

To analyze a potential crosstalk between chloroplasts and mitochondria, expression of the mitochondrial gene NAD4 was analyzed, which encodes a protein that is involved in respiration. The gene expression was found to be up regulated in *tic22dm* in the DNA Microarray as well as in the Real-Time RT PCR experiments, whereas no differences to WT were detected in *tic22IVsm*. This suggests a potential relation between the developmental state of chloroplasts and mitochondria as exemplified by NAD4. It has already been shown that plastids and mitochondria are tightly connected in the metabolic framework within plant cells. Oxygen and carbohydrates for mitochondrial energy conversion and metabolism are supplied by chloroplasts, and mitochondria support the chloroplast through the respiratory pathway and citric acid cycle (Noctor *et al.*, 2007; Yoshida *et al.*, 2007). Since these metabolic processes in mitochondria and chloroplasts are closely connected, a similar correlation between gene expression of nuclear-encoded mitochondrial and chloroplast genes has been proposed: the expression of nuclear-encoded mitochondrial genes, such as AOX, was found to be up regulated under high light conditions (Finnegan *et al.*, 1997; Yoshida

et al., 2007), and this up regulation is additionally dependent on the developmental status of plastids (Yoshida *et al.*, 2008). Moreover, it has been described that the transcript levels of mitochondrial genes are affected in mutants that comprise defects in plastid development (Hedtke *et al.*, 1999).

5.1.7 Potential flexible loops might avoid the crystallization of synTic22

In order to obtain further structural and thus functional information about Tic22, one aim of the project was to solve the protein structure of the Tic22 orthologues *A. thaliana*, *P. sativum*, *P. falciparum*, *T. gondii* and *G. theta*. All Tic22 proteins were overexpressed and since Tic22 from *Synechocystis* (synTic22) comprised optimal soluble expression properties, further purification and crystallization steps were performed with this orthologue.

Homology analysis by blast of the synTic22 amino acid sequence against other cyanobacterial species (*Anabaena* sp. PCC 7120, *Microcystis aeruginosa* NIES-843, *Cyanothece* sp. ATCC 51142, *Trichodesmium erythraeum* IMS101, *Crocospaera watsonii* WH 8501, *Microcoleus* sp. PCC 7113, *Fischerella* sp. JSC-11, *Oscillatoria nigro-viridis* PCC 7112) revealed four domains comprising highly conserved hydrophobic amino acids in all Tic22 isoforms of cyanobacteria (Figure 39). One of these isoforms (Tic22 of *Anabaena* sp. PCC 7120) has recently been published in terms of structure and function of the protein (Tripp *et al.*, 2012). In this study, Tic22 from *Anabaena* was supposed to play a role in OM biogenesis. It was found to be dually localized in the periplasm and the thylakoid system. The structure of the protein, which was solved by crystallization revealed a symmetric butterfly structure with a mixed $\alpha\beta$ -topology, as well as a hydrophobic surface and conserved functional hydrophobic pockets within the protein, which are thought to mediate protein-protein interactions as described for chaperones (Xu *et al.*, 2007; Bechtluft *et al.*, 2010).

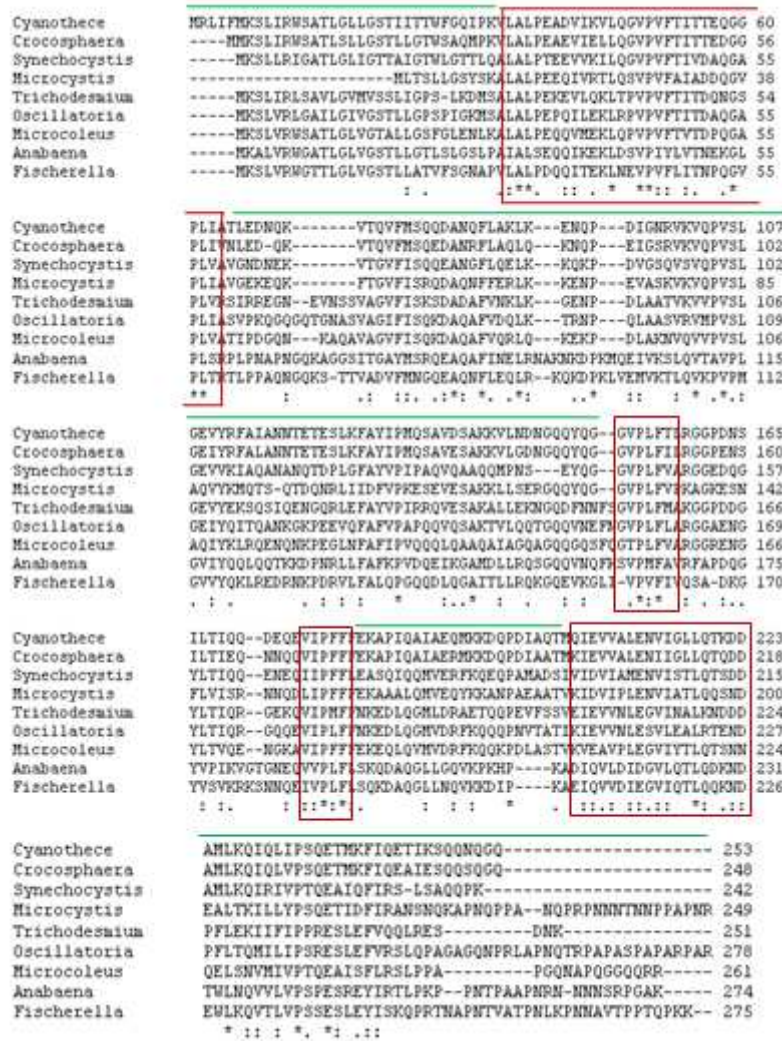


Figure 39 Protein alignment of Tic22 from cyanobacteria

For the alignment, Tic22 amino acid sequences from the cyanobacteria *Synechocystis sp.* PCC6803, *Cyanothece sp.* ATCC 51142, *Crocospaera watsonii* WH 8501, *Trichodesmium erythraeum* IMS101, *Oscillatoria nigro-viridis* PCC 7112, *Microcoleus sp.* PCC 7113, *Microcystis aeruginosa* NIES-843, *Anabaena sp.* PCC 7120 and *Fischerella sp.* JSC-11 were used. Asterisks depict identical and thus conserved amino acids in all sequences. Double dots show highly similar amino acids of most sequences, one dot describes similar amino acids. Red boxes indicate regions for highly conserved hydrophobic domains and green lines depict potential flexible loops within the sequences. The alignment was performed with the sequences from NCBI and the multi alignment tool MAFFT (<http://mafft.cbrc.jp/alignment/server/>).

Additionally, the Tic22 proteins of apicoplasts of *P. falciparum* and *T. gondii* have also been published during this study with regard to their function (TgTic22) and structure (PfTic22) (Glaser and Higgins, 2012), gradually completing the picture of Tic22 function and its conservation in many organisms. In this study, they describe Tic22 to be an essential protein mediating the protein import into apicoplasts, enforcing the predominant hypothesis that Tic22 could represent a chaperone for incoming preproteins. TgTic22 was found to be essential for parasite survival, although the apicoplast in all organisms bears reduced functional features like synthesis of fatty acids, heme, iron-sulfur clusters and isoprenoids

compared to chloroplasts (for review see Lim and McFadden, 2010). Furthermore, TgTic22 was found to be involved in protein import in apicoplasts and the crystallization trial of the mature form of PfTic22 revealed a monomeric protein, consisting of seven α -helices and two four-stranded β -sheets and interestingly similar hydrophobic pockets as found for the cyanobacterial homologue in *Anabaena* (Tripp *et al.*, 2012). These findings indicate that PfTic22 might function as a chaperone similar to Tic22 of *Anabaena*. Investigating the protein structures of other Tic22 orthologs could further verify this assumption in the future. In the present thesis, synTic22 was shown to solubly overexpress in high amounts and the purification resulted in pure protein, sufficient for crystallization trials (Figure 27). Nevertheless, no protein crystals were obtained in spite of numerous approaches. Since a large variety of conditions was tested unsuccessfully, it can be concluded that the tertiary structure adopted by this particular protein does not allow the formation of stable crystals. Beside the mentioned regions of conserved amino acids, the protein comprises amino acid sections in between, which could represent “flexible loops” (Figure 39, green line). Since Tic22 seems to contain several of these loops, the flexibility of one or more of them might prevent the proper formation of regularly arranged units, which are prerequisite for crystal formation, thus possibly hampering the crystallization processes.

It is widely accepted that even small changes in the amino acid sequence of proteins can dramatically change the properties of the protein. The full-length TgTic22 failed to crystallize although high amounts of soluble protein were obtained Glaser and Higgins (2012). Thus it was concluded that crystal formation might be prevented due to the N-terminal extension and/or low complexity insertions (flexible loops). However, crystallization trials with the predicted mature form of PfTic22 successfully led to crystal formation (Glaser and Higgins 2012). Furthermore, crystallization of Tic22 of *Anabaena* was successfully performed utilizing an N-terminally shortened form of the protein (amino acid 32-274) (Tripp *et al.*, 2012). Due to the high homology of synTic22 and Tic22 of *Anabaena* (Figure 40), it is disputable, whether the crystallization of synTic22 might offer new insights in structural features.

```

Synechocystis MKSLLRIGATLGLIGTTAIGTWLGTTLQALALPTEEVVKILQGVVFTIVDAQGAPLVAV 60
Anabaena      MKALVRFMGATLGLVGSSTLLGTLGSLPAIALSEQQIKEKLDSPPIYLVITNEKGLPLSRP 60
              **:*: * *****:*: * **: * * **: . : : * :. **: : : : * **
Synechocystis GNDNEK-----VTGVFISQQEANGFLQELKKQK-----PDVGSQVSVQPVSLGCVVK 107
Anabaena      LPMAPNGQKAGGSITGAYMSRQEAQAFINELRNAKMKDPKMQEIVKSLQVTAVPLGVIIQ 120
              : : : **: *: *: *: *: *: * : : . : . * . *: * : :
Synechocystis IAQANANQTDPLGFAYVPIPAQVQAAQMPNSEYQGG-----VPLFVARGGEDQGYLTIQ 162
Anabaena      QLQQTKKDPNRLLFAPKPVQEIKGAMDLLRQSGQVNVQFKSVPMFAVRFAPDQGYVPIK 180
              * . : : : * **: * : : : . * : : . * * : * . * : * : * :
Synechocystis Q--ENEQIIPFFLEASQIQMVERFKQEQPAMADSIVIDVIAMENVISTLQTSDDAMLKQ 220
Anabaena      VGTGNEQVVPLFLSKQDAQGLLGQVKPKHPKAD----IQVLDIDGVLQTLQDKNDTWLNQ 236
              ***: *: * . : * : : . * : : * * : * : : . * : * : * : * :
Synechocystis IRIVPTQEAIQFIRLSAQPK----- 242
Anabaena      VVLVPSPEFREYIRTLPKPNTPAAPNRMNNSRPGAK 274
              : **: * : : **: * . .

```

Figure 40 Protein alignment of Tic22 from *Synechocystis sp.* PCC6803 and *Anabaena sp.* PCC 7120

Asterisks depict conserved and homologous amino acids and double dots show amino acids which are similar in respect to their properties.

5.2 Tic62 and Trol and their potential role in photosynthetic processes

The second project of this thesis deals with the characterization of Tic62/Trol double knock-out mutants (*tic62/trol*), two proteins, which contain FNR binding domains and are thus closely related to photosynthetic processes. FNR carries out the last step of LEF by transferring the electrons from ferredoxin to NADP^+ , thus generating the reduction equivalent NADPH. Tic62 features a triple localization at the IE, in the stroma and at the thylakoids of chloroplasts. Furthermore, it is thought that the FNR is tethered to the thylakoid membrane by Tic62 in times of a decreased activity of photosynthetic processes (Stengel *et al.*, 2008; Benz *et al.*, 2009). However, the significance of this FNR storage at the thylakoids and the interaction with Tic62 in the stroma is still not fully understood. In addition, a second FNR binding protein Trol has been discovered, which is exclusively localized at the thylakoid membrane. Trol deficient plants were shown to be slightly slower in development and to produce smaller rosettes. The morphology of the chloroplasts of these mutant plants was shown to be altered, indicating that the decreased LEF rate leads to slower plant growth (Juric *et al.*, 2009). In this study, the effect of *tic62/trol* plants, lacking both binding partners of FNR was analyzed in order to determine the potential regulatory mechanisms provoked by the absence of membrane-bound FNR.

According to previous studies (Juric *et al.*, 2009), it was expected that the double knock-out of both Tic62 and Trol might lead to severe defects in photosynthesis. Although it was shown that FNR is photosynthetically active when it is present as a soluble protein in the stroma, the membrane bound form was still considered to be more important. However, no significant differences were observed regarding photosynthetic activity and characterization

of the phenotype between *tic62trol* and WT, though FNR was completely missing from the thylakoids in *tic62trol* (Figure 31, 32 and 33 B).

Interestingly, *tic62trol* plants showed metabolic alterations. Plants, grown at 100 μmol light intensity revealed no difference in starch content between *tic62trol* and WT (Figure 35 A). During the day, when photosynthesis takes place, starch is produced and stored. During the night, starch is mobilized and used as carbon and energy source. The plants, which were grown at 50 μmol light intensity showed an increase of the starch amount over the day as mentioned before (Figure 35 B). *Tic62trol* plants contain in general more starch than the WT, although exclusively the difference at the end of the night was found to be significant ($p \leq 0.1$). However, considering the consistent higher amount of starch in *tic62trol* plants (Figure 35 B, end of day) indicates that the electrons deriving from LEF might be transferred to targets, which influence or even enhance starch biosynthesis. This led to the hypothesis that the thioredoxin system might be affected in *tic62trol* plants compared to WT plants, since many thioredoxin regulated proteins are known to be involved in starch synthesis (Balmer *et al.*, 2006). However, the increased starch amount at the end of the night was more striking. These observations indicated that during night, starch was either degraded in a reduced manner or that starch production was still ongoing.

AGPase catalyzes the first step in starch biosynthesis, converting glucose-1-phosphate to ADP-glucose in the chloroplast stroma by using ATP as an energy source. The enzyme is activated by reduction of a disulfide bridge between two cysteine residues connecting the two small subunits (APS1) of the heterotetrameric enzyme by thioredoxin (Hendriks *et al.*, 2003; Kolbe *et al.*, 2005) and alterations in one of these functional cystein residues prevents the dimerization and therefore have impact on starch turnover (Hädrich *et al.*, 2012). Furthermore, it has been shown that the activation of the enzyme is not exclusively achieved by the light-dependent ferredoxin/thioredoxin system, but also in the dark involving the NAPDH/NADP-thioredoxin reductase (NTRC system) in response to sugars (Tiessen *et al.*, 2002, Michalska *et al.*, 2009).

Analyzing *tic62trol* in regard to the AGPase monomerization state compared to WT revealed a significantly higher monomerization and therefore activation of the enzyme in *tic62trol* plants at the end of the night (Figure 36 A). Since redox dependent AGPase activation is increased at the end of the night but not after onset of light, electrons cannot be transferred via Trx. As mentioned before, AGPase can also be reduced and thereby activated by NTRC,

which itself is able to accept electrons from NADPH produced during the night in the oxidative pentose-phosphat pathway. Thus, NTRC might activate AGPase instead of the light dependent Fd/Trx system and continue starch synthesis at night.

Finally, the NADPH/NADP⁺ and NADH/NAD⁺ ratio in *tic62trol* and WT plants was measured. The ratio of these reduction equivalents provides information about the current redox state in the chloroplast and the surrounding cell. In the chloroplast, NADPH is photosynthetically generated by FNR, which reduces NADP⁺ at the end of the electron transport chain.

In *tic62trol*, NADPH is strongly reduced after 8 h light exposure and at the end of the day (Figure 37 A), whereas the difference to WT is not significant at the end of the night. This could be due to a decrease of FNR activity in the light, potentially provoked by the overall reduction of the total FNR amount (Figure 31) or the loss of FNR attachment in *tic62trol* plants. Furthermore, it is conceivable that further metabolic reactions using or generating NADPH might be altered in *tic62trol* plants due to the dysfunction of FNR tethering. Therefore, measurements of the enzyme activity of proteins which are proposed to be involved in NADPH metabolism, such as NADP-isocitrate dehydrogenase and glucose-6-phosphate dehydrogenase could be performed in the future in order to analyze if a decrease of the enzyme activity might be responsible for the reduced NADPH consumption.

On the other hand, the NADH/NAD⁺ ratio is slightly increased in *tic62trol* at the end of the night compared to WT (Figure 37 B), indicating that the cytosolic redox state is linked to the stromal redox state via the malate valve. As mentioned before, in contrast to the unchanged FNR amounts (in total) in the *tic62* and *trol* single mutants, *tic62trol* possess a 20% decreased total FNR amount. Therefore, it cannot be excluded that observed and described alterations in *tic62trol* might be due to the decreased amount of FNR.

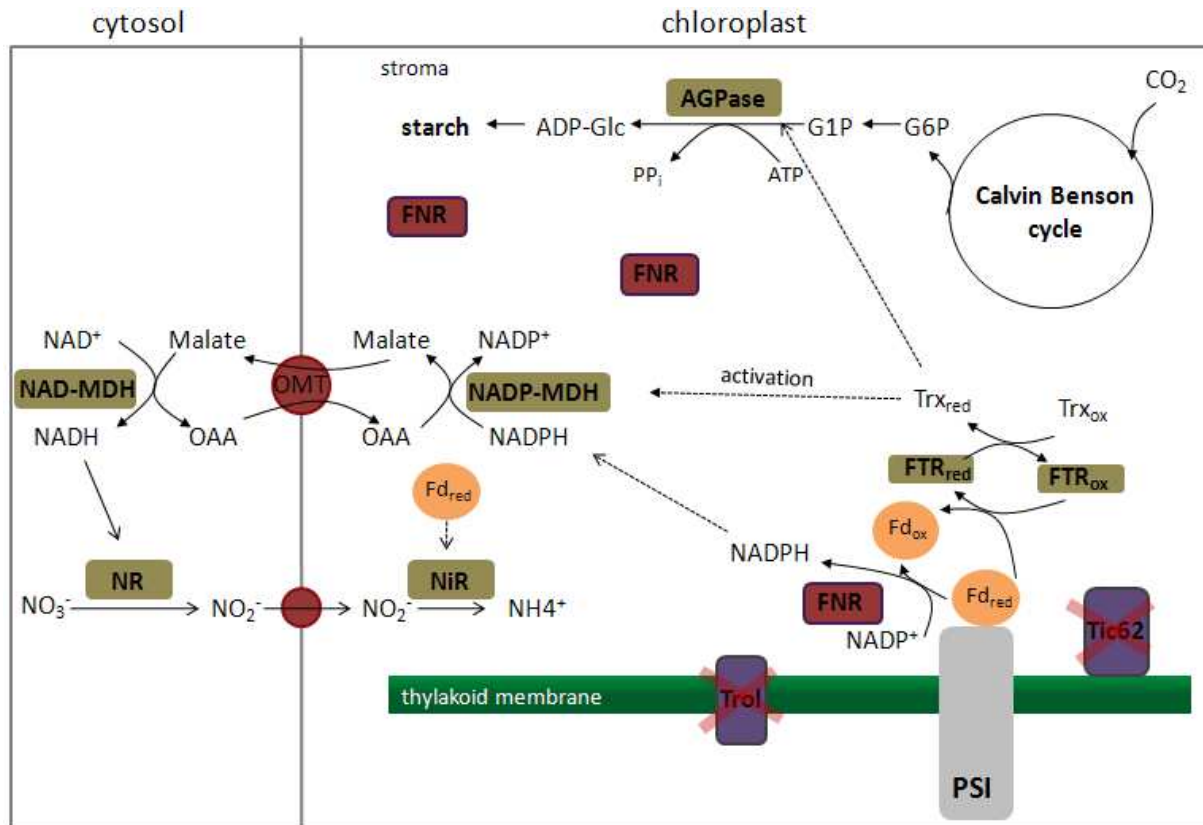


Figure 41 Metabolic pathways influenced by *Tic62* and *Trol* double knock-out

FNR enables the transfer of electrons from ferredoxin to NADP⁺ in the stroma. The lack of FNR at the thylakoids or the overall reduction of the protein in *tic62trol* leads to an alteration in starch amount, AGPase activity and NADP⁺/NADPH and NAD⁺/NADH ratios. Potentially involved is the ferredoxin-thioredoxin-reductase (FTR), subsequently reducing and activating thioredoxin (Trx). Trx triggers the activation of e.g. AGPase, catalyzing the first reaction in starch biosynthesis. During night, this is achieved by NTRC (not depicted). The activation of NADP-malate dehydrogenase (NADP-MDH) leads to the production of malate, which is transferred to the cytosol by the oxalacetate-malate-transporter (OMT). Malate is utilized in the cytosol to produce NADH by generation of oxalacetate (OAA) by the NADH-MDH. In the cytosol, NADH is used to activate nitrate reductase (NR), converting nitrate to nitrite, which is translocated to the stroma and metabolized to ammonium (NH₄⁺) by the nitrite reductase (NiR).

In summary, the obvious differences between *tic62trol* and WT concerning redox related components of plants metabolism suggest a clear relation between light-driven photosynthesis and subsequent metabolic pathways (Figure 41). Since *tic62trol* plants do not possess a visible phenotype and no alterations in photosynthetic activity were detected, the electron transfer rate might be the same as in WT plants. Interestingly, the photosynthesis is not altered in *tic62trol* but simultaneously differences in the metabolism were detected.

Further analysis of enzymes and metabolites, which are closely related to redox regulated processes, such as malate dehydrogenase and nitrate/nitrite reductase, is a conceivable approach for the near future in order to investigate the importance of thylakoid-stroma shuttling of FNR.

6 References

- Altschul, S. F., T. L. Madden, A. A. Schaffer, J. Zhang, Z. Zhang, W. Miller and D. J. Lipman** (1997). "Gapped BLAST and PSI-BLAST: A new generation of protein database search programs." *Nucleic Acids Res* 25 (17): 3389-3402.
- Arnon, D. I.** (1949). "Copper enzymes in isolated chloroplasts: Polyphenoloxidase in *Beta-vulgaris*." *Plant Physiol.* 24 (1): 1-15.
- Aronsson, H. and P. Jarvis** (2002). "A simple method for isolating import-competent *Arabidopsis* chloroplasts." *FEBS Lett* 529(2-3): 215-220.
- Aronsson, H. and P. Jarvis** (2011). "Dimerization of TOC receptor GTPases and its implementation for the control of protein import into chloroplasts." *Biochem J* 436(2): e1-2.
- Bagos, P. G., E. P. Nikolaou, T. D. Liakopoulos, K. D. Tsirigos** (2010). "Combined prediction of Tat and Sec signal peptides with hidden Markov models." *Bioinformatics (Oxford, England)* 26 (22): 2811-2817.
- Balmer, Y., W. H. Vensel, N. Cai, W. Manieri, P. Schurmann, W. J. Hurkman and B. B. Buchanan** (2006). "A complete ferredoxin/thioredoxin system regulates fundamental processes in amyloplasts." *Proc Natl Acad Sci U S A* 103(8): 2988-2993.
- Balsera, M., T. A. Goetze, E. Kovacs-Bogdan, P. Schurmann, R. Wagner, B. B. Buchanan, J. Soll and B. Bolter** (2009). "Characterization of Tic110, a channel-forming protein at the inner envelope membrane of chloroplasts, unveils a response to Ca²⁺ and a stromal regulatory disulfide bridge." *J Biol Chem* 284(5): 2603-2616.
- Balsera, M., A. Stengel, J. Soll and B. Bolter** (2007). "Tic62: a protein family from metabolism to protein translocation." *BMC Evol Biol* 7: 43.
- Balsera, M., J. Soll, B.B. Buchanan** (2009b). "Protein import into chloroplasts: An emerging regulatory role for redox." *Advances in Botanical Research* 52, 277-332.
- Bauer, J., K. Chen, A. Hiltbunner, E. Wehrli, M. Eugster, D. Schnell and F. Kessler** (2000). "The major protein import receptor of plastids is essential for chloroplast biogenesis." *Nature* 403(6766): 203-207.
- Bechthold, N., J. Ellis and G. Pelletier** (1993). "In planta *Agrobacterium* mediated gene transfer by infiltration of adult *Arabidopsis thaliana* plants " *C.R.Acad.Sci.Paris/Life sciences* 316: 1194-1199.
- Bechtluft, P., A. Kedrov, D. J. Slotboom, N. Nouwen, S. J. Tans and A. J. Driessen** (2010). "Tight hydrophobic contacts with the SecB chaperone prevent folding of substrate proteins." *Biochemistry* 49(11): 2380-2388.
- Becker, T., J. Hritz, M. Vogel, A. Caliebe, B. Bukau, J. Soll and E. Schleiff** (2004). "Toc12, a

novel subunit of the intermembrane space preprotein translocon of chloroplasts." *Mol Biol Cell* 15(11): 5130-5144.

Benz, J. P., J. Soll and B. Bolter (2009). "Protein transport in organelles: The composition, function and regulation of the Tic complex in chloroplast protein import." *FEBS J* 276(5): 1166-1176.

Benz, J. P., A. Stengel, M. Lintala, Y. H. Lee, A. Weber, K. Philippar, I. L. Gugel, S. Kaieda, T. Ikegami, P. Mulo, J. Soll and B. Bolter (2009). "Arabidopsis Tic62 and ferredoxin-NADP(H) oxidoreductase form light-regulated complexes that are integrated into the chloroplast redox poise." *Plant Cell* 21(12): 3965-3983.

Bruce, B. D. (2000). "Chloroplast transit peptides: structure, function and evolution." *Trends Cell Biol* 10(10): 440-447.

Buchanan, B. B. and Y. Balmer (2005). "Redox regulation: a broadening horizon." *Annu Rev Plant Biol* 56: 187-220.

Catanzariti, A. M., T. A. Soboleva, D. A. Jans, P. G. Board, R. T. Baker (2004). "An efficient system of high-level expression and easy purification of authentic recombinant proteins." *Protein Sci* 13 (5): 1331-1339

Chang, C. H., H. I. Wang, H. C. Lu, C. E. Chen, H. H. Chen, H. H. Yeh and C. Y. Tang (2012). "An efficient RNA interference screening strategy for gene functional analysis." *BMC Genomics* 13: 491.

Chen, X., M. D. Smith, L. Fitzpatrick and D. J. Schnell (2002). "In vivo analysis of the role of atTic20 in protein import into chloroplasts." *Plant Cell* 14(3): 641-654.

Chigri, F., F. Hormann, A. Stamp, D. K. Stammers, B. Bolter, J. Soll and U. C. Vothknecht (2006). "Calcium regulation of chloroplast protein translocation is mediated by calmodulin binding to Tic32." *Proc Natl Acad Sci U S A* 103(43): 16051-16056.

Chiu, C. C., L. J. Chen and H. M. Li (2010). "Pea chloroplast DnaJ-J8 and Toc12 are encoded by the same gene and localized in the stroma." *Plant Physiol* 154(3): 1172-1182.

Chou, M. L., L. M. Fitzpatrick, S. L. Tu, G. Budziszewski, S. Potter-Lewis, M. Akita, J. Z. Levin, K. Keegstra and H. M. Li (2003). "Tic40, a membrane-anchored co-chaperone homolog in the chloroplast protein translocon." *EMBO J* 22(12): 2970-2980.

Clausen, C., I. Ilkavets, R. Thomson, K. Philippar, A. Vojta, T. Mohlmann, E. Neuhaus, H. Fulgosi and J. Soll (2004). "Intracellular localization of VDAC proteins in plants." *Planta* 220(1): 30-37.

Clough, S. J. and A. F. Bent (1998). "Floral dip: a simplified method for *Agrobacterium*-mediated transformation of *Arabidopsis thaliana*." *Plant J* 16(6): 735-743.

- Constan, D., J. E. Froehlich, S. Rangarajan and K. Keegstra** (2004). "A stromal Hsp100 protein is required for normal chloroplast development and function in Arabidopsis." *Plant Physiol* 136(3): 3605-3615.
- Detlef, W. and J. Glazebrook** (2001). "Arabidopsis: A laboratory Manual." Cold Spring Harbor Laboratory, Cold Spring Harbor Press, New York.
- Duy, D., R. Stübe, G. Wanner and K. Philippar** (2011). "The Chloroplast Permease PIC1 Regulates Plant Growth and Development by Directing Homeostasis and Transport of Iron." *Plant Physiology* 155(4): 1709-1722.
- Emanuelsson O, H. Nielsen, G. von Heijne** (1999) ChloroP, a neural network-based method for predicting chloroplast transit peptides and their cleavage sites. *Protein Sci* 8: 978-984.
- Emanuelsson O, H. Nielsen, S. Brunak, G. von Heijne** (2000) Predicting subcellular localization of proteins based on their N-terminal amino acid sequence. *J Mol Biol* 300: 1005-1016.
- Fellerer, C., R. Schweiger, K. Schongruber, J. Soll and S. Schwenkert** (2011). "Cytosolic HSP90 cochaperones HOP and FKBP interact with freshly synthesized chloroplast preproteins of Arabidopsis." *Mol Plant* 4(6): 1133-1145.
- Finnegan, P. M., J. Whelan, A. H. Millar, Q. Zhang, M. K. Smith, J. T. Wiskich and D. A. Day** (1997). "Differential expression of the multigene family encoding the soybean mitochondrial alternative oxidase." *Plant Physiol* 114(2): 455-466.
- Firlej-Kwoka, E., P. Strittmatter, J. Soll and B. Bolter** (2008). "Import of preproteins into the chloroplast inner envelope membrane." *Plant Mol Biol* 68(4-5): 505-519.
- Flores-Perez, U. and P. Jarvis** (2013). "Molecular chaperone involvement in chloroplast protein import." *Biochim Biophys Acta* 1833(2): 332-340.
- Fulda, S., S. Mikkat, W. Schroder and M. Hagemann** (1999). "Isolation of salt-induced periplasmic proteins from *Synechocystis* sp. strain PCC 6803." *Arch Microbiol* 171(3): 214-217.
- Fulda, S., B. Norling, A. Schoor and M. Hagemann** (2002). "The Slr0924 protein of *Synechocystis* sp. strain PCC 6803 resembles a subunit of the chloroplast protein import complex and is mainly localized in the thylakoid lumen." *Plant Mol Biol* 49(1): 107-118.
- Gasteiger E, Gattiker A, Hoogland C, Ivanyi I, Appel RD, Bairoch A** (2003) ExpASY: the proteomics server for in-depth protein knowledge and analysis. *Nucleic Acids Research* 31: 3784-3788.
- Gelhaye, E., N. Rouhier, N. Navrot and J. P. Jacquot** (2005). "The plant thioredoxin system." *Cell Mol Life Sci* 62(1): 24-35.

- Gibon, Y., O.E. Blaesing, J. Hannemann, P. Carillo, M. Höhne, J. H. M. Hendriks, N. Palacios, J. Cross, J. Selbig, M. Stitt** (2004). "A robot-based platform to measure multiple enzyme activities in Arabidopsis using a set of cycling assays: Comparison of changes of enzyme activities and transcript levels diurnal cycles and in prolonged darkness." *Plant Cell* 16 (12): 3304-3325.
- Glaser, S. and M. K. Higgins** (2012). "Overproduction, purification and crystallization of PfTic22, a component of the import apparatus from the apicoplast of *Plasmodium falciparum*." *Acta Crystallogr Sect F Struct Biol Cryst Commun* 68(Pt 3): 351-354.
- Glaser, S., G. G. van Dooren, S. Agrawal, C. F. Brooks, G. I. McFadden, B. Striepen and M. K. Higgins** (2012). "Tic22 is an essential chaperone required for protein import into the apicoplast." *J Biol Chem* 287(47): 39505-39512.
- Gorrec, F.** (2009). "The MORPHEUS protein crystallization screen." *J Appl Crystallogr* 42(Pt 6): 1035-1042.
- Gould, S. B., R. F. Waller and G. I. McFadden** (2008). "Plastid evolution." *Annu Rev Plant Biol* 59: 491-517.
- Hadrich, N., J. H. Hendriks, O. Kotting, S. Arrivault, R. Feil, S. C. Zeeman, Y. Gibon, W. X. Schulze, M. Stitt and J. E. Lunn** (2012). "Mutagenesis of cysteine 81 prevents dimerization of the APS1 subunit of ADP-glucose pyrophosphorylase and alters diurnal starch turnover in *Arabidopsis thaliana* leaves." *Plant J* 70(2): 231-242.
- Hanahan, D.** (1983). "Studies on transformation of *Escherichia coli* with plasmids." *J Mol Biol* 166(4): 557-580.
- Hebbelmann, I., J. Selinski, C. Wehmeyer, T. Goss, I. Voss, P. Mulo, S. Kangasjarvi, E. M. Aro, M. L. Oelze, K. J. Dietz, A. Nunes-Nesi, P. T. Do, A. R. Fernie, S. K. Talla, A. S. Raghavendra, V. Linke and R. Scheibe** (2012). "Multiple strategies to prevent oxidative stress in *Arabidopsis* plants lacking the malate valve enzyme NADP-malate dehydrogenase." *J Exp Bot* 63(3): 1445-1459.
- Hedtke, B., I. Wagner, T. Borner and W. R. Hess** (1999). "Inter-organellar crosstalk in higher plants: impaired chloroplast development affects mitochondrial gene and transcript levels." *Plant J* 19(6): 635-643.
- Hendriks, J. H., A. Kolbe, Y. Gibon, M. Stitt and P. Geigenberger** (2003). "ADP-glucose pyrophosphorylase is activated by posttranslational redox-modification in response to light and to sugars in leaves of *Arabidopsis* and other plant species." *Plant Physiol* 133(2): 838-849.
- Hinnah, S. C., R. Wagner, N. Sveshnikova, R. Harrer and J. Soll** (2002). "The chloroplast protein import channel Toc75: pore properties and interaction with transit peptides." *Biochem J* 363(2): 899-911.

- Hirsch, S., E. Muckel, F. Heemeyer, G. von Heijne and J. Soll** (1994). "A receptor component of the chloroplast protein translocation machinery." *Science* 266(5193): 1989-1992.
- Hormann, F., M. Kuchler, D. Sveshnikov, U. Oppermann, Y. Li and J. Soll** (2004). "Tic32, an essential component in chloroplast biogenesis." *J Biol Chem* 279(33): 34756-34762.
- Inaba, T., M. Alvarez-Huerta, M. Li, J. Bauer, C. Ewers, F. Kessler and D. J. Schnell** (2005). "Arabidopsis tic110 is essential for the assembly and function of the protein import machinery of plastids." *Plant Cell* 17(5): 1482-1496.
- Inaba, T., M. Li, M. Alvarez-Huerta, F. Kessler and D. J. Schnell** (2003). "atTic110 functions as a scaffold for coordinating the stromal events of protein import into chloroplasts." *J Biol Chem* 278(40): 38617-38627.
- Inoue, H., M. Li and D. J. Schnell** (2013). "An essential role for chloroplast heat shock protein 90 (Hsp90C) in protein import into chloroplasts." *Proc Natl Acad Sci U S A* 110(8): 3173-3178.
- Jarvis, P.** (2008). "Targeting of nucleus-encoded proteins to chloroplasts in plants." *New Phytol* 179(2): 257-285.
- Jelic, M., N. Sveshnikova, M. Motzkus, P. Horth, J. Soll and E. Schleiff** (2002). "The chloroplast import receptor Toc34 functions as preprotein-regulated GTPase." *Biol Chem* 383(12): 1875-1883.
- Juric, S., K. Hazler-Pilepic, A. Tomasic, H. Lepedus, B. Jelacic, S. Puthiyaveetil, T. Bionda, L. Vojta, J. F. Allen, E. Schleiff and H. Fulgosi** (2009). "Tethering of ferredoxin:NADP+ oxidoreductase to thylakoid membranes is mediated by novel chloroplast protein TROL." *Plant J* 60(5): 783-794.
- Kalanon, M. and G. I. McFadden** (2008). "The chloroplast protein translocation complexes of *Chlamydomonas reinhardtii*: a bioinformatic comparison of Toc and Tic components in plants, green algae and red algae." *Genetics* 179(1): 95-112.
- Kalanon, M., C. J. Tonkin and G. I. McFadden** (2009). "Characterization of two putative protein translocation components in the apicoplast of *Plasmodium falciparum*." *Eukaryot Cell* 8(8): 1146-1154.
- Kessler, F., G. Blobel, H. A. Patel and D. J. Schnell** (1994). "Identification of two GTP-binding proteins in the chloroplast protein import machinery." *Science* 266(5187): 1035-1039.
- Kolbe, A., A. Tiessen, H. Schluempmann, M. Paul, S. Ulrich and P. Geigenberger** (2005). "Trehalose 6-phosphate regulates starch synthesis via posttranslational redox activation of ADP-glucose pyrophosphorylase." *Proc Natl Acad Sci U S A* 102(31): 11118-11123.
- Koncz, C. and J. Schell** (1986). "The Promoter of TI-DNA Gene 5 Controls the Tissue-Specific Expression of Chimeric Genes Carried by a Novel Type of Agrobacterium Binary Vector." *Molecular & General Genetics* 204(3): 383-396.

- Kouranov, A., X. Chen, B. Fuks and D. J. Schnell** (1998). "Tic20 and Tic22 are new components of the protein import apparatus at the chloroplast inner envelope membrane." *J Cell Biol* 143(4): 991-1002.
- Kouranov, A. and D. J. Schnell** (1997). "Analysis of the interactions of preproteins with the import machinery over the course of protein import into chloroplasts." *J Cell Biol* 139(7): 1677-1685.
- Kouranov, A., H. Wang and D. J. Schnell** (1999). "Tic22 is targeted to the intermembrane space of chloroplasts by a novel pathway." *J Biol Chem* 274(35): 25181-25186.
- Kovacs-Bogdan, E., J. P. Benz, J. Soll and B. Bolter** (2011). "Tic20 forms a channel independent of Tic110 in chloroplasts." *BMC Plant Biol* 11: 133.
- Kuchler, M., S. Decker, F. Hormann, J. Soll and L. Heins** (2002). "Protein import into chloroplasts involves redox-regulated proteins." *EMBO J* 21(22): 6136-6145.
- Kyhse-Andersen, J.** (1984). "Electroblotting of multiple gels: a simple apparatus without buffer tank for rapid transfer of proteins from polyacrylamide to nitrocellulose." *J Biochem Biophys Methods* 10(3-4): 203-209.
- Laemmli, U. K.** (1970). "Cleavage of structural proteins during assembly of head of bacteriophage-T4. *Nature* 227 (5259): 680-685
- Lamesch P, T. Z. Berardini , D. Li , D. Swarbreck , C. Wilks, R. Sasidharan , R. Muller , K. Dreher , D. L. Alexander , M. Garcia-Hernandez , A. S. Karthikeyan, C. H. Lee , W. D. Nelson, L. Ploetz , S. Singh , A. Wensel, E. Huala** (2011) *The Arabidopsis Information Resource (TAIR): improved gene annotation and new tools. Nucleic Acids Res* 40: 1202-1210.
- Larkin, R. M., J. M. Alonso, J. R. Ecker and J. Chory** (2003). "GUN4, a regulator of chlorophyll synthesis and intracellular signaling." *Science* 299(5608): 902-906.
- Leister, D.** (2003). "Chloroplast research in the genomic age." *Trends Genet* 19(1): 47-56.
- Li, H. M., T. Moore and K. Keegstra** (1991). "Targeting of proteins to the outer envelope membrane uses a different pathway than transport into chloroplasts." *Plant Cell* 3(7): 709-717.
- Lim, L. and G. I. McFadden** (2010). "The evolution, metabolism and functions of the apicoplast." *Philos Trans R Soc Lond B Biol Sci* 365(1541): 749-763.
- Lindahl, M. and T. Kieselbach** (2009). "Disulphide proteomes and interactions with thioredoxin on the track towards understanding redox regulation in chloroplasts and cyanobacteria." *J Proteomics* 72(3): 416-438.
- Lopez-Juez, E.** (2007). "Plastid biogenesis, between light and shadows." *J Exp Bot* 58(1): 11-26.

- Martin, W. and R. G. Herrmann** (1998). "Gene transfer from organelles to the nucleus: how much, what happens, and Why?" *Plant Physiol* 118(1): 9-17.
- Martin, W., T. Rujan, E. Richly, A. Hansen, S. Cornelsen, T. Lins, D. Leister, B. Stoebe, M. Hasegawa and D. Penny** (2002). "Evolutionary analysis of Arabidopsis, cyanobacterial, and chloroplast genomes reveals plastid phylogeny and thousands of cyanobacterial genes in the nucleus." *Proc Natl Acad Sci U S A* 99(19): 12246-12251.
- Martin, W., B. Stoebe, V. Goremykin, S. Hapsmann, M. Hasegawa and K. V. Kowallik** (1998). "Gene transfer to the nucleus and the evolution of chloroplasts." *Nature* 393(6681): 162-165.
- May, T. and J. Soll** (2000). "14-3-3 proteins form a guidance complex with chloroplast precursor proteins in plants." *Plant Cell* 12(1): 53-64.
- McFadden, G. and G. van Dooren** (2004). "Evolution: Red algal genome affirms a common origin of all plastids." *Curr. Biol.* 14 (13): R514-516.
- Michalska, J., H. Zauber, B. Buchanan, F. Cejudo and P. Geigenberger** (2009). "NTRC links built-in thioredoxin to light and sucrose in regulating starch synthesis in chloroplasts and amyloplasts." *Proc Natl Acad Sci U S A* 106 (24): 9908-9913
- Murashige, T. S. F.** (1962). "A revised medium for rapid growth and bio assays with tobacco tissue cultures." *Physiologia Plantarum* 15: 473-497.
- Nicholas KB and Nicholas HB** (1997) GeneDoc: a tool for editing and annotating multiple sequence alignments. Distributed by the authors.
- Noctor, G., R. De Paepe and C. H. Foyer** (2007). "Mitochondrial redox biology and homeostasis in plants." *Trends Plant Sci* 12(3): 125-134.
- Orzechowski, S.** (2008). "Starch metabolism in leaves." *Acta Biochim Pol* 55(3): 435-445.
- Ossowski, S., R. Schwab and D. Weigel** (2008). "Gene silencing in plants using artificial microRNAs and other small RNAs." *Plant J* 53(4): 674-690.
- Perry, S. E. and K. Keegstra** (1994). "Envelope membrane proteins that interact with chloroplastic precursor proteins." *Plant Cell* 6(1): 93-105.
- Pfalz, J., M. Liebers, M. Hirth, B. Grubler, U. Holtzegel, Y. Schroter, L. Dietzel and T. Pfanschmidt** (2012). "Environmental control of plant nuclear gene expression by chloroplast redox signals." *Front Plant Sci* 3: 257.
- Porra, R. J. T. W. A. K. P. E.** (1989). "Determination of accurate extinction coefficient and simultaneous equations for assaying chlorophylls a and b extracted with four different solvents: verification of the concentration of chlorophyll standards by atomic absorption spectroscopy." *Biochim Biophys Acta* 975: 384-394.

- Qbadou, S., T. Becker, T. Bionda, K. Reger, M. Ruprecht, J. Soll and E. Schleiff (2007).** "Toc64--a preprotein-receptor at the outer membrane with bipartite function." *J Mol Biol* 367(5): 1330-1346.
- Qbadou, S., T. Becker, O. Mirus, I. Tews, J. Soll and E. Schleiff (2006).** "The molecular chaperone Hsp90 delivers precursor proteins to the chloroplast import receptor Toc64." *EMBO J* 25(9): 1836-1847.
- Richter, S. and G. K. Lamppa (1999).** "Stromal processing peptidase binds transit peptides and initiates their ATP-dependent turnover in chloroplasts." *J Cell Biol* 147(1): 33-44.
- Robbens, S., E. Derelle, C. Ferraz, J. Wuyts, H. Moreau and Y. Van de Peer (2007).** "The complete chloroplast and mitochondrial DNA sequence of *Ostreococcus tauri*: organelle genomes of the smallest eukaryote are examples of compaction." *Mol Biol Evol* 24(4): 956-968.
- Rokka, A., M. Suorsa, A. Saleem, N. Battchikova and E. M. Aro (2005).** "Synthesis and assembly of thylakoid protein complexes: multiple assembly steps of photosystem II." *Biochem J* 388(Pt 1): 159-168.
- Rudolf, M., A. B. Machettira, L. E. Gross, K. L. Weber, K. Bolte, T. Bionda, M. S. Sommer, U. G. Maier, A. P. Weber, E. Schleiff and J. Tripp (2013).** "In Vivo Function of Tic22, a Protein Import Component of the Intermembrane Space of Chloroplasts." *Mol Plant*. 6 (3): 817-829.
- Ruprecht, M., T. Bionda, T. Sato, M. S. Sommer, T. Endo and E. Schleiff (2010).** "On the impact of precursor unfolding during protein import into chloroplasts." *Mol Plant* 3(3): 499-508.
- Saiki, R. K., D. H. Gelfand, S. Stoffel, S. J. Scharf, R. Higuchi, G. T. Horn, K. B. Mullis and H. A. Erlich (1988).** "Primer-directed enzymatic amplification of DNA with a thermostable DNA polymerase." *Science* 239(4839): 487-491.
- Sambrook, J. F., EF and Maniatis, T. (1989).** "Molecular Cloning. A Laboratory Manual. Cold Spring Harbour Laboratory, Cold Spring Harbour Press, New York."
- Scheibe, R. (2004).** "Malate valves to balance cellular energy supply." *Physiol Plant* 120(1): 21-26.
- Schindler, C. H., R; Soll J (1987).** "Protein transport in chloroplasts: ATP is prerequisite." *Z. Naturforsch.* 42c: 103-108.
- Schmid M, Davison TS, Henz SR, Pape UJ, Demar M, Vingron M, Scholkopf B, Weigel D, Lohmann JU (2005)** A gene expression map of *Arabidopsis thaliana* development. *Nature Genetics* 37: 501–506.
- Schwacke, R., A. Schneider, E. van der Graaff, K. Fischer, E. Catoni, M. Desimone, W. B. Frommer, U. I. Flugge and R. Kunze (2003).**"ARAMEMNON, a novel database for Arabidopsis integral membrane proteins." *Plant Physiol*. 131(1): 16-26.

- Schwenkert, S., J. Soll and B. Bolter** (2011). "Protein import into chloroplasts--how chaperones feature into the game." *Biochim Biophys Acta* 1808(3): 901-911.
- Seedorf, M., K. Waegemann and J. Soll** (1995). "A constituent of the chloroplast import complex represents a new type of GTP-binding protein." *Plant J* 7(3): 401-411.
- Seigneurin-Berny, D., D. Salvi, A. J. Dorne, J. Joyard and N. Rolland** (2008). "Percoll-purified and photosynthetically active chloroplasts from *Arabidopsis thaliana* leaves." *Plant Physiol Biochem* 46(11): 951-955.
- Sirpio, S., Y. Allahverdiyeva, M. Suorsa, V. Paakkarinen, J. Vainonen, N. Battchikova and E. M. Aro** (2007). "TLP18.3, a novel thylakoid lumen protein regulating photosystem II repair cycle." *Biochem J* 406(3): 415-425.
- Sohrt, K. and J. Soll** (2000). "Toc64, a new component of the protein translocon of chloroplasts." *J Cell Biol* 148(6): 1213-1221.
- Soll, J. and E. Schleiff** (2004). "Protein import into chloroplasts." *Nat Rev Mol Cell Biol* 5(3): 198-208.
- Spurr, A. R.** (1969). "A low-viscosity epoxy resin embedding medium for electron microscopy." *J Ultrastruct Res* 26(1): 31-43.
- Stengel, A., J. P. Benz, B. B. Buchanan, J. Soll and B. Bolter** (2009). "Preprotein import into chloroplasts via the Toc and Tic complexes is regulated by redox signals in *Pisum sativum*." *Mol Plant* 2(6): 1181-1197.
- Stengel, A., J. P. Benz, J. Soll and B. Bolter** (2010). "Redox-regulation of protein import into chloroplasts and mitochondria: similarities and differences." *Plant Signal Behav* 5(2): 105-109.
- Stengel, A., P. Benz, M. Balsera, J. Soll and B. Bolter** (2008). "TIC62 redox-regulated translocon composition and dynamics." *J Biol Chem* 283(11): 6656-6667.
- Su, P. H. and H. M. Li** (2010). "Stromal Hsp70 is important for protein translocation into pea and *Arabidopsis* chloroplasts." *Plant Cell* 22(5): 1516-1531.
- Tamura, K., D. Peterson, N. Peterson, G. Stecher, M. Nei and S. Kumar** (2011). "MEGA5: molecular evolutionary genetics analysis using maximum likelihood, evolutionary distance, and maximum parsimony distance" *Mol Biol Evol* 28 (10): 2731-2739
- Taniguchi, M. and H. Miyake** (2012). "Redox-shuttling between chloroplast and cytosol: integration of intra-chloroplast and extra-chloroplast metabolism." *Curr Opin Plant Biol* 15(3): 252-260.
- Thompson JD, Gibson TJ, Plewniak F, Jeanmougin F und Higgins DG** (1997) The CLUSTAL_X windows interface: flexible strategies for multiple sequence alignment aided by quality analysis tools. *Nucleic Acids Res* 25: 4876-4882.

- Thormahlen, I., J. Ruber, E. von Roepenack-Lahaye, S. M. Ehrlich, V. Massot, C. Hummer, J. Tezycka, E. Issakidis-Bourguet and P. Geigenberger (2013).** "Inactivation of thioredoxin f1 leads to decreased light activation of ADP-glucose pyrophosphorylase and altered diurnal starch turnover in leaves of Arabidopsis plants." *Plant Cell Environ* 36(1): 16-29.
- Tiessen, A., J. H. Hendriks, M. Stitt, A. Branscheid, Y. Gibon, E. M. Farre and P. Geigenberger (2002).** "Starch synthesis in potato tubers is regulated by post-translational redox modification of ADP-glucose pyrophosphorylase: a novel regulatory mechanism linking starch synthesis to the sucrose supply." *Plant Cell* 14(9): 2191-2213.
- Tikkanen, M., P. J. Gollan, M. Suorsa, S. Kangasjarvi and E. M. Aro (2012).** "STN7 Operates in Retrograde Signaling through Controlling Redox Balance in the Electron Transfer Chain." *Front Plant Sci* 3: 277.
- Tripp, J., A. Hahn, P. Koenig, N. Flinner, D. Bublak, E. M. Brouwer, F. Ertel, O. Mirus, I. Sinning, I. Tews and E. Schleiff (2012).** "Structure and conservation of the periplasmic targeting factor Tic22 protein from plants and cyanobacteria." *J Biol Chem* 287(29): 24164-24173.
- Vojta, L., J. Soll and B. Bolter (2007).** "Protein transport in chloroplasts - targeting to the intermembrane space." *FEBS J* 274(19): 5043-5054.
- Waegemann, K. and J. Soll (1995).** "Characterization and isolation of the chloroplast protein import machinery." *Methods Cell Biol* 50: 255-267.
- Wielopolska, A., H. Townley, I. Moore, P. Waterhouse and C. Helliwell (2005).** "A high-throughput inducible RNAi vector for plants." *Plant Biotechnol J* 3(6): 583-590.
- Woodson, J. D., J. M. Perez-Ruiz, R. J. Schmitz, J. R. Ecker and J. Chory (2012).** "Sigma factor-mediated plastid retrograde signals control nuclear gene expression." *Plant J*.
- Xu, X., S. Wang, Y. X. Hu and D. B. McKay (2007).** "The periplasmic bacterial molecular chaperone SurA adapts its structure to bind peptides in different conformations to assert a sequence preference for aromatic residues." *J Mol Biol* 373(2): 367-381.
- Yoshida, K., I. Terashima and K. Noguchi (2007).** "Up-regulation of mitochondrial alternative oxidase concomitant with chloroplast over-reduction by excess light." *Plant Cell Physiol* 48(4): 606-614.
- Yoshida, K., C. Watanabe, Y. Kato, W. Sakamoto and K. Noguchi (2008).** "Influence of chloroplastic photo-oxidative stress on mitochondrial alternative oxidase capacity and respiratory properties: a case study with Arabidopsis yellow variegated 2." *Plant Cell Physiol* 49(4): 592-603.
- Zeeman, S. C., J. Kossmann and A. M. Smith (2010).** "Starch: its metabolism, evolution, and biotechnological modification in plants." *Annu Rev Plant Biol* 61: 209-234.

Zeeman, S. C., S. M. Smith and A. M. Smith (2007). "The diurnal metabolism of leaf starch." *Biochem J* 401(1): 13-28.

Zhou, C., Y. Yang and A. Y. Jong (1990). "Mini-prep in ten minutes." *Biotechniques* 8(2): 172-173.

7 Supplementary data

7.1 DNA Microarray analysis

Table 8 Regulation of the gene expression in *tic22dm* plants grown under long day conditions (100 μ mol). Up- and down regulated genes in *tic22dm* are listed (50 genes per regulation). The order is based on the intensity of the fold change (quantitative evaluation of the differential gene expression). The MapMan Bin Code classifies single genes to certain categories.

AGI	Name and function	Bin Code
Up regulated genes		
At5g48570	ROF2, ATKBP65 peptidyl-prolyl cis-trans isomerase, putative / FK506-binding protein, putative	31.3.1 cell.cycle.peptidylprolyl isomerase
At3g12580	HSP70 HSP70 (heat shock protein 70); ATP binding	20.2.1 stress.abiotic.heat
Atcg00660	RPL20 encodes a chloroplast ribosomal protein L20, a constituent of the large subunit of the ribosomal complex	29.2.1.1.1.2.20 protein.synthesis.ribosomal protein.prokaryotic.chloroplast.50S subunit.L20
At5g52640	HSP81-1, ATHS83, HSP81.1, HSP83, ATHSP90.1 ATHSP90.1 (HEAT SHOCK PROTEIN 90.1); ATP binding / unfolded protein binding	20.2.1 stress.abiotic.heat
Atcg01120	RPS15 encodes a chloroplast ribosomal protein S15, a constituent of the small subunit of the ribosomal complex	29.2.1.1.1.1.15 protein.synthesis.ribosomal protein.prokaryotic.chloroplast.30S subunit.S15
Atmg00080, Atmg00090	MULTIPLE HITS:atmg00080: Symbols: RPL16 encodes a mitochondrial ribosomal protein L16, which is a constituent of the large ribosomal subunit atmg00090: ribosomal protein S3	29.2.1.1.2.1.3 protein.synthesis.ribosomal protein.prokaryotic.mitochondrion.30S subunit.S3 AND 29.2.1.1.2.1.16 protein.synthesis.ribosomal protein.prokaryotic.mitochondrion.30S subunit.S16

At5g12030	(AT-HSP17.6A, HSP17.6 AT-HSP17.6A (ARABIDOPSIS THALIANA HEAT SHOCK PROTEIN 17.6A); unfolded protein binding	20.2.1 stress.abiotic.heat
Atcg01060	PSAC Encodes the PsaC subunit of photosystem I.	1.1.2.2 PS.lightreaction.photosystem I.PSI polypeptide subunits
At5g12110	elongation factor 1B alpha-subunit 1 (eEF1Balpha1)	29.2.4 protein.synthesis.elongation
At5g51440	23.5 kDa mitochondrial small heat shock protein (HSP23.5-M)	20.2.1 stress.abiotic.heat
At3g30720	QQS QQS (QUA-QUINE STARCH)	2.1.2 major CHO metabolism.synthesis.starch
At1g36180	ACC2 ACC2 (ACETYL-COA CARBOXYLASE 2); acetyl-CoA carboxylase	11.1.1 lipid metabolism.FA synthesis and FA elongation.Acetyl CoA Carboxylation
At3g13470	chaperonin, putative	29.6 protein.folding
At5g37670	15.7 kDa class I-related small heat shock protein-like (HSP15.7-CI)	20.2.1 stress.abiotic.heat
At5g09590	MTHSC70-2, HSC70-5 MTHSC70-2 (MITOCHONDRIAL HSP70 2); ATP binding	20.2.1 stress.abiotic.heat
At2g21640	Encodes a protein of unknown function that is a marker for oxidative stress response.	35.2 not assigned.unknown
At4g12400	stress-inducible protein, putative	20 stress
Atmg00580	NAD4 NADH dehydrogenase subunit 4	9.1.2 mitochondrial electron transport / ATP synthesis.NADH-DH.localisation not clear
At1g59860, At1g07400	MULTIPLE HITS: at1g59860: 17.6 kDa class I heat shock protein (HSP17.6A-CI) at1g07400: 17.8 kDa class I heat shock protein (HSP17.8-CI)	20.2.1 stress.abiotic.heat
At4g25990	chloroplast gene regulation CIL	35.2 not assigned.unknown
At2g26150	ATHSFA2, HSFA2 ATHSFA2; DNA binding / transcription factor	20.2.1 stress.abiotic.heat AND 27.3.23 RNA.regulation of transcription.HSF,Heat-shock transcription factor family

At2g40960	nucleic acid binding	35.2 not assigned.unknown
Atcg00590	ORF31 hypothetical protein	1.1.3 PS.lightreaction.cytochrome b6/f
At5g08610	DEAD box RNA helicase (RH26)	27.1.2 RNA.processing.RNA helicase
At5g23480	DNA binding	35.2 not assigned.unknown
At5g47500	pectinesterase family protein	10.8.1 cell wall.pectin*esterases.PME
At5g66960	prolyl oligopeptidase family protein	29.5 protein.degradation
At1g63100	AtSCL28 scarecrow transcription factor family protein	27.3.21 RNA.regulation of transcription.GRAS transcription factor family
At5g09300	2-oxoisovalerate dehydrogenase, putative / 3-methyl-2-oxobutanoate dehydrogenase, putative / branched-chain alpha-keto acid dehydrogenase E1 alpha subunit, putative	13.2.4.1 amino acid metabolism.degradation.branched-chain group.shared
At2g18220	INVOLVED IN: biological_process unknown; LOCATED IN: cellular_component unknown; EXPRESSED IN: 22 plant structures; EXPRESSED DURING: 13 growth stages	35.2 not assigned.unknown
At1g20390	transposable element gene	28.1.1.1 DNA.synthesis/chromatin structure.retrotransposon/transposase.gypsy-like retrotransposon
At5g24240	phosphatidylinositol 3- and 4-kinase family protein / ubiquitin family protein	29.5.11 protein.degradation.ubiquitin
At1g24822 At1g25097 At1g24996	MULTIPLE DISAGREEING HITS: at1g24822: unknown protein at1g25097: unknown protein at1g24996: unknown protein	35.3 not assigned.disagreeing hits
At2g22650	FAD-dependent oxidoreductase family protein	35.1 not assigned.no ontology

At1g72440	EDA25 EDA25 (embryo sac development arrest 25)	27.3.13 RNA.regulation of transcription.CCAAT box binding factor family, DR1
At4g38280	MULTIPLE HITS: at4g38280: unknown protein at4g38330: unknown protein at2g45250: unknown protein	35.2 not assigned.unknown
At4g38330		
At2g45250		
At4g38950	kinesin motor family protein	31.1 cell.organisation
At5g55915	OLI2 nucleolar protein, putative	28.1 DNA.synthesis/chromatin structure
At3g53230	cell division cycle protein 48, putative / CDC48, putative	31.2 cell.division
At3g48500	PDE312, PTAC10 RNA binding	35.2 not assigned.unknown
At3g21300	RNA methyltransferase family protein	26.1 misc.misc2
At3g57150	Symbols: NAP57, AtNAP57, CBF5, AtCBF5 NAP57 (Arabidopsis thaliana homologue of NAP57); pseudouridine synthase	28.1 DNA.synthesis/chromatin structure
Atcg00170	RPOC2 RNA polymerase beta' subunit-2 chrC:15938-20068 REVERSE	27.2 RNA.transcription
At1g74310	ATHSP101, HSP101, HOT1 ATHSP101 (ARABIDOPSIS THALIANA HEAT SHOCK PROTEIN 101); ATP binding / ATPase/ nucleoside-triphosphatase/ nucleotide binding / protein binding	20.2.1 stress.abiotic.heat
At1g44910	protein binding	35.1 not assigned.no ontology
At5g55450	protease inhibitor/seed storage/lipid transfer protein (LTP) family protein	26.21 misc.protease inhibitor/seed storage/lipid transfer protein (LTP) family protein
At1g76820	GTP binding / GTPase	29.2.99 protein.synthesis.misc
At1g17960	threonyl-tRNA synthetase, putative / threonine--tRNA ligase, putative	29.1.3 protein.aa activation.threonine-tRNA ligase

Atcg01000 Atcg01130	MULTIPLE HITS: atcg01000: Symbols: YCF1.1 hypothetical protein atcg01130: Symbols: YCF1.2 hypothetical protein	29.8 protein.assembly and cofactor ligation
Down regulated genes		
Atcg01110	NDHH Encodes the 49KDa plastid NAD(P)H dehydrogenase subunit H protein. Its transcription is regulated by an ndhF-specific plastid sigma factor, SIG4.	1.1.40 PS.lightreaction.cyclic electron flow-chlororespiration
At3g47340	ASN1, DIN6, AT-ASN1 ASN1 (GLUTAMINE-DEPENDENT ASPARAGINE SYNTHASE 1); asparagine synthase (glutamine-hydrolyzing)	13.1.3.1.1 amino acid metabolism.synthesis.aspartate family.asparagine.asparagine synthetase
Atcg00120	ATPA Encodes the ATPase alpha subunit, which is a subunit of ATP synthase and part of the CF1 portion which catalyzes the conversion of ADP to ATP using the proton motive force. This complex is located in the thylakoid membrane of the chloroplast	1.1.4.1 PS.lightreaction.ATP synthase.alpha subunit
At2g26020	(PDF1.2b PDF1.2b (plant defensin 1.2b)	20.1.7.12 stress.biotic.PR-proteins.plant defensins
Atcg00350	PSAA Encodes psaA protein comprising the reaction center for photosystem I along with psaB protein; hydrophobic protein encoded by the chloroplast genome.	1.1.2.2 PS.lightreaction.photosystem I.PSI polypeptide subunits
Atcg00580	PSBE PSII cytochrome b559. There have been many speculations about the function of Cyt b559, but the most favored at present is that it plays a protective role by acting as an electron acceptor or electron donor under conditions when electron flow through PSII is not optimized.	1.1.1.2 PS.lightreaction.photosystem II.PSII polypeptide subunits
At1g72910 At1g72930	MULTIPLE HITS: at1g72910: disease resistance protein (TIR-NBS class), putative at1g72930: Symbols: TIR TIR (TOLL/INTERLEUKIN-1 RECEPTOR-LIKE); transmembrane receptor	20.1.2 stress.biotic.receptors AND 20.1.7 stress.biotic.PR-proteins
At2g30520	RPT2 RPT2 (ROOT PHOTOTROPISM 2); protein binding	30.11 signalling.light
At4g16990	RLM3 RLM3 (RESISTANCE TO LEPTOSPHAERIA MACULANS 3); ATP binding / transmembrane receptor	20.1.7 stress.biotic.PR-proteins

Atcg00710	PSBH Encodes a 8 kD phosphoprotein that is a component of the photosystem II oxygen evolving core. Its exact molecular function has not been determined but it may play a role in mediating electron transfer between the secondary quinone acceptors, QA and QB, associated with the acceptor side of PSII.	1.1.1.2 PS.lightreaction.photosystem II.PSII polypeptide subunits
At1g53890 At1g53870	MULTIPLE HITS: at1g53890: unknown protein at1g53870: unknown protein	35.1 not assigned.no ontology AND 35.2 not assigned.unknown
At4g13560	UNE15 UNE15 (unfertilized embryo sac 15)	33.99 development.unspecified
At3g46780	PTAC16 PTAC16 (PLASTID TRANSCRIPTIONALLY ACTIVE 16); binding / catalytic	35.2 not assigned.unknown
At5g20230	ATBCB, BCB ATBCB (ARABIDOPSIS BLUE-COPPER-BINDING PROTEIN); copper ion binding / electron carrier	26.19 misc.plastocyanin-like
At2g45670	calcineurin B subunit-related	30.3 signalling.calcium
At3g02020, At5g14060	MULTIPLE HITS: at3g02020: Symbols: AK3 AK3 (ASPARTATE KINASE 3); aspartate kinase at5g14060: Symbols: CARAB-AK-LYS CARAB-AK-LYS; amino acid binding / aspartate kinase	13.1.3.6.1.1 amino acid metabolism.synthesis.aspartate family.misc.homoserine.aspartate kinase
At3g28220	meprin and TRAF homology domain-containing protein / MATH domain-containing protein	35.1 not assigned.no ontology
At3g62950	glutaredoxin family protein	21.4 redox.glutaredoxins
At5g24770 At5g24780	MULTIPLE HITS: at5g24770: Symbols: VSP2, ATVSP2 VSP2 (VEGETATIVE STORAGE PROTEIN 2); acid phosphatase chr5:8500476-8502224 REVERSE at5g24780: Symbols: VSP1, ATVSP1 VSP1 (VEGETATIVE STORAGE PROTEIN 1); acid phosphatase/ transcription factor binding	33.1 development.storage proteins
At2g01520	MLP328 MLP328 (MLP-LIKE PROTEIN 328); copper ion binding	20.2.99 stress.abiotic.unspecified
At1g57990 At1g57980	MULTIPLE HITS: at1g57990: Symbols: ATPUP18 ATPUP18; purine transmembrane transporter at1g57980: purine permease-related	34.10 transport.nucleotides

At1g19660, At1g75380	MULTIPLE HITS: at1g19660: wound-responsive family protein at1g75380: wound-responsive protein-related	20.2.4 stress.abiotic.touch/wounding
At5g03350	(legume lectin family protein	26.16 misc.myrosinases-lectin-jacalin
At2g20570	GPRI1, GLK1 GPRI1 (GBF'S PRO-RICH REGION-INTERACTING FACTOR 1); transcription factor/transcription regulator	27.3.20 RNA.regulation of transcription.G2-like transcription factor family, GARP
At5g44420	Symbols: PDF1.2, PDF1.2A, LCR77 PDF1.2	20.1.7.12 stress.biotic.PR-proteins.plant defensins
At5g02160	unknown protein	35.2 not assigned.unknown
At1g70900	unknown protein	35.2 not assigned.unknown
At1g14230, At1g14250	MULTIPLE HITS: at1g14230: nucleoside phosphatase family protein / GDA1/CD39 family protein at1g14250: nucleoside phosphatase family protein / GDA1/CD39 family protein	23.2 nucleotide metabolism.degradation
At5g62000	ARF2, ARF1-BP, HSS ARF2 (AUXIN RESPONSE FACTOR 2); protein binding / transcription factor	27.3.4 RNA.regulation of transcription.ARF, Auxin Response Factor family
At5g44190	GLK2, ATGLK2, GPRI2 GLK2 (GOLDEN2-LIKE 2); DNA binding / transcription factor/transcription regulator	27.3.20 RNA.regulation of transcription.G2-like transcription factor family, GARP
At3g29270	ubiquitin-protein ligase	29.5.11.4.2 protein.degradation.ubiquitin.E3.RING
At4g32020	unknown protein	35.2 not assigned.unknown
At1g67865	unknown protein	35.2 not assigned.unknown
At5g66400	RAB18, ATDI8 RAB18 (RESPONSIVE TO ABA 18	20.2.99 stress.abiotic.unspecified
At4g04330	RbcX1	35.2 not assigned.unknown

At3g13750	BGAL1 BGAL1 (Beta galactosidase 1); beta-galactosidase/ catalytic/ cation binding / heme binding / peroxidase/ sugar binding	26.3.2 misc.gluco-, galacto- and mannosidases.beta-galactosidase
At3g50970	LTI30, XERO2 LTI30 (LOW TEMPERATURE-INDUCED 30)	20.2.99 stress.abiotic.unspecified
At5g03040	iqd2 (IQ-domain 2); calmodulin binding	30.3 signalling.calcium
At4g16490	binding	35.1.3 not assigned.no ontology.armadillo/beta-catenin repeat family protein
At5g65380	MATE efflux carrier put	33.99 development.unspecified
At2g39190	ATATH8 ATATH8; transporter	35.1.1 not assigned.no ontology.ABC1 family protein
At3g28740	CYP81D1 CYP81D1; electron carrier/ heme binding / iron ion binding / monooxygenase/ oxygen binding	26.10 misc.cytochrome P450
At4g35770	SEN1, ATSEN1, DIN1 SEN1 (SENESCENCE 1)	33.99 development.unspecified
At2g33830	dormancy/auxin associated family protein	17.2.3 hormone metabolism.auxin.induced-regulated-responsive-activated
At2g46340	SPA1 SPA1 (SUPPRESSOR OF PHYA-105 1); protein binding / signal transducer	30.11 signalling.light
At5g09530	hydroxyproline-rich glycoprotein family protein	35.1.41 not assigned.no ontology.hydroxyproline rich proteins
At4g31080	(at4g31080): unknown protein chr4:15120888-15123486 FORWARD	35.2 not assigned.unknown
At1g34760	GRF11, GF14 OMICRON GRF11 (GENERAL REGULATORY FACTOR 11); ATPase binding / amino acid binding / protein binding / protein phosphorylated amino acid binding	30.7 signalling.14-3-3 proteins
At5g44100, At1g03930	MULTIPLE HITS: at5g44100: Symbols: ckl7 ckl7 (Casein Kinase I-like 7); ATP binding / kinase/ protein kinase/ protein serine/threonine kinase at1g03930: Symbols: ADK1, CKL9ALPHA, CKL9BETA ADK1 (dual specificity kinase 1); kinase/ protein serine/threonine/tyrosine kinase	29.4 protein.postranslational modification

Table 9 Regulated genes in *tic22dm* used for specified analysis. The AGI-code (*Arabidopsis* Genome Initiative), averaged signal values (n=4) of WT and *tic22dm*, the fold change and the statistical significance (p-value) is depicted. The value of the fold change is increased (, if the expression of the gene is up regulated compared to WT and negative, when the gene expression is down regulated compared to WT:

Name	AGI	WT	<i>tic22dm</i>	FCH	P-value
Up regulated genes					
RPL20	Atcg00660	94	564	5,97	5,95E-06
RPS15	Atcg01120	114	562	4,94	2,07E-04
PSAC	Atcg01060	129	528	4,10	1,63E-05
ACC2	At1g36180	49	154	3,13	2,19E-04
NAD4	Atmg00580	495	1475	2,98	1,6E-04
Down regulated genes					
NDHH	Atcg01110	246	28	0,11	2,0E-04
ATPA	Atcg00120	1805	330	0,18	2,8E-04
PSAC	Atcg00350	396	76	0,19	2,1E-04
PSBE	Atcg00580	3549	740	0,21	1,3E-04

Curriculum vitae

Persönliche Daten

Name	Natalie Schuck
Geburtsdaten	29. April 1983 in München
Familienstand	ledig
Staatsangehörigkeit	deutsch

Hochschulbildung

<i>08/2009-05/2013</i>	Promotion, Ludwig-Maximilians-Universität München, Lehrstuhl für Biochemie und Physiologie der Pflanzen (Prof. Dr. Jürgen Soll) Abschluss voraussichtlich Mai/Juni 2013
<i>09/2004-07/2009</i>	Studium der Biologie mit Schwerpunkt Zellbiologie, Ludwig-Maximilians-Universität München, Abschluss: Diplom

Berufserfahrung

<i>05/2005-12/2007</i>	Studentische Hilfskraft, Proteros biostructures GmbH, Martinsried
------------------------	--

Danksagung

Als erstes möchte ich mich bei Prof. Dr. Jürgen Soll bedanken, dass er mir ermöglicht hat, diese Doktorarbeit in seiner Arbeitsgruppe anzufertigen. Neben seinem stetigen wissenschaftlichen Input und seinem offenen Ohr für sämtliche Fragen und Belange, hat er mit beständigen Herausforderungen meinen persönlichen und beruflichen Horizont erweitert. Vielen Dank für alles!!

Ein herzliches Dankeschön auch an meine Betreuerin Dr. Bettina Bölter für die Betreuung dieser Arbeit und das Beantworten aller Fragen während der gesamten Zeit.

Ein Riesendankeschön geht an meine allerliebsten Kollegen der gesamten AG Soll, die in der Zeit nicht nur ein tolles Team waren, sondern für mich echte Freunde geworden sind: Anna, vielen Dank für die Korrektur dieser Arbeit und dass Du so schöne gemeinsame Events organisierst! Vielen Dank auch an Andi, dass man bei allen Fragen rund um die ÄKTA und Proteinaufreinigung immer zu Dir kommen konnte. Deine Hilfsbereitschaft ist unglaublich! Danke auch an Katja, dass Du nach wie vor immer für mich da bist! Danke auch Eike, WaiLing, Carsten, Erika, und Betty für die tolle Laboratmosphäre!

Ein herzliches Dankeschön auch an Roland für die Einarbeitung in die Pflanzenmethoden und für die tollen Gespräche (und natürlich auch für die Einladung in die USA!). Ein großes Dankeschön an Irene, die mit mir Stunden beim Schneiden der mikroskopischen Blatteile verbracht hat, und für die Anfertigung der TEM-Bilder. Danke auch an Betty und Ulrike, für das Fortführen der Schnipselei. Vielen Dank auch an Kathrin und Karl für das Durchführen der Affymetrixanalysen. Danke an die gesamte Arbeitsgruppe für die tolle Teamarbeit und das schöne Arbeitsklima! Es war mir eine Ehre, ein Teil dessen gewesen zu sein! Ein herzliches Dankeschön auch an die finnischen Mädls Minna, Nina und Paula für die tolle Kooperation und die Gastfreundschaft in Turku! Ein großes Dankeschön auch an Ira für die unermüdlichen Kristallisationsversuche und an Ina für die Metabolitanalysen.

Der größte und für mich wichtigste Dank geht an meine Mama und meine Freunde, ganz besonders an Amelie und Hanni: Eure stetige Ermutigung und bedingungslose Unterstützung hat mir immer Kraft gegeben. Ihr glaubt an mich und seid immer für mich da, dafür kann ich Euch nicht genug danken. Ein ganz besonderer Dank geht an meinen persönlichen Lichtblick Tommi: Du hast mit mir sowohl schwierige als auch schöne Zeiten durchgestanden und ich freue mich sehr auf unsere vielversprechende gemeinsame Zukunft.

Eidesstattliche Versicherung

Hiermit versichere ich an Eides statt, dass die vorgelegte Dissertation von mir selbstständig und ohne unerlaubte Hilfe angefertigt wurde.

München, den 23. Mai 2013

Natalie Schuck

Erklärung

Hiermit erkläre ich, dass ich zuvor nicht versucht habe, anderweitig eine Dissertation einzureichen oder mich einer Doktorprüfung zu unterziehen. Die vorliegende Dissertation wurde weder in Teilen noch als Ganzes einer weiteren Prüfungskommission vorgelegt.

München, den 23. Mai 2013

Natalie Schuck